

**NASA CONTRACTOR
REPORT**



NASA CR-2464

NASA CR-2464

(NASA-CR-2464) A GENERAL THEORY OF
UNSTEADY COMPRESSIBLE POTENTIAL
AERODYNAMICS (Boston Univ.) 201 p
HC \$7.25

CSCL 01A

✓ N75-12893
Unclas
H1/01 06125

**A GENERAL THEORY OF UNSTEADY
COMPRESSIBLE POTENTIAL AERODYNAMICS**

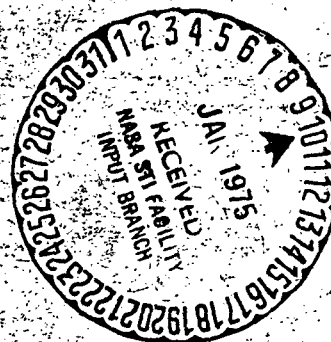
by Luigi Morino

Prepared by

**BOSTON UNIVERSITY
COLLEGE OF ENGINEERING**

Boston, Mass. 02215

for Langley Research Center



NATIONAL AERONAUTICS AND SPACE ADMINISTRATION • WASHINGTON, D. C. • DECEMBER 1974

REPRODUCED BY
U.S. DEPARTMENT OF COMMERCE
NATIONAL TECHNICAL INFORMATION SERVICE
SPRINGFIELD, VA. 22161

202

1. Report No. NASA CR-2464	2. Government Accession No.	3. Recipient's Catalog No.	
4. Title and Subtitle A GENERAL THEORY OF UNSTEADY COMPRESSIBLE POTENTIAL AERODYNAMICS		5. Report Date December 1974	
		6. Performing Organization Code	
7. Author(s) LUIGI MORINO		8. Performing Organization Report No. TR-73-01	
		10. Work Unit No.	
9. Performing Organization Name and Address BOSTON UNIVERSITY COLLEGE OF ENGINEERING BOSTON, MASSACHUSETTS 02215		11. Contract or Grant No. NGR 22-004-030	
		13. Type of Report and Period Covered CONTRACTOR REPORT	
12. Sponsoring Agency Name and Address NATIONAL AERONAUTICS AND SPACE ADMINISTRATION WASHINGTON, D.C. 20546		14. Sponsoring Agency Code	
15. Supplementary Notes THIS REPORT SUPERSEDES BOSTON UNIVERSITY REPORT TR-72-01 TOPICAL REPORT.			
16. Abstract THE GENERAL THEORY OF POTENTIAL AERODYNAMIC FLOW AROUND A LIFTING BODY HAVING ARBITRARY SHAPE AND MOTION IS PRESENTED. BY USING THE GREEN FUNCTION METHOD, AN INTEGRAL REPRESENTATION FOR THE POTENTIAL IS OBTAINED FOR BOTH SUPERSONIC AND SUBSONIC FLOW. UNDER SMALL PERTURBATION ASSUMPTION, THE POTENTIAL AT ANY POINT, P , IN THE FIELD DEPENDS ONLY UPON THE VALUES OF THE POTENTIAL AND ITS NORMAL DERIVATIVE ON THE SURFACE, Σ , OF THE BODY. HENCE, IF THE POINT P APPROACHES THE SURFACE OF THE BODY, THE REPRESENTATION REDUCES TO AN INTEGRO-DIFFERENTIAL EQUATION RELATING THE POTENTIAL AND ITS NORMAL DERIVATIVE (WHICH IS KNOWN FROM THE BOUNDARY CONDITIONS) ON THE SURFACE Σ . FOR THE IMPORTANT PRACTICAL CASE OF SMALL HARMONIC OSCILLATION AROUND A REST POSITION, THE EQUATION REDUCES TO A TWO-DIMENSIONAL FREDHOLM INTEGRAL EQUATION OF SECOND-TYPE. IT IS SHOWN THAT THIS EQUATION REDUCES PROPERLY TO THE LIFTING SURFACE THEORIES AS WELL AS OTHER CLASSICAL MATHEMATICAL FORMULAE. THE QUESTION OF UNIQUENESS IS EXAMINED AND IT IS SHOWN THAT, FOR THIN WINGS, THE OPERATOR BECOMES SINGULAR AS THE THICKNESS APPROACHES ZERO. THIS FACT MAY YIELD NUMERICAL PROBLEMS FOR VERY THIN WINGS. HOWEVER, NUMERICAL RESULTS OBTAINED FOR A RECTANGULAR WING IN SUBSONIC FLOW SHOW THAT THESE PROBLEMS DO NOT APPEAR EVEN FOR THICKNESS RATIO $\tau = .001$. COMPARISON WITH EXISTING RESULTS SHOWS THAT THE PROPOSED METHOD IS NOT ONLY MORE GENERAL AND FLEXIBLE, BUT ALSO AT LEAST AS FAST AND ACCURATE AS EXISTING ONES.			
17. Key Words (Suggested by Author(s)) POTENTIAL FLOW LIFTING SURFACE THEORY UNSTEADY FLOW AIRCRAFT AERODYNAMICS		18. Distribution Statement UNCLASSIFIED - UNLIMITED STAR CATEGORY: 01	
19. Security Classif. (of this report) UNCLASSIFIED	20. Security Classif. (of this page) UNCLASSIFIED	21. No. of Pages 204	22. Price* \$5.75

* For sale by the National Technical Information Service, Springfield, Virginia 22151

FOREWORD

This research, initially supported by a Boston University Grant-in-Aid Program, (Grants No. UG-112-ENG and UG-143-ENG), was completed under a NASA Grant No. 22-004-030. Dr. E. Carson Yates, Jr. of NASA acted as technical advisor. The author wishes to express his appreciation to his colleagues P. T. Hsu, D. G. Udelson and C. C. Kuo for the discussions and criticisms, as well as Mr. E. Chiuchiolo for his help on the numerical calculations and Miss B. Wright for her patience in editing and typing the report.

CONTENTS

<u>Section</u>	<u>Page</u>
1. INTRODUCTION	1
1.1 Definition of the Problem	1
1.2 Formulation of the Problem	3
1.3 Method of Solution	6
2. THE GREEN FUNCTION FOR SUBSONIC AND SUPERSONIC LINEAR UNSTEADY POTENTIAL FLOW	8
2.1 Introduction	8
2.2 Galilean Transformation	9
2.3 Subsonic Green's Function	14
2.4 The Supersonic Green Function	15
3. GENERALIZED HUYGENS' PRINCIPLE FOR THE NONLINEAR EQUATION OF THE UNSTEADY AERODYNAMIC POTENTIAL	18
3.1 Introduction	18
3.2 Green's Theorem for the Equation of Aerodynamic Potential	21
3.3 Generalized Subsonic Huygens' Principle	23
3.4 Steady Subsonic Flow	26
3.5 Generalized Supersonic Huygens' Principle	28
4. SIMPLIFIED FORMULATIONS	31
4.1 Introduction	31
4.2 Subsonic and Supersonic Small Perturbation Flow	32
4.3 Quasi-fixed Surface in Small-Perturbation Flow	36
4.4 Complex-Exponential Flow	37

CONTENTS CONTINUED

<u>Section</u>	<u>Page</u>
5. LIFTING SURFACE THEORIES	40
5.1 Introduction	40
5.2 Oscillating Wing in Subsonic Flow	40
6. NUMERICAL FORMULATION	46
6.1 Introduction	46
6.2 Integral Equation Formulation; Existence and Uniqueness of the Solution	47
6.3 The Wake	50
6.4 Numerical Solution of the Integral Equation	54
6.5 Limiting Behavior for Zero Thickness	57
6.6 Generalization to Unsteady Subsonic Flow	60
7. NUMERICAL RESULTS	66
7.1 Introduction	66
7.2 The Geometry of the Wing	66
7.3 The Numerical Procedure	68
7.4 Numerical Results	72
7.4.1 Thickness Effect	73
7.4.2 Convergence	76
7.5 Comparison with Existing Results	76
8. DISCUSSION	80
8.1 General Comments	80
8.2 Applicability of the Method	80
9. CONCLUDING REMARKS	84
REFERENCES	85

CONTENTS CONTINUED

<u>Section</u>	<u>Page</u>
FIGURES	87
 <u>APPENDICES</u>	
A TWO FUNDAMENTAL FORMULAE	106
B REDUCTION TO ELEMENTARY CASES	110
B.1 Huygens' Principle	110
B.2 Integral Representation of Solution of Poisson's Equation	112
B.3 Poisson's Formula	112
C THE VALUE OF THE FUNCTION E ON THE SURFACE	114
C.1 Introduction	114
C.2 Steady Incompressible Flow	116
C.3 Unsteady Compressible Subsonic Flow	121
C.3.1 Frame of Reference with $U_{\infty} = 0$	122
C.3.2 Frame of Reference with $U_{\infty} \neq 0$	129
D UNSTEADY WAKE AND LIFTING SURFACE THEORY KERNEL	136
D.1 Introduction	136
D.2 Unsteady Subsonic Wake	136
D.3 An Explicit Expression for \tilde{J}_W	139
D.4 The Kernel of the Lifting Surface Theory	146
D.5 Evaluation of the Integral \hat{F}	149

CONTENTS CONTINUED

<u>Section</u>	<u>Page</u>
E SOURCES AND DOUBLETS ON A TRAPEZOIDAL ELEMENT	154
E.1 Trapezoidal Element	154
E.2 Doublet Distribution	154
E.3 Source Distribution	161
F INITIAL CONDITIONS	165
G SMALL THICKNESS FORMULATION	167
G.1 Introduction	167
G.2 Leading and Trailing Edges	167
G.3 Vortex Layer	170
G.4 Alternative Formulation	170
H SUPERSONIC DOUBLET	173
H.1 Introduction	173
H.2 Modified Supersonic Doublet Integral	174
H.3 Supersonic Doublet Integral	178

LIST OF FIGURES

<u>Figure</u>		<u>Page</u>
Fig. 1	The supersonic flow pattern	87
Fig. 2	The hypersurface Σ	88
Fig. 3a	The surface Σ'	89
Fig. 3b	The surfaces Σ_B and Σ_W	89
Fig. 4	Solid angle Ω	90
Fig. 5	Treatment of the wake	91
Fig. 6	Boxes and control points	92
Fig. 7	Definition of opposite boxes	93
Fig. 8	Transformation $(\bar{x}, \bar{y}) \rightarrow (\bar{\xi}, \bar{\eta})$	94
Fig. 9	Geometry of the problem	95
Fig. 10	Transformation $(\bar{\xi}, \bar{\eta}) \rightarrow (\bar{X}, \bar{Y})$	96
Fig. 11	Potential Distribution for a rectangular wing with aspect ratio $b/c = 3$, angle of attack $\alpha = 5^\circ$ and Mach number $M = .24$	97
Fig. 12	Lift coefficient distribution for a rectangular wing with aspect ratio $b/c = 3$, angle of attack $\alpha = 5^\circ$ and Mach number $M = .24$	98
Fig. 13	Effect of decreasing thickness on the numerical scheme: Potential difference at the trailing edge boxes for $NX = NY = 4$ and different values of the thickness ratio, τ , for a rectangular wing with aspect ratio $b/c = 3$, angle of attack $\alpha = 5^\circ$ and Mach number $M = .24$	99

- Fig. 14 Effect of decreasing thickness on the numerical scheme: Potential difference at the root boxes for $NX = NY = 4$ and different values of the thickness ratio, τ , for a rectangular wing with aspect ratio $b/c = 3$, angle of attack $\alpha = 5^\circ$ and Mach number $M = .24$ 100
- Fig. 15 Effect of decreasing thickness on the numerical scheme: Lifting pressure coefficient at the root boxes for $NX = NY = 4$ and different values of the thickness ratio, τ , for a rectangular wing with aspect ratio $b/c = 3$, angle of attack $\alpha = 5^\circ$ and Mach number $M = .24$ 101
- Fig. 16 Potential difference at trailing edge boxes for thickness ratio $\tau = .001$ and different values of NX and NY for a rectangular wing with aspect ratio $b/c = 3$, angle of attack $\alpha = 5^\circ$ and Mach number $M = .24$ 102
- Fig. 17 Potential difference at the root boxes for thickness ratio $\tau = .001$ and different values of NX and NY for a rectangular wing with aspect ratio $b/c = 3$, angle of attack $\alpha = 5^\circ$ and Mach number $M = .24$ 103
- Fig. 18 Lifting pressure coefficient at root boxes for thickness ratio $\tau = .001$ and different values of NX and NY for a rectangular wing with aspect ratio $b/c = 3$, angle of attack $\alpha = 5^\circ$ and Mach number $M = .24$ 104

<u>Figure</u>	<u>Page</u>
Fig. 19 Comparison with existing results for a rectangular wing with aspect ratio $b/c = 3$, angle of attack $\alpha = 5^\circ$ and Mach number $M = .24$	105
Fig. C.1 The surface Σ in the neighborhood of P_*	134
Fig. C.2 The surface Σ^T in the neighborhood of P_*	135
Fig. D.1 The contour of integration	153
Fig. E.1 The projection of the trapezoidal element in the plane X_1, Y_1	164
Fig. G.1 Surfaces Σ and Σ'	172
Fig. H.1 Modified Supersonic Source	180
Fig. H.2 Surface $\Sigma_0 = \Sigma_1 + \Sigma_2 + \Sigma_3$	180

LIST OF SYMBOLS

a	speed of sound
a_{∞}	speed of sound in undisturbed air
a_{ki}	see Eq. 6.27
b	span of wing (Eq. 7.2)
b_k	see Eq. 6.21
$B = \sqrt{M^2 - 1}$	
c	chord of wing (Eq. 7.2)
\bar{c}	speed of surface of body at $P = P_*$ (Eq. C.25)
\bar{c}_0	see Eq. C.55
c_p	pressure coefficient (Eq. 1.18)
$c_l = -\Delta c_p = c_{p,l} - c_{p,u}$	lifting pressure coefficient (Eq. 7.21)
c_{ki}	see Eq. 6.22
\hat{c}_{ki}	see Eq. 7.9
d_m, d_p	see Eq. E.2
\vec{D}_0	see Eq. C.54
E	domain function (Eq. 3.1 and Eq. 3.33)
F	sum of nonlinear terms (Eq. 1.8)
f	"good function" (see Eq. A.1 and A.2)
f_n	see Eqs. D.53 and D.55
F_i	see Eq. 4.9
\hat{F}	see Eqs. D.34 and D.56
\hat{F}_n	see Eqs. D.41 and D.57
G	Green's function
h	thickness of wing (Eq. 7.1)

PRECEDING PAGE BLANK NOT FILMED

$H(\tau)$	Heaviside step function (Eq. 5.21)
\vec{H}	see Eq. C.31
\vec{H}_0	see Eq. C.54
$i = \sqrt{-1}$	
I_W	see Eq. 6.12
$I_n(\kappa)$	Modified Bessel function of first kind of order n
\tilde{I}_W	see Eq. D.2
\hat{I}_W	see Eq. D.4
\hat{I}	see Eq. D.20
\hat{I}_C	see Eq. D.22
\bar{I}_i	see Eq. D.24
\hat{I}_5	see Eq. D.28
\hat{I}_3	see Eq. D.29
\hat{I}_D	see Eq. E.3
\hat{I}_S	see Eq. E.27
\hat{I}_1	see Eq. E.19
\hat{I}_2	see Eq. E.30
\hat{I}	see Eq. E.23
I_\perp^e	see Eq. C.16
$J = \frac{\partial(x_1, y_1, z_1)}{\partial(\xi_1, \eta_1, \zeta_1)}$	Jacobian of transformation given by Eq. 2.26
J_W	see Eq. 6.13
\tilde{J}_W	see Eq. D.11
\hat{J}_W	see Eq. D.13
K	lifting surface Kernel function (see Eq. 5.18)

K_z	see Eq. 5.15
$K_n(\kappa)$	modified Bessel function of second kind of order n
\vec{k}	unit vector in direction z (see Eq. C.29)
\vec{k}_0	see Eq. C.54
\hat{k}	see Eq. D.46
L	Layer function (Eq. A.4)
$L_1(\kappa)$	Struve function (Eq. D.66)
$M = U_\infty / a_\infty$	Mach number for undisturbed flow
\vec{n}_1	normal to the surface Σ at P_1
$N = 2 \cdot NX \cdot NY$	(Eq. 7.17)
NX, NY	number of boxes in direction X, Y
p	pressure
p_∞	pressure in undisturbed air
\tilde{p}	see Eq. 5.7
\hat{p}	see Eq. 6.63
$P \equiv (X, Y, Z)$	control point
$P_1 \equiv (X_1, Y_1, Z_1)$	dummy point of integration on Σ
$P^{(k)}$	center of box Σ_k
P_*	control point on Σ (see Eq. C.1)
Q	see Eq. 2.12
Q_n	normal component of perturbation velocity (Eq. 1.13)
\tilde{Q}_n	see Eq. 4.1
\bar{Q}_n	see Eq. 4.6

\hat{Q}_n

see Eq. 6.49

$$r = [(x - x_1)^2 + (y - y_1)^2 + (z - z_1)^2]^{1/2}$$

$$r_\beta = \left\{ (x - x_1)^2 + \beta^2 [(y - y_1)^2 + (z - z_1)^2] \right\}^{1/2}$$

$$r_B = \left\{ (x - x_1)^2 - B^2 [(y - y_1)^2 + (z - z_1)^2] \right\}^{1/2}$$

$$\hat{r} = \left\{ (x - x_1)^2 + (1 - M^2) [(y - y_1)^2 + (z - z_1)^2] \right\}^{1/2}$$

$$r_\lambda = \left\{ \lambda^2 + \beta^2 [(y - y_1)^2 + (z - z_1)^2] \right\}^{1/2}$$

 $r_{\lambda,}$

see Eq. D.5

$$r_0 = [(x_0 - x_{01})^2 + (y_0 - y_{01})^2 + (z_0 - z_{01})^2]^{1/2}$$

 R

see Eq. C.8

$$s = \mu + i\omega$$

complex frequency (see Eq. 4.2)

 S function describing the hypersurface Σ S_B

function describing the hypersurface

$$\sum_B \text{ (Eq. 1.9)}$$

 S_W

function describing the hypersurface

$$\sum_W$$

 t time for x, y, z system

$$t_0 = a_\infty \beta t$$

 \hat{t}

see Eq. E.20

 T

subsonic time delay (Eq. 2.38)

 T^\pm

supersonic time delays (Eq. 2.48)

$$T_0 = a_\infty \beta T$$

see Eq. 6.43

 U_∞

velocity of undisturbed flow

 w_{ki}

see Eqs. 6.24 and 6.25

\hat{w}_{ki}	see Eq. 7.8
w_t	see Eq. 6.19
x, y, z	Cartesian coordinate system in which the undisturbed air travels at velocity U_∞ in positive x direction
x_0, y_0, z_0	Prandtl-Glauert cartesian coordinate (Eq. 3.35)
X, Y, Z	see Eq. 7.4 and 7.5
X, Y, Z, X_1, Y_1, Z_1	see Eqs. C.6 and C.7
\bar{X}, \bar{Y}	see Eq. 7.12
$\bar{X}_m^{(c)}, \bar{Y}_n^{(c)}$	see Eq. 7.14
$\bar{X}_m^{(M)}, \bar{Y}_n^{(M)}, \bar{X}_m^{(P)}, \bar{Y}_n^{(P)}$	see Eq. 7.16
\tilde{z}, \tilde{z}_1	see Eqs. C.34 and C.36
α	angle of attack (Eq. 7.5)
$\bar{\alpha}$	see Eqs. E.1 and E.5
$\beta = \sqrt{1 - M^2}$	
$\bar{\beta}$	see Eqs. E.1 and E.5
γ	specific heat coefficient ratio
$\Gamma = \bar{c}/a_\infty$	see Eq. C.39
Γ_0	see Eq. 2.16
$\delta(\tau)$	Dirac's delta function
$\bar{\delta}$	see Eq. E.6
$\delta_\tau = \delta(t_1 - t + \tau)$	see Eq. 3.21
$\delta_z = \frac{\partial E}{\partial n}$	see Eq. 3.6
δ_{ki}	Kronecker delta
δ_ϵ	see Eq. C.4

$\Delta\bar{X}, \Delta\bar{Y}$	see Eq. 7.13
ε	radius of circular surface element Σ_ε
$\bar{\varepsilon}$	see Eq. 4.4
$\hat{\varepsilon}$	see Eq. 4.18
ε'	see Eq. A.3
ε''	see Eq. A.12
$\hat{\eta}_p, \hat{\eta}_m$	see Eq. E.13
θ	see Eq. C.8
κ	see Eq. D.21
μ	real part of complex frequency s
\vec{v}	fourdimensional (space and time) normal to hypersurface Σ
ξ, η, ζ	Cartesian coordinate connected with undisturbed air
$\hat{\xi}, \hat{\eta}, \hat{\zeta}$	see Eq. E.9
$\bar{\xi}, \bar{\eta}$	see Eq. 7.2
$\hat{\xi}_p, \hat{\xi}_m$	see Eqs. E.14 and E.16
$\hat{\xi}_{op}, \hat{\xi}_{ip}, \hat{\xi}_{om}, \hat{\xi}_{im}$	see Eqs. E.15 and E.17
$\rho = [(\xi - \xi_1)^2 + (\eta - \eta_1)^2 + (\zeta - \zeta_1)^2]^{1/2}$	
$\hat{\rho} = (\hat{\xi}^2 + \hat{\eta}^2 + \hat{\zeta}^2)^{1/2}$	see Eq. E.12
ρ_∞	density of undisturbed air
Σ	surface surrounding body and wake
Σ_B	surface surrounding body
Σ_W	surface surrounding wake
Σ^T	subsonic deformed surface (defined by Eq. 3.31)

$\Sigma^{T\pm}$	supersonic deformed surfaces (defined by $S^{T\pm} = 0$)
$\Sigma^{(u)}$	portion of upper side of plane $z_1 = 0$ where $\Delta\varphi \neq 0$
Σ_w	surface of the wing
τ	time for ξ, η, ζ system
τ	thickness ratio (Eq. 7.3)
φ	perturbation aerodynamic potential (Eq. 1.4)
φ_k	value of φ at $P^{(k)}$
$\bar{\varphi}$	see Eq. 4.8
φ_s	see Eq. 4.24
φ_v	see Eq. 4.24
$\tilde{\varphi}$	see Eq. 4.25
$\hat{\varphi}$	see Eq. 6.50
φ_{lc}	initial conditions contribution (Eq. F.2)
ϕ	aerodynamic potential
ω	imaginary part of complex frequency s
Ω	solid angle (Eq. 6.8)
Ω_n	solid angle for strip Σ_n (see Eq. 6.9)

SPECIAL SYMBOLS

$\frac{D}{Dt} = \frac{\partial}{\partial t} + \nabla\phi \cdot \nabla$	total time derivative (Eq. 1.2)
--	---------------------------------

$\frac{d}{dt} = \frac{\partial}{\partial t} + U_{\infty} \frac{\partial}{\partial x}$	linearized total time derivative
∇	gradient operator
∇^2	Laplacian operator
\square	fourdimensional (space and time)
	gradient operator

$|\nabla, s^T|$ see Eq. 3.29

$|\nabla, s|^T$ see Eq. 3.30

$|\square, s|$ see Eq. 3.5

$\Delta() = ()$ upper - $()$ lower

$\left[\begin{array}{c} \end{array} \right]^{\rho/a_{\infty}} = \left[\begin{array}{c} \end{array} \right]_{\tau_1 = \tau - \rho/a_{\infty}} \quad (\text{Eq. 2.22})$

$\left[\begin{array}{c} \end{array} \right]^{\tau} = \left[\begin{array}{c} \end{array} \right]_{t_1 = t - \tau} \quad (\text{Eq. 3.27})$

$\left[\begin{array}{c} \end{array} \right]^{\tau_2} = \left[\begin{array}{c} \end{array} \right]_{t_1 = t - \tau_2} \quad (\text{Eq. 2.47})$

$\left[\begin{array}{c} \end{array} \right]^{\tau_0} = \left[\begin{array}{c} \end{array} \right]_{t_{01} = t_0 - \tau_0} \quad (\text{Eq. 6.42})$

$\left[\begin{array}{c} \end{array} \right]^+ = \left[\begin{array}{c} \end{array} \right]_{t_1 = t - r/a_{\infty}}$

SUBSCRIPTS

0	Prandtl-Glauert variables (Eq. 3.35 and 6.39)
1	Dummy variables
01	Dummy Prandtl-Glauert variables
TE	trailing edge
*	evaluation at $P = P_*$

SECTION 1

INTRODUCTION

1.1 Definition of the Problem

The evaluation of the aerodynamic pressure is an important tool for the design of aeronautical and space vehicles. Current methods do not satisfy the requirements of generality, flexibility and efficiency.* A general theory of potential aerodynamic flow around a lifting body having arbitrary shape and motion is presented here. The theory is based upon the classical Green theorem approach, and provides a tool for the evaluation of the aerodynamic pressure acting on the surface of the body. Comparison with existing results shows that the proposed method is not only more general and flexible, but also at least as fast and accurate as existing ones. The concept of the Green function is fundamental to the theory and therefore an ample discussion of this concept is given in Section 2, where the classical expressions for the subsonic and supersonic Green function are derived using a novel approach which, it is hoped, gives a clear physical interpretation for these expressions. A detailed outline of this report is given in Subsection 1.3. In the following, a short analysis of the method (lifting surface theory) currently used in the design of aircraft is presented.

*An excellent analysis of the state of the art is given by Ashley and Rodden.²⁵

The problem of the evaluation of the pressure acting on a surface of a body immersed in a fluid stream has always attracted the attention of the scientists. In particular, interest in the theory of unsteady potential aerodynamics, which is a basic tool in dynamic aeroelasticity, has been growing steadily in the last fifty years.^{1,2,3} Until recently, the attention of the researchers has been concentrated on lifting-surface theories in which the body is assumed to have zero thickness; the solution of the problem is reduced to an integral equation relating pressure and downwash or similar quantities. An excellent analysis of the recent literature in this field is given in Refs. 2 and 3.

Two major objections can be raised about the lifting-surface theories. First, the numerical solution of the problem is rather complicated. The difficulties are related to the complicated form of the kernel function and the numerical integration of improper integrals. An excellent analysis of the numerical problems which are encountered in the various lifting-surface formulations is given in Ref. 3. Attempts to circumvent these difficulties have been presented more recently,⁴ but the present situation can be considered still unsatisfactory.

The second objection is that the lifting-surface theory cannot be easily generalized to include more complicated geometries and motions. Geometries which need further exploration are for instance the effect of thickness of the wings, and the wing-body interference.²⁵ The results shown in Ref. 5 show that the lifting-surface theory is being used beyond the limit of its validity and that, in some cases, the results are still unsatisfactory. Similar is the situation for motions which do not fall into the categories of either harmonic oscillation or impulsive start.

An attempt to circumvent the present "impasse" situation is described in Ref. 6, where a three-dimensional body of arbitrary geometry which executes an arbitrary motion in an incompressible fluid is considered. The method has the advantage of satisfying the boundary conditions on the true location of the surface of the body. This is a considerable improvement with respect to the lifting surface theories since it does not involve the use of zero thickness. Thus, complicated geometries can be easily analyzed. Furthermore, the formulation is suitable for treating arbitrary motions. On the other hand, the formulation still involves a singular kernel, which implies the above-mentioned difficulty of evaluating the integrals in the principal sense. In addition, the method is limited to incompressible flow, since the Green theorem for the Laplace equation is used.

1.2. Formulation of the Problem

In the following, the isentropic inviscid flow of a perfect gas, initially irrotational, is considered. Under this hypothesis, the flow can be described by the velocity potential Φ . The equation of the unsteady aerodynamic potential, given by Garrick¹ is

$$a^2 \nabla^2 \Phi = \frac{D_c^2 \Phi}{Dt^2} \quad 1.1$$

where a is the speed of sound, ∇^2 is the Laplacian operator, and

$$\frac{D_c}{Dt} = \frac{\partial}{\partial t} + \nabla \Phi \cdot \nabla \quad 1.2$$

is the total time derivative (the subscript "c" reminds that $\nabla \Phi$ should be treated as a constant in order to obtain the second total time derivative). Consider a frame of reference such that the undisturbed flow has velocity U_∞ in the direction of the positive x-axis. Then the speed of sound is given by

$$a^2 = a_\infty^2 - (\gamma - 1) \left\{ \frac{\partial \Phi}{\partial t} + \frac{1}{2} \left[\left(\frac{\partial \Phi}{\partial x} \right)^2 + \left(\frac{\partial \Phi}{\partial y} \right)^2 + \left(\frac{\partial \Phi}{\partial z} \right)^2 - U_\infty^2 \right] \right\} \quad 1.3$$

Furthermore, it is convenient to introduce the perturbation potential ψ , such that

$$\Phi = U_\infty (x + \psi) \quad 1.4$$

Note that $\psi \equiv 0$ in the undisturbed flow. Combining Eqs. 1.1, 1.3 and 1.4 yields the equation for the perturbation potential

$$\begin{aligned}
a_{\omega}^2 \nabla^2 \varphi = & U_{\omega}^2 \left[(1 + \varphi_x)^2 \varphi_{xx} + \varphi_y^2 \varphi_{yy} + \varphi_z^2 \varphi_{zz} \right] + \varphi_{tt} \\
& + 2 U_{\omega}^2 \left[(1 + \varphi_x) \varphi_y \varphi_{xy} + (1 + \varphi_x) \varphi_z \varphi_{xz} + \varphi_y \varphi_z \varphi_{yz} \right] \\
& + 2 U_{\omega} \left[(1 + \varphi_x) \varphi_{xt} + \varphi_y \varphi_{yt} + \varphi_z \varphi_{zt} \right] \\
& + (\gamma - 1) U_{\omega} \left[\varphi_t + U_{\omega} \varphi_x + \frac{1}{2} U_{\omega} (\varphi_x^2 + \varphi_y^2 + \varphi_z^2) \right] \nabla^2 \varphi
\end{aligned} \tag{1.5}$$

For the sake of simplicity, it is convenient to separate the linear terms from the nonlinear ones; thus Eq. 1.5 is rewritten as

$$\begin{aligned}
& \nabla^2 \varphi - \frac{1}{a_{\omega}^2} \frac{d^2 \varphi}{dt^2} \\
& = F(\varphi_x, \varphi_y, \varphi_z, \varphi_{xx}, \varphi_{yy}, \varphi_{zz}, \varphi_{tt}, \varphi_{xy}, \varphi_{yz}, \varphi_{xz}, \varphi_{xt}, \varphi_{yt}, \varphi_{zt})
\end{aligned} \tag{1.6}$$

where

$$\frac{d}{dt} = \frac{\partial}{\partial t} + U_{\omega} \frac{\partial}{\partial x} \tag{1.7}$$

is the linearized total time derivative and the nonlinear terms are given by

$$\begin{aligned}
F = & \frac{U_{\omega}^2}{a_{\omega}^2} \left\{ (2\varphi_x + \varphi_x^2) \varphi_{xx} + \varphi_y^2 \varphi_{yy} + \varphi_z^2 \varphi_{zz} \right. \\
& + 2 \left[(1 + \varphi_x) \varphi_y \varphi_{xy} + (1 + \varphi_x) \varphi_z \varphi_{xz} + \varphi_y \varphi_z \varphi_{yz} \right. \\
& + \left. \frac{1}{U_{\omega}} (\varphi_x \varphi_{xt} + \varphi_y \varphi_{yt} + \varphi_z \varphi_{zt}) \right] \\
& + (\gamma - 1) \left[\frac{1}{U_{\omega}} \varphi_t + \varphi_x + \frac{1}{2} (\varphi_x^2 + \varphi_y^2 + \varphi_z^2) \right] \nabla^2 \varphi \left. \right\}
\end{aligned} \tag{1.8}$$

This is the equation for the unsteady potential compressible (subsonic or supersonic) aerodynamic flow.

A very general approach is considered here by assuming that the body immersed in this flow has arbitrary shape and is moving with arbitrary motion. Thus, the surface of the body is represented in the general form

$$S_B(x, y, z, t) = 0 \quad 1.9$$

where the subscript B stands for Body. The boundary condition on the body is given by

$$\frac{DS_B}{Dt} = 0 \quad 1.10$$

or

$$\frac{\partial S_B}{\partial t} + \nabla \phi \cdot \nabla S_B = 0 \quad 1.11$$

By using Eq. 1.4, Eq. 1.11 yields

$$\nabla \phi \cdot \nabla S_B = - \frac{1}{U_\infty} \left(\frac{\partial S_B}{\partial t} + U_\infty \frac{\partial S_B}{\partial x} \right) \quad 1.12$$

or

$$\frac{\partial \phi}{\partial n} = Q_n \quad 1.13$$

with

$$Q_n = - \frac{1}{U_\infty} \frac{1}{|\nabla S_B|} \frac{dS_B}{dt} \quad 1.14$$

Furthermore, as mentioned above, the boundary condition at infinity is given by

$$\phi = 0 \quad 1.15$$

Finally, the pressure can be evaluated from the Bernoulli

Theorem

$$\frac{p}{p_\infty} = \left[1 - \frac{\gamma-1}{a_\infty^2} \left(\frac{\partial \phi}{\partial t} + \frac{1}{2} \nabla \phi \cdot \nabla \phi - \frac{1}{2} U_\infty^2 \right) \right]^{\frac{\gamma}{\gamma-1}} \quad 1.16$$

or the linearized Bernoulli Theorem

$$p - p_\infty = - \rho_\infty U_\infty \left(\frac{\partial \phi}{\partial t} + U_\infty \frac{\partial \phi}{\partial x} \right) \quad 1.17$$

which yields, for the pressure coefficient

$$C_p = \frac{p - p_\infty}{\frac{1}{2} \rho_\infty U_\infty^2} = -2 \left(\frac{1}{U_\infty} \frac{\partial \phi}{\partial t} + \frac{\partial \phi}{\partial x} \right) = -2 \frac{d\phi}{dt} \quad 1.18$$

Note that no assumption was made on the Mach number

$$M = \frac{U_\infty}{a_\infty} \quad 1.19$$

Thus, the above equations are valid for both subsonic and supersonic flow.

1.3. Method of Solution

The method of solution presented here is based upon the well known Green function technique. The Green functions for the linear unsteady subsonic and supersonic flow are derived in Section 2, and used in Section 3 to derive an integral representation of the potential ϕ at any point in the field (control point) in terms of the values of ϕ and $\partial \phi / \partial n$ on a surface surrounding the body and the wake. In Section 4, it is shown that the integral representation

can be simplified under the assumption of small perturbation; and even further simplified for small vibration around a configuration fixed with respect to the frame of reference. Next, in Section 5, it is shown how lifting surface theories can be obtained as limiting cases of the formulation presented here.

Finally, in Section 6, the problem of small vibration around a fixed configuration in subsonic flow is analyzed in detail. It is shown (Appendix C), that if the control point is on the surface of the body, the problem reduces to an integral equation. The question of existence and uniqueness is also discussed in Section 6 and, in particular, it is shown that, for a zero-thickness flat wing, the integral equation operator becomes singular.

Hence, in order to verify the limit of applicability for low values of the thickness ratio, the steady subsonic flow around very thin wings is solved numerically. The results are presented in Section 7, whereas the conclusions are discussed in Section 8.

SECTION 2.

THE GREEN FUNCTION FOR SUBSONIC AND SUPERSONIC LINEAR UNSTEADY POTENTIAL FLOW

2.1. Introduction

The Green function for the linear unsteady potential flow for the whole space (which represents a unit-impulsive-source) is the solution of the problem

$$\nabla^2 G - \frac{1}{a_\infty^2} \frac{d^2 G}{dt^2} = \delta(x-x_1, y-y_1, z-z_1, t-t_1) \quad 2.1$$

with

$$G = 0 \quad \text{at infinity} \quad 2.2$$

In Eq. 2.1, δ is the well known Dirac delta function defined by

$$\iiint_{-\infty}^{\infty} F \delta \, dV \, dt_1 = \iiint_{-\infty}^{\infty} F(x, y, z, t_1) \delta(x-x_1, y-y_1, z-z_1, t-t_1) \, dx \, dy \, dz \, dt_1 = F(x, y, z, t) \quad 2.3$$

The solution of Eq. 2.1 for the subsonic case (subsonic Green's function) is given by

$$G = - \frac{1}{4\pi r_\beta} \delta(t_1 - t + T) \quad 2.4$$

where $\delta(t_1 - t + T)$ is the usual Dirac delta function and

$$r_\beta = \left\{ (x-x_1)^2 + \beta^2 [(y-y_1)^2 + (z-z_1)^2] \right\}^{\frac{1}{2}} \quad 2.5$$

and

$$T = \frac{1}{a_\infty \beta^2} \left[r_\beta - M(x-x_1) \right] \quad 2.6$$

where

$$\beta = \sqrt{1 - M^2} \quad 2.7$$

Although this result is well known,^{8,9} for the sake of completeness, Eq. 2.4 is derived here (Subsection 2.3) using a particularly instructive procedure.

Similarly, the supersonic Green function is given by^{9,10}

$$G = -\frac{1}{4\pi r_B} \left[\delta(t_1 - t + T^-) + \delta(t_1 - t + T^+) \right] \quad 2.8$$

with

$$r_B = \left\{ (x - x_1)^2 - B^2 \left[(y - y_1)^2 + (z - z_1)^2 \right] \right\}^{\frac{1}{2}} \quad 2.9$$

and

$$T^\pm = \frac{1}{a_\infty B^2} \left[M(x - x_1) \pm r_B \right] \quad 2.10$$

where

$$B = \sqrt{M^2 - 1} \quad 2.11$$

Equation 2.8 is derived in Subsection 2.4.

2.2. Galilean Transformation

In order to obtain the Green function of the linear unsteady potential flow, it is convenient to use a Galilean transformation, such that the new frame of reference is rigidly connected to the undisturbed flow. Then the differential equation reduces to the well known wave equation for which the Green function is well known. Then, by using

the inverse transformation, the Green function for the unsteady linear potential flow is derived.

In order to avoid transformation of generalized functions (distributions) it is convenient to consider the nonhomogeneous equation of the linear unsteady potential *

$$\nabla^2 \varphi - \frac{1}{a_\infty^2} \left(\frac{\partial}{\partial t} + U_\infty \frac{\partial}{\partial x} \right)^2 \varphi = Q(x, y, z, t) \quad 2.12$$

This equation reduces to the nonhomogeneous wave equation for a coordinate system ξ, η, ζ, τ rigidly connected to the undisturbed flow. The Galilean transformation relating the two systems is given by

$$x = \xi + U_\infty \tau \quad y = \eta \quad z = \zeta \quad t = \tau \quad 2.13$$

whose inverse is given by

$$\xi = x - U_\infty t \quad \eta = y \quad \zeta = z \quad \tau = t \quad 2.14$$

Since

$$\frac{\partial}{\partial \xi} = \frac{\partial}{\partial x} \quad \frac{\partial}{\partial \eta} = \frac{\partial}{\partial y} \quad \frac{\partial}{\partial \zeta} = \frac{\partial}{\partial z} \quad \frac{\partial}{\partial \tau} = \frac{\partial}{\partial t} + U_\infty \frac{\partial}{\partial x} \quad 2.15$$

Equation 2.12, in the new frame of reference, reduces to

$$\frac{\partial^2 \varphi}{\partial \xi^2} + \frac{\partial^2 \varphi}{\partial \eta^2} + \frac{\partial^2 \varphi}{\partial \zeta^2} - \frac{1}{a_\infty^2} \frac{\partial^2 \varphi}{\partial \tau^2} = \Gamma_0(\xi, \eta, \zeta, \tau) \quad 2.16$$

with

$$\Gamma_0(\xi, \eta, \zeta, \tau) = Q(\xi + U_\infty \tau, \eta, \zeta, \tau) \quad 2.17$$

* Note that Q is a fictitious prescribed source distribution, while F in Eq. 1.6 depends on the unknown itself.

The solution of Eq. 2.16 is given by¹¹

$$\varphi(\xi, \eta, \zeta, \tau) = -\frac{1}{4\pi} \iiint_{-\infty}^{\infty} \frac{1}{\rho} [\Gamma_0]^{p/a_w} d\xi_1 d\eta_1 d\zeta_1 \quad 2.18$$

where

$$\rho = \left[(\xi - \xi_1)^2 + (\eta - \eta_1)^2 + (\zeta - \zeta_1)^2 \right]^{\frac{1}{2}} \quad 2.19$$

and

$$[\Gamma_0]^{p/a_w} = \Gamma_0(\xi_1, \eta_1, \zeta_1, \tau_1) \quad 2.20$$

with

$$\tau_1 = \tau - \rho/a_w \quad 2.21$$

or

$$[\Gamma_0]^{p/a_w} = \Gamma_0 \Big|_{\tau_1 = \tau - \rho/a_w} \quad 2.22$$

Equation 2.18 is equivalent to saying that the Green function for the wave equation in the space is¹¹

$$G_w = \frac{-1}{4\pi\rho} \delta(\tau, -\tau + \rho/a_w) \quad 2.23$$

Finally, in order to obtain the solution of Eq. 2.12, it is sufficient to express Eq. 2.18 in terms of the original variables x, y, z and t . It should be noted however, that the inverse transformation is not given by Eq. 2.14, since, according to Eq. 2.21, one has

$$\tau - \tau_1 = \rho / a_\infty \quad 2.24$$

Thus, the inverse of the transformation

$$x - x_1 = \xi - \xi_1 + U_\infty (\tau - \tau_1) = \xi - \xi_1 + M \rho \quad 2.25a$$

$$y - y_1 = \eta - \eta_1 \quad 2.25b$$

$$z - z_1 = \zeta - \zeta_1 \quad 2.25c$$

$$t - t_1 = \tau - \tau_1 = \rho / a_\infty \quad 2.25d$$

has to be considered. The inverse is given by (*)

$$\xi - \xi_1 = \frac{1}{1 - M^2} (x - x_1 \pm M \hat{r}) \quad 2.26a$$

$$\eta - \eta_1 = y - y_1 \quad 2.26b$$

$$\zeta - \zeta_1 = z - z_1 \quad 2.26c$$

$$\tau - \tau_1 = \rho / a_\infty = \frac{1}{a_\infty} \left| \frac{1}{1 - M^2} [\hat{r} \pm M(x - x_1)] \right| \quad 2.26d$$

(*) Equation 2.25a yields

$$[(x - x_1) - (\xi - \xi_1)]^2 = M^2 \rho^2 = M^2 [(\xi - \xi_1)^2 + (\eta - \eta_1)^2 + (\zeta - \zeta_1)^2]$$

By solving for $\xi - \xi_1$, one obtains

$$\xi - \xi_1 = \frac{1}{1 - M^2} (x - x_1) \pm M \hat{r}$$

that is, Eq. 2.26a. Combining this equation with Eq. 2.19, yields, in agreement with Eq. 2.26d

$$\begin{aligned} \rho^2 &= \frac{1}{(1 - M^2)^2} \left[(x - x_1)^2 \pm 2M \hat{r} (x - x_1) + M^2 \hat{r}^2 \right] + (y - y_1)^2 + (z - z_1)^2 \\ &= \frac{1}{(1 - M^2)^2} [M(x - x_1) \pm \hat{r}]^2 \end{aligned}$$

with

$$\hat{r} = \left\{ (x-x_1)^2 + (1-M^2) \left[(y-y_1)^2 + (z-z_1)^2 \right] \right\}^{\frac{1}{2}} \quad 2.27$$

The interpretation of the double sign which appears in Eq. 2.26a is discussed later in this section. For clarity, it is convenient to consider the subsonic case and the supersonic one independently (Subsections 2.3 and 2.4, respectively).

Note that, in either case*

$$\hat{r} = \left| M(\xi-\xi_1) + \rho \right| \quad 2.28$$

and that the Jacobian of the transformation is given by

$$J = \frac{\partial(x, y, z)}{\partial(\xi, \eta, \zeta)} = \text{Det} \begin{bmatrix} 1 + M \frac{\xi-\xi_1}{\rho} & M \frac{\eta-\eta_1}{\rho} & M \frac{\zeta-\zeta_1}{\rho} \\ 0 & 1 & 0 \\ 0 & 0 & 1 \end{bmatrix} = \frac{\rho + M(\xi-\xi_1)}{\rho} \quad 2.29$$

which shows that

$$|J| = \frac{\hat{r}}{\rho} \quad 2.30$$

*By combining Eqs. 2.25 and 2.27 yields

$$\begin{aligned} \hat{r}^2 &= (x-x_1)^2 + (1-M^2) (y-y_1)^2 + (z-z_1)^2 \\ &= (\xi-\xi_1)^2 + 2 M \rho (\xi-\xi_1) + M^2 \rho^2 + (1-M^2) [(\eta-\eta_1)^2 + (\zeta-\zeta_1)^2] \\ &= (\xi-\xi_1)^2 + 2 M \rho (\xi-\xi_1) + M^2 (\xi-\xi_1)^2 + (\eta-\eta_1)^2 + (\zeta-\zeta_1)^2 \\ &= [M (\xi-\xi_1) + \rho]^2 \end{aligned}$$

2.3. Subsonic Green's Function

Consider the subsonic case. For $M < 1$, one has $\hat{r} = r_\beta$ and

$$M |x - x_1| < r_\beta \quad 2.31$$

Thus, Eq. 2.26d, by eliminating the absolute-value sign, may be rewritten as

$$\rho = \frac{1}{\beta^2} [\pm M(x - x_1) + r_\beta] \quad 2.32$$

By substituting this equation and Eq. 2.26a into Eq. 2.25a, one obtains

$$x - x_1 = \frac{1}{\beta^2} (x - x_1 \pm M r_\beta) + M \frac{1}{\beta^2} [\pm M(x - x_1) + r_\beta] \quad 2.33$$

which is satisfied only if the lower sign is used.

Thus, by using the lower sign, the inverse transformation for the subsonic case is given by

$$\begin{aligned} \xi - \xi_1 &= \frac{1}{\beta^2} [(x - x_1) - M r_\beta] \\ \eta - \eta_1 &= y - y_1 \\ \zeta - \zeta_1 &= z - z_1 \\ \tau - \tau_1 &= \rho / a_\infty = \frac{1}{a_\infty \beta^2} [r_\beta - M(x - x_1)] \end{aligned} \quad 2.34$$

with

$$r_\beta = \rho + M(\xi - \xi_1) \quad 2.35$$

This transformation may be used in order to express Eq. 2.18 in the frame of reference (x, y, z, t) . This yields

$$\varphi(x, y, z, t) = \iiint \frac{-1}{4\pi\rho} \tau_0 \Big|_{\tau_1 = \tau - \rho/a_\infty} d\xi_1 d\eta_1 d\zeta_1$$

$$\begin{aligned}
&= \iiint \frac{1}{4\pi\rho} Q \Big|_{t_1 = t - \rho/a_\infty} \Big| J \Big|^{-1} dx, dy, dz, \\
&= \iiint \frac{1}{4\pi r_\beta} [Q]^T dx, dy, dz,
\end{aligned} \tag{2.36}$$

where

$$[Q]^T = Q \Big|_{t_1 = t - T} = Q(x, y, z, t - T) \tag{2.37}$$

with

$$T = \frac{1}{a_\infty \beta^2} [r_\beta - M(x - x_1)] \tag{2.38}$$

Equation 2.36 shows that the Green function for subsonic case is

$$G = -\frac{1}{4\pi r_\beta} \delta(t_1 - t + T) \tag{2.39}$$

as shown in Eq. 2.4.

2.4. The Supersonic Green Function

Consider the supersonic case. For $M > 1$, Eq. 2.25a yields

$$x - x_1 > 0 \tag{2.40}$$

which shows the well known property of supersonic flow that any point can influence only the points downstream.

Equation 2.40 implies

$$M(x - x_1) > r_\beta \tag{2.41}$$

Thus, Eq. 2.26d may be rewritten as

$$\rho = \frac{1}{B^2} [M(x - x_1) \pm r_\beta] \tag{2.42}$$

Note that $B^2 = M^2 - 1 > 0$. Finally, combining Eq. 2.25a, and 2.42 yields

$$x - x_1 = - \frac{1}{B^2} (x - x_1 \pm M r_B) + \frac{M}{B^2} [M(x - x_1) \pm r_B] \quad 2.43$$

which is satisfied by both signs.

The interpretation of this double sign lies in the well known fact that a disturbance A, (Fig. 1) traveling at supersonic speed, influences a given point B two times. The first by "backward-traveling waves" coming from position A^+ , and the second by "forward-traveling waves" coming from position A^- . In other words, the supersonic inverse transformation is not a one-to-one but a one-to-two transformation. Thus, for supersonic case, the inverse transformation is given by

$$\begin{aligned} \xi - \xi_1 &= - \frac{1}{B^2} (x - x_1 \pm M r_B) \\ \eta - \eta_1 &= y - y_1 \\ \zeta - \zeta_1 &= z - z_1 \\ \tau - \tau_1 &= \rho / a_\infty = \frac{1}{a_\infty B^2} [M(x - x_1) \pm r_B] \end{aligned} \quad 2.44$$

with

$$r_B = \pm [\rho + M(\xi - \xi_1)] \quad 2.45$$

This transformation may now be used in order to express Eq. 2.18 in the frame of reference (x, y, z, t) . This yields, in analogy to the subsonic case,

$$\varphi(x, y, z, t) = \iiint_V \frac{-1}{4\pi r_B} \left([Q]^{T_+} + [Q]^{T_-} \right) dx, dy, dz, \quad 2.46.$$

where

$$[Q]^{T_{\pm}} = Q \Big|_{t_1 = t - T_{\pm}} \quad 2.47$$

with

$$T_{\pm} = \frac{1}{a_{\infty} B^2} \left[M(x - x_1) \pm r_B \right] \quad 2.48$$

Equation 2.46 shows that the supersonic Green function is given by

$$G = \frac{-1}{4\pi r_B} \left[\delta(t_1 - t + T_+) + \delta(t_1 - t + T_-) \right] \quad 2.49$$

in agreement to Eq. 2.8.

SECTION 3

GENERALIZED HUYGENS' PRINCIPLE FOR THE NONLINEAR EQUATION OF THE UNSTEADY AERODYNAMIC POTENTIAL

3.1. Introduction

As mentioned in the introduction, the purpose of this analysis is to obtain a representation of the potential in terms of its values (and the values of its derivatives) on the surface of the body and the wake. A representation of this type for the wave equation is called Huygens' Principle¹¹ (or Kirchhoff's formula). The corresponding formula for the unsteady compressible (subsonic or supersonic) aerodynamic potential will be called Generalized Huygens' Principle.

In order to obtain this principle, it is convenient to follow a procedure similar to the one used in Ref. 11 to derive the Huygens' Principle. There are two major differences between the two problems. The first is that Eq. 1.6 is more complicated than the wave equation examined in Ref. 11. The second is that the surface is assumed to be changing in time. This assumption is necessary if enough generality is desired, in order to include arbitrary motions, like the roll for instance. In order to simplify the generalization of the procedure used in Ref. 11, it is convenient to make use of the theory of distributions developed by Schwartz.⁷

In order to do this, it is convenient to introduce a few basic definitions.

Note first that the equation of the aerodynamic potential given by Eq. 1.6, is not valid on the wake, where discontinuities on φ exist. Thus, consider the volume V in which Eq. 1.6 is valid. At any instant of time, this volume is given by the whole physical space except the volume, V_B , occupied by the body and an infinitesimally thin layer, V_W , representing the wake. Define the function E (see Fig. 2)

$$\begin{aligned} E(x,y,z,t) &= 1 && \text{on } V \\ &= 0 && \text{otherwise} \end{aligned} \quad 3.1$$

This function represents the domain of validity of the equation of the potential and will be called "domain function". Consider the surface of discontinuity of the function E , that is the surface, Σ , surrounding the volume $V_B + V_W$. Let

$$S(x, y, z, t) = 0 \quad 3.2$$

be the equation of the surface Σ .

Note that the surface Σ is composed of two branches. The first, Σ_B , is the surface of the body given by Eq. 1.9. The second is the surface, Σ_W , of the wake

$$S_W(x, y, z, t) = 0 \quad 3.3$$

Note that this surface Σ_W is considered twice, since Σ is a closed surface. In other words, the upper side and the lower side of the wake are considered to be two independent surfaces having the same equation (but opposite outwardly-directed normal).

Finally, for later convenience, the four-dimensional gradient of the function E is introduced. Consider first the four-dimensional outwardly-directed* normal to the surface Σ defined by

$$\vec{\nu} = \frac{\square S}{|\square S|} = \frac{1}{|\square S|} \begin{pmatrix} \partial S / \partial x \\ \partial S / \partial y \\ \partial S / \partial z \\ \partial S / \partial t \end{pmatrix} \quad 3.4$$

with

$$|\square S| = \left[\left(\frac{\partial S}{\partial x} \right)^2 + \left(\frac{\partial S}{\partial y} \right)^2 + \left(\frac{\partial S}{\partial z} \right)^2 + \left(\frac{\partial S}{\partial t} \right)^2 \right]^{\frac{1}{2}} \quad 3.5$$

It should be noted that, in writing Eq. 3.4, it has been assumed implicitly that the vector $\square S$ is equidirected with the four dimensional normal $\vec{\nu}$. This condition can always be satisfied (by a suitable change of sign in Eq. 1 if necessary).

Next, note that along the direction of the normal $\vec{\nu}$, the function E behaves as a step-function. Thus its directional derivative in the direction of the normal $\vec{\nu}$ is a Dirac delta function on the surface Σ , which will be indicated with the symbol δ_{Σ}

$$\delta_{\Sigma} = \frac{\partial E}{\partial n} \quad 3.6$$

It may be worth noting that the integrals of δ_{Σ} are equivalent to hypersurface integrals (the surface Σ is on the four dimensional space),

*"Outwardly" is understood as "going from the body into the fluid", that is, from the region $E = 0$ into the region $E = 1$ (see Fig. 1)

$$\iiint F \delta_{\Sigma} dx, dy, dz, dt, = \oint F d\Sigma \quad 3.7$$

By using Eq. 3.6, the four-dimensional gradient of the function E can be written immediately, since Eq. 3.6 is equivalent to

$$\square E = \frac{\partial E}{\partial n} \vec{n} = \delta_{\Sigma} \frac{\partial S}{|\partial S|} \quad 3.8$$

where Eq. 3.4 has also been used.

By separating the spatial components from the time component, Eq. 3.8 yields

$$\begin{aligned} \nabla E &= \delta_{\Sigma} \nabla S \frac{1}{|\partial S|} \\ \frac{\partial E}{\partial t} &= \delta_{\Sigma} \frac{\partial S}{\partial t} \frac{1}{|\partial S|} \end{aligned} \quad 3.9$$

Note that

$$\frac{dE}{dt} = \frac{\partial E}{\partial t} + U_{\infty} \frac{\partial E}{\partial x} = \delta_{\Sigma} \frac{dS}{dt} \frac{1}{|\partial S|} \quad 3.10$$

3.2. Green's Theorem for the Equation of Aerodynamic Potential

In order to obtain the generalized Huygens' principle, it is convenient to follow the general method that leads to the Green theorem. Multiply the equation of the aerodynamic potential (in the form given by Eq. 1.6) by the Green function G and subtract Eq. 2.1 (definition of the Green formula) multiplied by φ :

$$G \left(\nabla^2 \varphi - \frac{1}{a_{\infty}^2} \frac{d^2 \varphi}{dt^2} \right) - \varphi \left(\nabla^2 G - \frac{1}{a_{\infty}^2} \frac{d^2 G}{dt^2} \right) = GF - \varphi \delta(x-x_1, y-y_1, z-z_1, t-t_1) \quad 3.11$$

where the arguments of φ and its derivatives are x_1, y_1, z_1 and t_1 , while the arguments of G and its derivatives are $x_1 - x, y_1 - y, z_1 - z$, and $t_1 - t$.

Making use of the identities

$$\nabla_i \cdot (a \nabla_i b) = \nabla_i a \cdot \nabla_i b + a \nabla_i^2 b \quad 3.12$$

and

$$\frac{d}{dt_i} \left(a \frac{db}{dt_i} \right) = \frac{da}{dt_i} \frac{db}{dt_i} + a \frac{d^2 b}{dt_i^2} \quad 3.13$$

Equation 3.11 reduces to

$$\nabla_i \cdot (G \nabla_i \varphi - \varphi \nabla_i G) - \frac{1}{a^2} \frac{d}{dt_i} \left(G \frac{d\varphi}{dt_i} - \varphi \frac{dG}{dt_i} \right) = GF - \varphi \delta \quad 3.14$$

Multiplying Eq. 3.14 by the domain function E, defined by Eq. 3.1, and integrating over the whole four-dimensional space yields

$$\begin{aligned} \iiint_{-\infty}^{\infty} E \left[\nabla_i \cdot (G \nabla_i \varphi - \varphi \nabla_i G) - \frac{1}{a^2} \frac{d}{dt_i} \left(G \frac{d\varphi}{dt_i} - \varphi \frac{dG}{dt_i} \right) \right] dV_i dt_i \\ = \iiint_{-\infty}^{\infty} E (GF - \varphi \delta) dV_i dt_i, \end{aligned} \quad 3.15$$

where the subscript 1 indicates the dummy variable of integration, and

$$\frac{d}{dt_i} = \frac{\partial}{\partial t_i} + U \frac{\partial}{\partial x_i} \quad 3.16$$

By suitable integrations by parts, Eq. 3.15 yields

$$\begin{aligned} - \iiint_{-\infty}^{\infty} \left[\nabla_i E \cdot (G \nabla_i \varphi - \varphi \nabla_i G) - \frac{1}{a^2} \frac{dE}{dt_i} \left(G \frac{d\varphi}{dt_i} - \varphi \frac{dG}{dt_i} \right) \right] dV_i dt_i \\ = \iiint_{-\infty}^{\infty} E (GF - \varphi \delta) dV_i dt_i, \end{aligned} \quad 3.17$$

or, by using Eqs. 3.9 and 3.10

$$\begin{aligned}
 & - \iiint_{-\infty}^{\infty} \left[\nabla_i S \cdot (G \nabla_i \varphi - \varphi \nabla_i G) - \frac{1}{a^2} \frac{dS}{dt_i} \left(G \frac{d\varphi}{dt_i} - \varphi \frac{dG}{dt_i} \right) \right] \delta_{\Sigma} |\nabla S|^{-1} dV, dt_i \\
 & = \iiint_{-\infty}^{\infty} E (GF - \varphi \delta) dV, dt_i,
 \end{aligned} \tag{3.18}$$

which is the Green theorem for the equation of the aerodynamic (subsonic and supersonic) potential. Note the presence of the factor δ_{Σ} which shows that the integral on the left hand side of Eq. 3.17 is a surface integral, as it is indicated by Eq. 3.7.

Finally, making use of the definition of the Dirac delta function (Eq. 2.3) yields

$$\begin{aligned}
 E\varphi &= \iiint_{-\infty}^{\infty} EGF dV, dt_i \\
 &+ \iiint_{-\infty}^{\infty} \left[\nabla_i S \cdot (G \nabla_i \varphi - \varphi \nabla_i G) - \frac{1}{a^2} \frac{dS}{dt_i} \left(G \frac{d\varphi}{dt_i} - \varphi \frac{dG}{dt_i} \right) \right] \delta_{\Sigma} |\nabla S|^{-1} dV, dt_i,
 \end{aligned} \tag{3.19}$$

3.3. Generalized Subsonic Huygens' Principle

In this subsection, Eq. 3.19 is specialized to the subsonic case for which the Green function is given by Eq. 2.4, which may be rewritten as

$$G = -\frac{1}{4\pi r_p} \delta_T \tag{3.20}$$

with

$$\delta_T = \delta(t_i - t + T) \tag{3.21}$$

where T is given by Eq. 2.38. Note that

$$\nabla_i \delta_T = \frac{\partial \delta_T}{\partial t_i} \nabla_i T \tag{3.22}$$

and

$$\frac{d\delta_T}{dt_1} = \left(\frac{\partial}{\partial t_1} + U_\omega \frac{\partial}{\partial x_1} \right) \delta_T = \frac{\partial \delta_T}{\partial t_1} \left(1 + U_\omega \frac{\partial T}{\partial x_1} \right) \quad 3.23$$

Combining Eqs. 3.19 to 3.23 yields

$$\begin{aligned} 4\pi E \varphi = & - \iiint_{-\infty}^{\infty} E \frac{1}{r_\rho} \delta_T F dV_1 dt_1 \\ & - \iiint_{-\infty}^{\infty} \left[\nabla_1 S \cdot \nabla_1 \varphi - \frac{1}{a_z^2} \frac{dS}{dt_1} \frac{d\varphi}{dt_1} \right] \frac{1}{r_\rho} \delta_z \delta_T |\Box S|^{-1} dV_1 dt_1 \\ & + \iiint_{-\infty}^{\infty} \left[\nabla_1 S \cdot \nabla_1 \left(\frac{1}{r_\rho} \right) - \frac{1}{a_z^2} \frac{dS}{dt_1} \frac{d}{dt_1} \left(\frac{1}{r_\rho} \right) \right] \varphi \delta_z \delta_T |\Box S|^{-1} dV_1 dt_1 \\ & + \iiint_{-\infty}^{\infty} \left[\nabla_1 S \cdot \nabla_1 T - \frac{1}{a_z^2} \frac{dS}{dt_1} \left(1 + U_\omega \frac{\partial T}{\partial x_1} \right) \right] \varphi \frac{1}{r_\rho} \delta_z \frac{\partial \delta_T}{\partial t_1} |\Box S|^{-1} dV_1 dt_1 \end{aligned} \quad 3.24$$

Note that the integrands of the integrals on the right hand side contain products of distributions (either $\delta_z \delta_T$ or $\delta_z \partial \delta_T / \partial t_1$). For the sake of convenience, integrals of this type are discussed in Appendix A where it is shown that, for any "regular" function f ,

$$\iiint_{-\infty}^{\infty} f \delta_z \delta_T |\Box S|^{-1} dV_1 dt_1 = \oint_{\Sigma^T} [f]^T |\nabla S^T|^{-1} d\Sigma^T \quad 3.25$$

and

$$\iiint_{-\infty}^{\infty} f \delta_z \frac{\partial \delta_T}{\partial t_1} |\Box S|^{-1} dV_1 dt_1 = - \frac{\partial}{\partial t} \oint_{\Sigma^T} [f]^T |\nabla S^T|^{-1} d\Sigma^T \quad 3.26$$

In Eqs. 3.25 and 3.26, the symbol $[\quad]^T$ indicates evaluation at time $t_1 = t - T$,

$$\left[\quad \right]^T = \left[\quad \right] \Big|_{t_1 = t - T} \quad 3.27$$

with T given by Eq. 2.6. In particular

$$\begin{aligned} S^T &= S(x_1, y_1, z_1, t - T) \\ &= S\left(x_1, y_1, z_1, t - \frac{1}{a_\infty \beta^2} [r - M(x - x_1)]\right) \end{aligned} \quad 3.28$$

Note the difference between $|\nabla_1 S^T|$ and $|\nabla_1 S|^T$:

$$\begin{aligned} |\nabla_1 S^T| &= |\nabla_1 S(x_1, y_1, z_1, t - T)| \\ &= \left[\left(\frac{\partial S}{\partial x_1} - \frac{\partial S}{\partial t} \frac{\partial T}{\partial x_1} \right)^2 + \left(\frac{\partial S}{\partial y_1} - \frac{\partial S}{\partial t} \frac{\partial T}{\partial y_1} \right)^2 + \left(\frac{\partial S}{\partial z_1} - \frac{\partial S}{\partial t} \frac{\partial T}{\partial z_1} \right)^2 \right]_{t=t-T}^{\frac{1}{2}} \end{aligned} \quad 3.29$$

$$\begin{aligned} |\nabla_1 S|^T &= |\nabla_1 S(x_1, y_1, z_1, t_1)|_{t_1=t-T} \\ &= \left[\left(\frac{\partial S}{\partial x_1} \right)^2 + \left(\frac{\partial S}{\partial y_1} \right)^2 + \left(\frac{\partial S}{\partial z_1} \right)^2 \right]_{t_1=t-T}^{\frac{1}{2}} \end{aligned} \quad 3.30$$

Finally, Σ^T indicates the surface defined by the equation

$$S^T = S(x_1, y_1, z_1, t - T) = 0 \quad 3.31$$

Note that Σ^T is a surface of the three-dimensional space (x_1, y_1, z_1) , which depends parametrically upon x, y, z and t .

Note that, for steady state, the surface Σ^T coincides with the surface Σ . For quasi-steady state, the surface Σ^T differs very little from the surface Σ . Thus the surface Σ^T will be called "deformed surface of the body and wake".

By using Eq. 3.25 and 3.26, Eq. 3.24 reduces to

$$\begin{aligned}
 4\pi E \varphi = & \oint_{\Sigma^T} \left[\nabla_i S \cdot \nabla_i \varphi - \frac{1}{a_\infty^2} \frac{dS}{dt_i} \frac{d\varphi}{dt_i} \right]^T \frac{1}{r_\beta} \frac{1}{|\nabla_i S^T|} d\Sigma^T \\
 & + \oint_{\Sigma^T} \left[\nabla_i S \cdot \nabla_i \left(\frac{1}{r_\beta} \right) - \frac{1}{a_\infty^2} \frac{dS}{dt_i} \frac{d}{dt_i} \left(\frac{1}{r_\beta} \right) \right]^T \varphi^T \frac{1}{|\nabla_i S^T|} d\Sigma^T \\
 & - \frac{\partial}{\partial t} \oint_{\Sigma^T} \left[\nabla_i S \cdot \nabla_i T - \frac{1}{a_\infty^2} \frac{dS}{dt_i} \left(1 + U_\infty \frac{\partial T}{\partial x_i} \right) \right]^T \varphi^T \frac{1}{r_\beta} \frac{1}{|\nabla_i S^T|} d\Sigma^T \\
 & - \iiint_V [EF]^T \frac{1}{r_\beta} dV_i
 \end{aligned} \tag{3.32}$$

Equation 3.32 is the desired generalized subsonic Huygens' principle. The reduction of Eq. 3.32 to the classical Huygens' principle and to other well known formulas is considered in Appendix B. The more general case in which initial conditions are also considered is analyzed in Appendix F.

Finally, in Appendix C, it is shown that Eq. 3.32 is still valid when the control point is on the surface Σ if the convention is made that $E = 1/2$ on Σ , that is, if Eq. 3.1 is replaced by:

$$\begin{aligned}
 E &= 0 && \text{inside } \Sigma \\
 &= 1/2 && \text{on } \Sigma \\
 &= 1 && \text{outside } \Sigma
 \end{aligned} \tag{3.33}$$

3.4. Steady Subsonic Flow

By assuming the time derivatives to be equal to zero, Eq. 3.32 reduces to the steady state case

$$\begin{aligned}
4\pi E\varphi = & - \oint_{\Sigma} \left[\nabla S \cdot \nabla \varphi - M^2 \frac{\partial S}{\partial x_1} \frac{\partial \varphi}{\partial x_1} \right] \frac{1}{r_p} \frac{1}{|\nabla S|} d\Sigma \\
& + \oint_{\Sigma} \left[\nabla S \cdot \nabla \left(\frac{1}{r_p} \right) - M^2 \frac{\partial S}{\partial x_1} \frac{\partial}{\partial x_1} \left(\frac{1}{r_p} \right) \right] \varphi \frac{1}{|\nabla S|} d\Sigma \\
& - \iiint_V F \frac{1}{r_p} dV,
\end{aligned} \tag{3.34}$$

Note that Eq. 3.34 differs from Eq. 2.6.10 of Ref. 13 in that, in Ref. 13:

- the convention on the normal is opposite
- the function represents the volume density of a fictitious creation of sources
- the terms which contain $M^2 \frac{\partial S}{\partial x_1}$ have been neglected* (see Ref. 13, p. 33).

The correctness of Eq. 3.34 results from the fact that, by using the well known Prandtl-Glauert transformation

$$X_0 = \frac{x}{\sqrt{1-M^2}} \quad y_0 = y \quad z_0 = z \tag{3.35}$$

Eq. 3.34 reduces (in agreement with Eq. B.8) to

$$\begin{aligned}
4\pi E\varphi = & - \oint_{\Sigma} \frac{\partial \varphi}{\partial n_0} \frac{1}{r_0} d\Sigma_0 \\
& + \oint_{\Sigma} \frac{\partial}{\partial n_0} \left(\frac{1}{r_0} \right) \varphi d\Sigma_0 \\
& - \iiint_V F \frac{1}{r_0} dV_0,
\end{aligned} \tag{3.36}$$

where \vec{n}_0 is the normal to Σ_0 , and

*The analysis of the order of magnitude of these terms is given in the next section.

$$r_o = \left[(x_o - x_{o1})^2 + (y_o - y_{o1})^2 + (z_o - z_{o1})^2 \right]^{\frac{1}{2}} \quad 3.37$$

and, having used the relation

$$\frac{1}{r_\beta} \frac{d\Sigma}{|\nabla_1 S|} = \frac{1}{r_\beta} \left| \frac{\partial S}{\partial x_1} \right| dy_1 dz_1 = \frac{1}{r_o} \left| \frac{\partial S}{\partial x_{o1}} \right| dy_{o1} dz_{o1} = \frac{1}{r_o} \frac{d\Sigma_o}{|\nabla_o S|} \quad 3.38$$

3.5. Generalized Supersonic Huygens' Principle

In this subsection, Eq. 3.19 is specialized to the supersonic case for which the Green function is given by Eq. 2.49 which may be rewritten as

$$G = \frac{-1}{4\pi r_\beta} (\delta_{T_+} + \delta_{T_-}) \quad 3.39$$

with

$$\delta_{T_\pm} = \delta(t_1 - t + T_\pm) \quad 3.40$$

where T_+ and T_- are given by Eq. 2.48.

The analysis for the supersonic case is obtained from the subsonic one by replacing each term with two, the first evaluated at time $t_1 = t - T_+$ and the second evaluated at time $t_1 = t - T_-$. The final result is obtained by modifying Eq. 3.32 to yield

$$4\pi E\varphi = - \oint_{\Sigma^{T_+}} \left[\nabla_1 S \cdot \nabla_1 \varphi - \frac{1}{a^2} \frac{dS}{dt_1} \frac{d\varphi}{dt_1} \right]^{T_+} \frac{1}{r_\beta} \frac{1}{|\nabla_1 S^{T_+}|} d\Sigma^{T_+} \\ - \oint_{\Sigma^{T_-}} \left[\nabla_1 S \cdot \nabla_1 \varphi - \frac{1}{a^2} \frac{dS}{dt_1} \frac{d\varphi}{dt_1} \right]^{T_-} \frac{1}{r_\beta} \frac{1}{|\nabla_1 S^{T_-}|} d\Sigma^{T_-}$$

(Eq. cont'd.)

$$\begin{aligned}
& + \oint_{\Sigma^{T_+}} \left[\nabla_i S \cdot \nabla_i \left(\frac{1}{r_B} \right) - \frac{1}{a_\infty^2} \frac{dS}{dt} \frac{d}{dt} \left(\frac{1}{r_B} \right) \right]^{T_+} \varphi^{T_+} \frac{1}{|\nabla_i S^{T_+}|} d\Sigma^{T_+} \\
& + \oint_{\Sigma^{T_-}} \left[\nabla_i S \cdot \nabla_i \left(\frac{1}{r_B} \right) - \frac{1}{a_\infty^2} \frac{dS}{dt} \frac{d}{dt} \left(\frac{1}{r_B} \right) \right]^{T_-} \varphi^{T_-} \frac{1}{|\nabla_i S^{T_-}|} d\Sigma^{T_-} \\
& - \frac{\partial}{\partial t} \oint_{\Sigma^{T_+}} \left[\nabla_i S \cdot \nabla_i T_+ - \frac{1}{a_\infty^2} \frac{dS}{dt} \left(1 + U_\infty \frac{\partial T_+}{\partial x_1} \right) \right]^{T_+} \varphi^{T_+} \frac{1}{r_B} \frac{1}{|\nabla_i S^{T_+}|} d\Sigma^{T_+} \\
& - \frac{\partial}{\partial t} \oint_{\Sigma^{T_-}} \left[\nabla_i S \cdot \nabla_i T_- - \frac{1}{a_\infty^2} \frac{dS}{dt} \left(1 + U_\infty \frac{\partial T_-}{\partial x_1} \right) \right]^{T_-} \varphi^{T_-} \frac{1}{r_B} \frac{1}{|\nabla_i S^{T_-}|} d\Sigma^{T_-} \\
& - \iiint_{-\infty}^{\infty} \left([EF]^{T_+} + [EF]^{T_-} \right) \frac{1}{r_B} dV
\end{aligned} \tag{3.41}$$

It may be worth noting that Σ^{T_+} and Σ^{T_-} are, in general, two different surfaces.

For steady state S is independent of t and Eq. 3.41 simplifies into

$$\begin{aligned}
2\pi E\varphi = & - \oint_{\Sigma} \left[\nabla_i S \cdot \nabla_i \varphi - M^2 \frac{\partial S}{\partial x_1} \frac{\partial \varphi}{\partial x_1} \right] \frac{1}{r_B} \frac{1}{|\nabla_i S|} d\Sigma \\
& + \oint_{\Sigma} \left[\nabla_i S \cdot \nabla_i \left(\frac{1}{r_B} \right) - M^2 \frac{\partial S}{\partial x_1} \frac{\partial}{\partial x_1} \left(\frac{1}{r_B} \right) \right] \varphi \frac{1}{|\nabla_i S|} d\Sigma - \iiint_V F \frac{1}{r_B} dV
\end{aligned} \tag{3.42}$$

Note that Eq. 3.42 differs formally from Eq. 3.34 only for the factor 2π instead of 4π on the left hand side. This is a consequence of the well known fact that the supersonic doublet is equal to twice the subsonic one: this is due to the fact that, as mentioned in Subsection 2.4, the supersonic inverse transformation is a one-to-two transformation.

It should be noted that, according to Eq. 2.40, a point can have influence only on the points located inside the

"downstream Mach cone" defined by

$$x - x_1 > B \sqrt{(y - y_1)^2 + (z - z_1)^2} \quad 3.43$$

Thus, it should be understood that the integration is extended to the part of the surface for which Eq. 3.43 is satisfied.

More precisely, G must be considered as a generalized function (or distribution according to Ref. 7) defined as

$$G = - \frac{1}{4\pi r_B} (\delta_{T_+} - \delta_{T_-}) \quad \begin{aligned} x - x_1 &> B \left[(y - y_1)^2 + (z - z_1)^2 \right]^{\frac{1}{2}} \\ &= 0 \quad x - x_1 \leq B \left[(y - y_1)^2 + (z - z_1)^2 \right]^{\frac{1}{2}} \end{aligned} \quad 3.44$$

This implies that the supersonic doublet cannot be integrated in the ordinary way, but must be integrated as the distribution theory indicates, that is, the Hadamard finite part of the integral⁷ must be considered (see Appendix H).

SECTION 4

SIMPLIFIED FORMULATIONS

4.1. Introduction

The formulae derived in Section 3, for subsonic flow, Eq. 3.32, and supersonic flow, Eq. 3.48, are very general, in that only the hypothesis of potential flow was assumed. Usually in practical applications, it is possible (and convenient) to introduce more restrictive assumptions, which allow considerable simplification of the above mentioned formulae.

In particular, one can make the assumption of small-perturbation flow, which is discussed in Subsection 4.2.

Furthermore, in most of the practical applications, the surface is almost fixed in space. Thus the case of almost fixed surface in small perturbation flow is discussed in Subsection 4.3.

Finally, in flutter problems, the surface of the body is vibrating with exponentially damped or growing oscillatory motion for which the boundary condition can be written as

$$\frac{\partial \phi}{\partial n} = Q_n = \tilde{Q}_n e^{st} \quad 4.1$$

where

$$s = \mu + i\omega \quad 4.2$$

is called the complex frequency. This problem is considered in Subsection 4.4. Note that, in particular for $\mu = 0$, one

obtains the harmonic motion.

It is important to note that the results obtained in this section do not require the general formulation of Section 3. In other words, using the procedure employed in Section 3 under the restrictive hypotheses considered here, yields the same results through a much simpler derivation. However, it is felt that going through the complicated general formulation and then simplifying under restrictive hypotheses gives a better understanding of the error introduced with the simplification.

4.2 Subsonic and Supersonic Small Perturbation Flow

As mentioned in Subsection 4.1, the results obtained thus far can be simplified considerably if the hypothesis of small perturbation is made. In the following, it is assumed that $M < 1$ (subsonic) or $M > 1$ (supersonic) but not $M \gg 1$ (hypersonic) nor $|M^2 - 1| \ll 1$ (transonic). Consider the boundary condition, which can be rewritten as

$$\frac{\partial \phi}{\partial n} = - \frac{1}{U_\infty} \frac{dS}{dt} \frac{1}{|\nabla S|} \quad 4.3$$

Assuming that $\frac{\phi}{L}$ (where L is a characteristic length of the problem) is small, say of order $\bar{\epsilon} \ll 1$,

$$\frac{\phi}{L} = O(\bar{\epsilon}) \quad 4.4$$

is equivalent to assume that the right hand side of Eq.

4.3 is small, also of order $\bar{\epsilon}$

$$\frac{1}{U_\infty} \frac{dS}{dt} \frac{1}{|\nabla S|} = O(\bar{\epsilon}) \quad 4.5$$

Thus Eq. 4.3 may be rewritten as

$$\frac{\partial \varphi}{\partial n} = - \frac{1}{U_\infty} \frac{dS}{dt} \frac{1}{|\nabla S|} = Q_n = \bar{\epsilon} \bar{Q}_n \quad 4.6$$

where $\bar{Q}_n = O(1)$. Hence, it is convenient to find an asymptotic solution for φ , as

$$\varphi = \bar{\epsilon} \varphi_1 + \bar{\epsilon}^2 \varphi_2 + \dots + O(\bar{\epsilon}^{N+1}) \quad 4.7$$

In particular, by limiting the analysis to $N = 1$, one may write

$$\varphi = \bar{\epsilon} \bar{\varphi} + O(\bar{\epsilon}^2) \quad 4.8$$

It may be noted that all the nonlinear terms are of order of $\bar{\epsilon}^2$ or higher and thus one can write

$$F = \bar{\epsilon}^2 F_2 + O(\bar{\epsilon}^3) \quad 4.9$$

By combining Eqs. 4.6, 4.8 and 4.9 with Eq. 3.32 yields

$$\begin{aligned} 4nE\bar{\epsilon}\bar{\varphi} = & - \oint_{\Sigma^T} \left[\bar{\epsilon} \bar{Q}_n \frac{1}{r_\beta} \right]^T \frac{|\nabla S|^T}{|\nabla S^T|} d\Sigma^T \\ & + \oint_{\Sigma^T} \left[\frac{\partial}{\partial n_i} \left(\frac{1}{r_\beta} \right) \bar{\epsilon} \bar{\varphi} \right]^T \frac{|\nabla S|^T}{|\nabla S^T|} d\Sigma^T \\ & - \frac{\partial}{\partial t} \oint_{\Sigma^T} \left[\frac{\partial T}{\partial n_i} \frac{\bar{\epsilon} \bar{\varphi}}{r_\beta} \right]^T \frac{|\nabla S|^T}{|\nabla S^T|} d\Sigma^T + O(\bar{\epsilon}^2) \end{aligned} \quad 4.10$$

Neglecting terms of order $\bar{\epsilon}^2$ in Eq. 4.10 and returning to the original variable yields

$$\begin{aligned}
4\pi E \varphi(x, y, z, t) = & - \oint_{\Sigma^+} \left[\frac{\partial \varphi}{\partial n_i} \frac{1}{r_B} \right]^T \frac{|\nabla S|^T}{|\nabla S^+|} d\Sigma^+ \\
& + \oint_{\Sigma^+} \left[\frac{\partial}{\partial n_i} \left(\frac{1}{r_B} \right) \varphi \right]^T \frac{|\nabla S|^T}{|\nabla S^+|} d\Sigma^+ \\
& - \frac{\partial}{\partial t} \oint_{\Sigma^+} \left[\frac{\partial T}{\partial n_i} \frac{\varphi}{r_B} \right]^T \frac{|\nabla S|^T}{|\nabla S^+|} d\Sigma^+
\end{aligned} \tag{4.11}$$

Equation 4.11 represents the small-perturbation subsonic Huygens' principle.

Similarly, by combining Eqs. 4.6, 4.8 and 4.9 with Eq. 3.41, one obtains, for supersonic flow

$$\begin{aligned}
4\pi E \varphi(x, y, z, t) = & - \oint_{\Sigma^{T+}} \left[\frac{\partial \varphi}{\partial n_i} \frac{1}{r_B} \right]^{T+} \frac{|\nabla S|^{T+}}{|\nabla S^{T+}|} d\Sigma^{T+} \\
& - \oint_{\Sigma^{T-}} \left[\frac{\partial \varphi}{\partial n_i} \frac{1}{r_B} \right]^{T-} \frac{|\nabla S|^{T-}}{|\nabla S^{T-}|} d\Sigma^{T-} \\
& + \oint_{\Sigma^{T+}} \left[\frac{\partial}{\partial n_i} \left(\frac{1}{r_B} \right) \varphi \right]^{T+} \frac{|\nabla S|^{T+}}{|\nabla S^{T+}|} d\Sigma^{T+} \\
& + \oint_{\Sigma^{T-}} \left[\frac{\partial}{\partial n_i} \left(\frac{1}{r_B} \right) \varphi \right]^{T-} \frac{|\nabla S|^{T-}}{|\nabla S^{T-}|} d\Sigma^{T-} \\
& - \frac{\partial}{\partial t} \oint_{\Sigma^{T+}} \left[\frac{\partial T_+}{\partial n_i} \varphi \right]^{T+} \frac{1}{r_B} \frac{|\nabla S|^{T+}}{|\nabla S^{T+}|} d\Sigma^{T+} \\
& - \frac{\partial}{\partial t} \oint_{\Sigma^{T-}} \left[\frac{\partial T_-}{\partial n_i} \varphi \right]^{T-} \frac{1}{r_B} \frac{|\nabla S|^{T-}}{|\nabla S^{T-}|} d\Sigma^{T-}
\end{aligned} \tag{4.12}$$

It should be noted that Eqs. 4.11 and 4.12 are not the exact solutions of the linear problem but an approximate (small perturbation) solution of the nonlinear problem. For, not only the nonlinear terms have been dropped, but the linear terms containing $\frac{dS}{dt}$ have been eliminated as well. It may be noted that one of the reasons to carry the effect of the nonlinear terms in the general analysis is to show that the order of magnitude of the terms which contain $\frac{dS}{dt}$ is of the same order of magnitude of the nonlinear terms. Thus, these terms can be consistently eliminated if the nonlinear effects are neglected.

It should be noted however, that once the value of φ has been obtained by using Eqs. 4.11 and 4.12, then the effect of the neglected terms can be obtained by studying the equation of terms of order $\bar{\epsilon}^2$ in Eq. 4.10, which has φ_2 as unknown (second order term of Eq. 4.7). It may be worth mentioning that this equation contains only known nonlinear terms and thus is linear with respect to the unknown φ_2 . It may be expected however, that the solution obtained in this way is not uniformly valid. Singular perturbation methods, which yield uniformly valid solutions, are now under consideration.

4.3. Quasi-fixed Surface in Small-Perturbation Flow

In many practical applications, the surface of the body is almost fixed with respect to the frame of reference. This is the case, for instance, of small elastic vibration of the wings of an airplane.* In this case, the surface may be considered to be fixed in space, although the time derivative cannot be neglected. Mathematically speaking, it is assumed that

$$S^T = S = S(x, y, z) \quad 4.13$$

and

$$|\nabla S|^T = |\nabla S^T| = |\nabla S| \quad 4.14$$

although

$$\frac{\partial S}{\partial t} \neq 0 \quad 4.15$$

in the boundary conditions.

Under these hypotheses, Eq. 4.11 reduces to

$$\begin{aligned} 4\pi E \varphi(x, y, z, t) = & - \oint_{\Sigma} \left[\frac{\partial \varphi}{\partial n_i} \right]^T \frac{1}{r_\beta} d\Sigma \\ & + \oint_{\Sigma} [\varphi]^T \frac{\partial}{\partial n_i} \left(\frac{1}{r_\beta} \right) d\Sigma \\ & - \oint_{\Sigma} \left[\frac{\partial \varphi}{\partial t} \right]^T \frac{1}{r_\beta} \frac{\partial T}{\partial n_i} d\Sigma \end{aligned} \quad 4.16$$

*Important exceptions are, for instance, the problems of helicopter blades and spinning missiles.

where Σ is the surface defined by the equation $S = 0$ and $\frac{\partial \varphi}{\partial n_i}$ is given by Eq. 1.13. Similarly, for supersonic case, Eq. 4.12 yields

$$\begin{aligned}
 4\pi E \varphi(x, y, z, t) = & - \oint_{\Sigma} \left(\left[\frac{\partial \varphi}{\partial n_i} \right]^{T+} + \left[\frac{\partial \varphi}{\partial n_i} \right]^{T-} \right) \frac{1}{r_B} d\Sigma \\
 & + \oint_{\Sigma} \left([\varphi]^{T+} + [\varphi]^{T-} \right) \frac{\partial}{\partial n_i} \left(\frac{1}{r_B} \right) d\Sigma \\
 & - \oint_{\Sigma} \left(\left[\frac{\partial \varphi}{\partial t} \right]^{T+} + \left[\frac{\partial \varphi}{\partial t} \right]^{T-} \right) \frac{1}{r_B} \frac{\partial T}{\partial n_i} d\Sigma
 \end{aligned} \tag{4.17}$$

with $\partial \varphi / \partial n_i$ given by Eq. 1.13.

4.4. Complex-Exponential Flow

As mentioned in Subsection 4.1, in flutter problems, the motion of the surface is exponentially damped or growing vibration. In this case, the surface of the body can be written as

$$Z = Z_0(x, y) + \hat{\varepsilon} z_1(x, y) e^{st} \tag{4.18}$$

or, in general

$$S_S(x, y, z) + \hat{\varepsilon} S_U(x, y, z) e^{st} = 0 \tag{4.19}$$

where S_S represents the steady state geometry, whereas S_U gives the unsteady contribution. For $\hat{\varepsilon} \ll 1$, the hypotheses assumed to derive Eqs. 4.16 and 4.17 are valid. Hence, Eqs. 4.16 and 4.17 can be used with the surface Σ described by $S_S = 0$ and boundary conditions given by Eqs. 1.13 and 1.14, with $|\nabla S|$ replaced by $|\nabla S_S|$, that is,

$$\begin{aligned}\frac{\partial \varphi}{\partial n} &= - \frac{1}{U_\infty} \frac{1}{|\nabla S_s|} \frac{dS}{dt} \\ &= - \frac{1}{U_\infty} \frac{1}{|\nabla S_s|} \left[\frac{\partial S_s}{\partial x} + \hat{\epsilon} \left(\frac{s}{U_\infty} S_u + \frac{\partial S_u}{\partial t} \right) e^{st} \right] = Q_{n,s} + Q_{n,u}\end{aligned}\quad 4.20$$

where

$$Q_{n,s} = - \frac{1}{|\nabla S_s|} \frac{\partial S_s}{\partial x} \quad 4.21$$

$$Q_{n,u} = - \hat{\epsilon} \frac{1}{|\nabla S_s|} \left(\frac{s}{U_\infty} S_u + \frac{\partial S_u}{\partial x} \right) e^{st} = \tilde{Q}_n e^{st} \quad 4.22$$

with

$$\tilde{Q}_n = - \frac{\hat{\epsilon}}{|\nabla S_s|} \left(\frac{s}{U_\infty} S_u + \frac{\partial S_u}{\partial x} \right) \quad 4.23$$

Since Eqs. 4.16 and 4.17 are linear, the steady and unsteady problems can be studied by setting

$$\varphi = \varphi_s + \varphi_u \quad 4.24$$

with

$$\varphi_u = \tilde{\varphi} e^{st} \quad 4.25$$

and separating the two problems, solving them independently and finally, superimposing the results.

Hence, only the unsteady state component is considered in the following. For the subsonic case, by combining Eq. 4.16, 4.22 and 4.25, one obtains

$$\begin{aligned}4\pi E \tilde{\varphi} &= - \oint_{\Sigma} \tilde{Q}_n \frac{e^{-s\tau}}{r_\beta} d\Sigma \\ &+ \oint_{\Sigma} \tilde{\varphi} e^{-s\tau} \frac{\partial}{\partial n_i} \left(\frac{1}{r_\beta} \right) - \oint_{\Sigma} \tilde{\varphi} s e^{-s\tau} \frac{1}{r_\beta} \frac{\partial \tau}{\partial n_i} d\Sigma\end{aligned}\quad 4.26$$

or

$$4\pi E \tilde{\varphi} = - \oint_{\Sigma} \tilde{Q}_n \frac{e^{-sT}}{r_B} d\Sigma + \oint_{\Sigma} \tilde{\varphi} \frac{\partial}{\partial n_i} \left(\frac{e^{-sT}}{r_B} \right) d\Sigma \quad 4.27$$

It may be of interest to note the similarity between Eq. 4.27 and the solution of Laplace's Equation given by Eq. 3.41.

Similarly, for the supersonic case, Eq. 4.17 yields

$$4\pi E \tilde{\varphi}(x, y, z) = - \oint_{\Sigma} \tilde{Q}_n \frac{e^{-sT_+} + e^{-sT_-}}{r_B} d\Sigma + \oint_{\Sigma} \tilde{\varphi} \frac{\partial}{\partial n_i} \left(\frac{e^{-sT_+} + e^{-sT_-}}{r_B} \right) d\Sigma \quad 4.28$$

where, according to Eq. 2.10,

$$e^{-sT_+} + e^{-sT_-} = e^{\frac{-sM(x-x_1)}{a_\infty B^2}} \left(e^{\frac{-s}{a_\infty B^2} r_B} + e^{\frac{s}{a_\infty B^2} r_B} \right) \quad 4.29$$

or, for $s = i\omega$ (harmonic motion),

$$e^{-sT_+} + e^{-sT_-} = 2 e^{\frac{-i\omega M(x-x_1)}{a_\infty B^2}} \cos\left(\frac{\omega r_B}{a_\infty B^2}\right) \quad 4.30$$

Finally, it should be remarked that Eqs. 4.27 and 4.28 are suitable for comparing this formulation to the lifting surface theory (see Section 5). However, from the numerical point of view, it is convenient to use a slightly different procedure described in Subsection 6.6. It should be noted that the two formulations differ only for terms of the same order of the terms neglected in Subsection 4.2.

SECTION 5

LIFTING SURFACE THEORIES

5.1. Introduction

As mentioned in Section 1, the methods currently available for evaluating the pressure acting on a wing are based on the assumption of zero-thickness-wings (lifting surface theories). The lifting surface theories generally used for aeroelastic application¹⁴ are those given in Refs. 8, 15 and 16. In this section, it is shown how lifting surface theories are related to the formulation presented here. It should be noted that, for the case considered here, all the hypotheses of Subsection 4.4 are satisfied. Thus the results obtained there will be used in this section. The subsonic flow is considered in Subsection 5.2 and the supersonic in Subsection 5.3.

5.2. Oscillating Wing in Subsonic Flow

Consider an oscillating thin wing in subsonic flow. If the thickness approaches zero, then Eq. 4.19 with $s = i\omega$ reduces to

$$4\pi\tilde{\varphi}(x, y, z) = \iint_{\Sigma^{(u)}} \Delta\tilde{\varphi} \frac{\partial}{\partial n_u} \left(\frac{e^{-i\omega\tau}}{r_\beta} \right) d\Sigma \quad 5.1$$

where $\tilde{n}_u = \tilde{n}_{upper}$,

$$\Delta\varphi = \varphi_{upper} - \varphi_{lower} \quad 5.2$$

and $\Sigma^{(u)}$ is the upper side of the surface of the wing and the wake. By assuming that this surface is contained in the plane $z_1 = 0$, Eq. 5.2 yields

$$4\pi \tilde{\varphi} = - \iint_{\Sigma_u} \Delta \tilde{\varphi} \frac{\partial}{\partial z} \left(\frac{e^{-i\omega T}}{r_\beta} \right) dx_1 dy_1 \quad 5.3$$

since

$$\frac{\partial}{\partial z_1} \frac{e^{-i\omega T}}{r_\beta} = - \frac{\partial}{\partial z} \left(\frac{e^{-i\omega T}}{r_\beta} \right) \quad 5.4$$

Note that $\Delta \varphi \equiv 0$ outside Σ_u ; thus it is convenient to replace the domain of integration, Σ_u , with the whole plane (in conformity with theory of distribution). Then, differentiating with respect to z yields

$$4\pi \frac{\partial \tilde{\varphi}}{\partial z} = - \int_{-\infty}^{\infty} \int_{-\infty}^{\infty} \Delta \tilde{\varphi} \frac{\partial^2}{\partial z^2} \left(\frac{e^{-i\omega T}}{r_\beta} \right) dx_1 dy_1 \quad 5.5$$

This is a relation between the downwash $\frac{\partial \tilde{\varphi}}{\partial z}$ and $\Delta \tilde{\varphi}$. Since the downwash is known at $z = 0$, Eq. 5.5 as z goes to zero yields an integral equation relating the downwash with $\Delta \tilde{\varphi}$. However, for practical applications it is convenient to have a relation between the downwash and the pressure distribution

$$\Delta p = p_{upper} - p_{lower} \quad 5.6$$

According to Eqs. 1.17, 4.18 and 5.6, Δp is given by

$$\Delta p = - \rho_\infty U_\infty \left(i\omega \Delta \tilde{\varphi} + U_\infty \frac{\partial \Delta \tilde{\varphi}}{\partial x} \right) e^{i\omega t} = \Delta \tilde{p} e^{i\omega t} \quad 5.7$$

with

$$\Delta \tilde{p} = -\rho_{\infty} U_{\infty} \left(i\omega \Delta \tilde{\varphi} + U_{\infty} \frac{\partial}{\partial x} \Delta \tilde{\varphi} \right) \quad 5.8$$

Equation 5.8 can be rewritten as

$$\Delta \tilde{p} = -\rho_{\infty} U_{\infty}^2 e^{-\frac{i\omega}{U_{\infty}} x} \frac{\partial}{\partial x} \left(e^{\frac{i\omega}{U_{\infty}} x} \Delta \tilde{\varphi} \right) \quad 5.9$$

By integrating Eq. 5.9 with the condition

$$\Delta \tilde{\varphi} = 0 \quad \text{at } x = -\infty \quad 5.10$$

one obtains

$$\Delta \tilde{\varphi} = -\frac{1}{\rho_{\infty} U_{\infty}^2} e^{-\frac{i\omega}{U_{\infty}} x} \int_{-\infty}^x e^{\frac{i\omega}{U_{\infty}} \lambda_2} \Delta \tilde{p}(\lambda_2, y) d\lambda_2 \quad 5.11$$

Combining Eq. 5.5 with 5.11 and integrating by parts, yields

$$\begin{aligned} 4\pi \frac{\partial \tilde{\varphi}}{\partial z} &= \frac{1}{\rho_{\infty} U_{\infty}^2} \int_{-\infty}^{\infty} \int_{-\infty}^{\infty} \left\{ \int_{-\infty}^{x_1} e^{\frac{i\omega \lambda_2}{U_{\infty}}} \Delta \tilde{p} d\lambda_2 \right\} e^{-\frac{i\omega x_1}{U_{\infty}}} \frac{\partial^2}{\partial z^2} \left(\frac{e^{-i\omega T}}{r_{\rho}} \right) dx_1 dy_1 \\ &= \frac{1}{\rho_{\infty} U_{\infty}^2} \iint_{-\infty}^{\infty} \Delta \tilde{p}(x_1, y_1) K_e(x_1 - x, y_1 - y) dx_1 dy_1 \end{aligned} \quad 5.12$$

with

$$K_e = e^{\frac{i\omega x_1}{U_{\infty}}} \int_{x_1}^{\infty} e^{-\frac{i\omega \lambda_1}{U_{\infty}}} \frac{\partial^2}{\partial z^2} \frac{e^{\frac{-i\omega}{a_2 \beta^2} \left[\sqrt{(x-\lambda_1)^2 + \beta^2 [(y-y_1)^2 + z^2]} - M(x-\lambda_1) \right]}}{\left\{ (x-\lambda_1)^2 + \beta^2 [(y-y_1)^2 + z^2] \right\}^{\frac{1}{2}}} d\lambda_1 \quad 5.13$$

Note that the finite terms of the integration by parts are

equal to zero because of Eq. 5.10 and the condition

$$K_z = 0 \quad \text{at} \quad x_1 = \infty \quad 5.14$$

which is obtained from Eq. 5.13. By using the transformation

$\lambda = x - x_1$, Eq. 5.13 yields a simpler expression for

$$K_z = e^{-\frac{i\omega}{U_\infty}(x-x_1)} \int_{-\infty}^{x-x_1} \frac{\partial^2}{\partial z^2} \left(\frac{e^{\frac{i\omega}{U_\infty \beta^2}(\lambda - M r_\lambda)}}{r_\lambda} \right) d\lambda \quad 5.15$$

with

$$r_\lambda = \left\{ \lambda^2 + \beta^2 [(y-y_1)^2 + z^2] \right\}^{\frac{1}{2}} \quad 5.16$$

Finally, as z goes to zero, Eq. 5.12 reduces to

$$\frac{\partial \tilde{\phi}}{\partial z}(x, y, 0) = \frac{1}{4\pi} \oint_{\Sigma_w} \frac{\Delta \tilde{p}}{\rho U_\infty^2} K \, dx, dy, \quad 5.17$$

with

$$K = \lim_{z \rightarrow 0} K_z(x-x_1, y-y_1) \quad 5.18$$

in agreement with results given by Watkins, Rynyan and

Woolston⁸. An explicit expression for K , given by Eq.

D.48, is derived in Appendix D. Note that in Eq. 5.17,

the integration can be limited to the surface, Σ_w , of wing,

since $\Delta \tilde{p} = 0$ outside the wing.

5.3. Oscillating Wing in Supersonic Flow

For the supersonic case, it is important to note that

the integration domain must be restricted to Mach cone defined by

$$x - x_1 > B \sqrt{(y - y_1)^2 + z^2} \quad 5.19$$

Thus, the supersonic case can be handled in a way similar to the subsonic case if a cutoff or unit function is used as a factor:¹⁵

$$H = H(x - x_1 - B \sqrt{(y - y_1)^2 + z^2}) \quad 5.20$$

where $H(\theta)$ is the Heavyside step function

$$\begin{aligned} H(\theta) &= 1 & \theta > 0 \\ &= 0 & \theta < 0 \end{aligned} \quad 5.21$$

By performing the same type of operations described in Subsection 5.2, one obtains

$$\frac{\partial \tilde{\phi}}{\partial z}(x, y, 0) = \frac{1}{4\pi} \oint_{\Sigma_w} \frac{\Delta p}{\rho_\infty U_\infty^2} K \, dx_1 dy_1 \quad 5.22$$

with

$$\begin{aligned} &K(x_1 - x, y_1 - y) \\ &= \lim_{z \rightarrow 0} 2e^{-i\frac{\omega}{U_\infty}(x - x_1)} \int_{-\infty}^{x - x_1} \frac{\partial^2}{\partial z^2} \left[H(\lambda - B \sqrt{(y - y_1)^2 + z^2}) e^{-i\frac{\omega}{U_\infty B} \lambda} \cos\left(\frac{M\omega}{U_\infty B^2} \sqrt{\lambda^2 - B^2[(y - y_1)^2 + z^2]}\right) \right] d\lambda \end{aligned} \quad 5.23$$

in agreement with the results given by Watkins and Berman.¹⁵

However, if the wings have only supersonic edges, then the two sides of the wing become independent and by assuming a

"symmetric flow", one obtains

$$\phi = \frac{-1}{\pi B} \iint_{\Sigma_w} \frac{\partial \phi}{\partial z_1} \frac{1}{r_B} e^{-i \frac{\omega M^2}{B^2 U_w} (x-x_1)} \cos \frac{\omega M r}{B^2 U_w} dx_1 dy_1, \quad 5.24$$

in agreement with Refs. 10 and 16.

SECTION 6

NUMERICAL FORMULATION

6.1. Introduction

In the preceding sections, a general theory of unsteady compressible potential aerodynamics is presented. In Section 1, the problem is formulated. Section 2 deals with the Green functions (for subsonic and supersonic linearized equations) which are used in Section 3 to derive an equation which relates the value of the potential ψ at any point in the field, the values of ψ and $\frac{\partial \psi}{\partial n}$ on the surface of the body and the value of $\Delta \psi$ on the wake with an additional contribution of the nonlinear terms. In Section 4, the formulation is simplified for (1) small perturbation, (2) almost fixed surface, (3) oscillatory motion, whereas in Section 5, it is shown how the classical lifting surface theories can be derived from the general formulation.

It is obvious that the general formulation presented here has no closed-form solution except for a few very special cases. Hence, in general, the use of high speed computers will be required. Thus, the numerical solution of the problem as formulated in Subsection 4.4 (small perturbation flow around an oscillating wing) is discussed here.

It should be emphasized that this discussion is given in order to focus a few difficulties which may arise during

the numerical computation. Furthermore, it may be noted that the difficulties of the unsteady flow (Eq. 4.19) are similar to the one of the steady flow. Hence, for the sake of simplicity, the numerical formulation is discussed for the steady incompressible flow. However, the generalization to the unsteady compressible flow is indicated.

It should be mentioned that the numerical problems arise especially on the treatment of a thin wing (see Subsection 6.4). Thus, in the discussion, it will be assumed that the body under consideration is a thin wing, although the formulation is valid for any body with sharp trailing edges (see Subsection 6.3).

6.2. Integral Equation Formulation; Existence and Uniqueness of the Solution.

For steady incompressible flow, Eq. 4.27 reduces to the classical equation

$$4\pi E\psi = - \oint_{\Sigma} \frac{\partial \psi}{\partial n_i} \frac{1}{r} d\Sigma + \oint_{\Sigma} \psi \frac{\partial}{\partial n_i} \left(\frac{1}{r} \right) d\Sigma \quad 6.1$$

In order to analyze the question of uniqueness of the solution, the surface Σ is replaced by a smooth surface Σ' surrounding (at very small, but finite, distance: the boundary layer thickness for instance) the body and the wake (Fig. 3a). The wake is truncated at a very large, but finite, distance from the wing. If the control point is on the surface Σ' the function E assumes the value $1/2$ and equation 6.1

reduces to

$$2\pi\varphi = - \oint_{\Sigma'} \frac{\partial\varphi}{\partial n_1} \frac{1}{r} d\Sigma' + \oint_{\Sigma'} \varphi \frac{\partial}{\partial n_1} \left(\frac{1}{r} \right) d\Sigma' \quad 6.2$$

If the geometry of the wake is known and if $\frac{\partial\varphi}{\partial n_1}$ is replaced by the value (see Eq. 1.12)

$$\frac{\partial\varphi}{\partial n_1} = - \frac{\partial S}{\partial x_1} / |\nabla S| \quad 6.3$$

which assumes on the body and the wake, then Eq. 6.2 is an integral equation relating the downwash integral to the unknown value of φ on the surface. Note that Eq. 6.2 gives the solution of the exterior Neumann problem and, in this case, the solution of the equation exists and is unique* for any smooth (Lyapunov) surface (Ref. 17, pp. 620-621).

Next, the surface Σ' (surrounding the body and the wake) is replaced by the surface Σ , composed of two branches, the surface Σ_b of the body and the surface Σ_w of the wake (Fig. 3b). Thus, Eq. 6.2, combined

*Note that, for the interior Neumann problem, the solution of the equation is not unique, for any arbitrary constant can be added to the solution. Physically speaking, one might say that, for the exterior problem, this arbitrariness is eliminated by the condition $\varphi = 0$ at infinity.

with Eq. 6.3, reduces to

$$2\pi\varphi = \oint_{\Sigma_B} \frac{\partial S}{\partial x_i} \frac{1}{r} \frac{d\Sigma}{|\nabla S|} + \oint_{\Sigma_B} \varphi \frac{\partial}{\partial n_i} \left(\frac{1}{r} \right) d\Sigma$$

$$+ \oint_{\Sigma_w^{(u)}} (\varphi_u - \varphi_e) \frac{\partial}{\partial n_i} \left(\frac{1}{r} \right) d\Sigma$$

6.4

In Eq. 6.4, $\Sigma_w^{(u)}$ is the upper side of the surface of the wake and hence, the normal \vec{n}_i is understood to be the upper normal. Note that, according to Eq. 1.17, for steady flow,

$$\frac{\partial}{\partial x_i} (\varphi_u - \varphi_e) = 0 \quad \text{on the wake} \quad 6.5$$

for no pressure jump is possible through the wake.

From physical considerations, the solution of Eq. 6.4 is "very close" to the one of Eq. 6.2. Thus, it will be assumed that, if the geometry of the wake is known, the solution of Eq. 6.4 exists and is unique. It should be emphasized however, that this conclusion is based upon physical reasoning. However, this reasoning is questionable, as shown by the remarks given in Subsection 6.5. Hence, a rigorous mathematical proof of the existence and uniqueness of the solution of Eq. 6.4 would be highly desirable.

However, there are still two important questions to be considered: first, the geometry of the wake and second, the special behaviour of Eq. 6.4 when the thickness

of the wing goes to zero. These two questions are discussed in Subsection 6.3 and 6.5, respectively.

6.3. The Wake

As mentioned in the preceding subsection, the surface of the wake in Eq. 6.4 is not known. Thus, Eq. 6.4, which is satisfied on the body, must be completed by the equation on the wake, which says that the velocity on the wake is tangent to the surface of the wake. Thus, one obtains two coupled integral equations, one on the body and one on the wake, with ϕ unknown on the body and $\frac{\partial \phi}{\partial n}$ unknown on the wake, whereas $\frac{\partial \phi}{\partial n}$ is known on the body and $\Delta \phi = \phi_u - \phi_t$ is constant along the x-direction on the wake. According to the Kutta condition, this constant value is equal to the value of $\Delta \phi$ at the trailing edge. Given the velocity on the wake, the geometry of the wake is obtained by the condition that the velocity is tangent to the wake. This approach has been successfully used in Ref. 6 to study the transient incompressible flow around a wing after a sudden start. However, from a practical point of view, this approach is too lengthy and a simplified treatment of the contribution of the wake is presented in the following.

Note first that

$$\iint \frac{\partial}{\partial n_i} \left(\frac{1}{r} \right) d\Sigma = - \iint \frac{\vec{n}_i \cdot \vec{r}}{r^3} d\Sigma = - \iint \vec{n}_i \cdot \frac{\vec{r}}{r^2} d\Sigma = - \iint \frac{d\Sigma_{(ni)}}{r^2} = - \iint d\Omega \quad 6.6$$

where

$$d\bar{\Sigma}_{(n)} = d\bar{\Sigma} \cos(\vec{n}, \vec{r}) \quad 6.7$$

is the projected area (into the plane normal to the direction \vec{r}) and

$$d\Omega = \frac{d\bar{\Sigma}_{(n)}}{r^2} \quad 6.8$$

is the solid angle (see Fig. 4).

Next, consider the wake integral as a sum of M strips in the x direction (see Fig. 5). Applying the mean value theorem, one obtains (note that $\Delta\varphi$ is only a function of y)

$$\begin{aligned} I_w &= \iint_{\Sigma_w^{(n)}} \Delta\varphi(y) \frac{\partial}{\partial n_1} \left(\frac{1}{r} \right) d\bar{\Sigma} = - \iint_{\Sigma_w^{(u)}} \Delta\varphi(y) d\Omega \\ &= - \sum_{m=1}^M \Delta\varphi(y_m) \iint_{\Sigma_m} d\Omega = - \sum_{m=1}^M \Delta\varphi(y_m) \Omega_m \end{aligned} \quad 6.9$$

where $\Delta\varphi(y_m)$ are the mean values of $\Delta\varphi$ for each strip Σ_m , and Ω_m are the solid angles of the strip Σ_m . Equation 6.9 shows that any changes of the wake such that solid angles Ω_m are not altered, do not have any influence on the value of the wake integral I_w .

This suggests that a "reasonable" geometry for the wake can be assumed, provided that the values of the associated solid angles are not excessively different from the true ones. Hence, it is possible (and convenient) to approximate the wake by straight vortex-lines, parallel to the direction of the flow, emanating

from the trailing edge of the wing. For, geometrical considerations show that the solid angles, Ω_m , are changed only slightly. With this assumption, the wake integral simplifies considerably and its contribution reduces to a line integral. For if the trailing edge is given by

$$\begin{aligned} X &= X_{TE}(y) \\ Z &= Z_{TE}(y) \end{aligned} \quad 6.10$$

then the equation of the surface of the wake is given by

$$S = z_1 - z_{TE}(y_1) = 0 \quad 6.11$$

and

$$\begin{aligned} I_w &= - \int_{-b/2}^{b/2} dy_1 \int_{x_{TE}(y_1)}^{\infty} \Delta \varphi(\nabla, S, \vec{r}) \frac{1}{r^3} dx_1 dy_1 \\ &= \int_{-b/2}^{b/2} \Delta \varphi J_w dy_1 \end{aligned} \quad 6.12$$

where b is the span of the wing and

$$\begin{aligned} J_w &= \left[(z_1 - z) - \frac{dz_{TE}}{dy_1}(y_1 - y) \right] \int_{x_{TE}}^{\infty} \frac{-1}{r^3} dx_1 \\ &= \left[(z_1 - z) - \frac{dz_{TE}}{dy_1}(y_1 - y) \right] \frac{-1}{(y_1 - y)^2 + (z_1 - z)^2} \left[1 - \left(\frac{x_1 - x}{r} \right)_{x_1 = x_{TE}(y_1)} \right] \end{aligned} \quad 6.13$$

with $z_1 = z_{TE}(y_1)$. In particular, if trailing edge is in the plane $z_1 = 0$ (i.e. $z_{TE}(y_1) \equiv 0$), Eq. 6.13 reduces to

$$J_w = \frac{z}{(y - y_1)^2 + z^2} \left[1 - \frac{x_{TE} - x}{[(x_{TE} - x)^2 + (y_1 - y)^2 + z^2]^{1/2}} \right] \quad 6.14$$

In conclusion, under the reasonable assumption of cylindrical wake (straight vortex-lines) the effect of the wake simplifies considerably and Eq. 6.4 reduces to

$$2\pi\varphi = \oint_{\Sigma} \frac{\partial S}{\partial x_i} \frac{1}{r} \frac{d\Sigma}{|VS|} + \oint_{\Sigma} \varphi \frac{\partial}{\partial n_i} \left(\frac{1}{r} \right) d\Sigma + \int_{-b/2}^{b/2} \Delta\varphi_{TE} J_w dy, \quad 6.15$$

with J_w given by Eq. 6.13.

Finally, an important remark about bodies without sharp trailing edge must be made. In the discussion presented in this subsection, it was assumed that the wing had a sharp trailing edge. Note that the results can be easily generalized to the case of general bodies with sharp trailing edge. However, for bodies without sharp trailing edge, the inviscid flow theory is incapable, in general, of predicting the location of the stagnation point from which the wake emanates. This can be easily seen in the case of rotating cylinder of finite length. From the experiments the location of the stagnation point depends upon the angular velocity, ω . On the other hand, the equation of the geometry of the cylinder does not depend upon ω and thus ω does not even appear in the equation of the inviscid flow.

In the following, it is assumed that the body under consideration has a sharp trailing edge. However, an

unsteady viscous theory which predicts the location of the stagnation point from which the wake emanates is necessary in order to extend this method to bodies without sharp trailing edges. Similar consideration holds for the case of detached flow (when this can be approximated by a wake emanating from a point different from the sharp trailing edge).

6.4. Numerical Solution of the Integral Equation

In order to solve Eq. 6.15, various approximate techniques are available. For lifting surface theories, one of the most successful ones is the collocation method. In this method, the unknown function is approximated by a linear combination of N prescribed functions with unknown coefficients. The functions are generally the first N ones of a complete set of functions, each of which satisfy the boundary conditions of the problem. The N unknown coefficients are determined by solving a linear system of N equations obtained by satisfying the integral equation at N points (collocation points). This method is being explored for the solution of Eq. 6.15. However, it should be noted that, for complex geometries, this approach is not feasible, for each geometry requires a different set of functions and the more complicated is the geometry, the more difficult it is to guess the appropriate set of functions.

Hence, a more flexible approach is desirable. A

representation of the unknown function similar to the one used in finite elements for structural problems seems to be more convenient. In finite elements, the domain of the equation is broken into small elements. The function inside the element is expressed in terms of its unknown values (and the values of its derivation, eventually) at nodes of the element. This general type of representation is now under examination. It should be noted that, in finite elements, the final equations are derived from variational principles. Here, the same type of representation is used, but the algebraic equations are obtained by satisfying Eq. 6.15 at prescribed points (control points).

The most elementary form of this approach is very close to the box method and is described in the following. Consider the surface Σ divided into small elements Σ_i (see Fig.6)

$$2\pi\varphi(P) = \oint_{\Sigma} \frac{\partial\varphi}{\partial n_i} \frac{1}{r} d\Sigma + \sum_{i=1}^N \iint_{\Sigma_i} \varphi \frac{\partial}{\partial n_i} \left(\frac{1}{r}\right) d\Sigma_i + I_w \quad 6.16$$

By the mean value theorem

$$\iint_{\Sigma_i} \varphi \frac{\partial}{\partial n_i} \left(\frac{1}{r}\right) d\Sigma_i = \bar{\varphi}_i \iint_{\Sigma_i} \frac{\partial}{\partial n_i} \left(\frac{1}{r}\right) d\Sigma_i \quad 6.17$$

where $\bar{\varphi}_i$ is an appropriate value within the element Σ_i . This suggests that $\bar{\varphi}_i$ may be approximated by the value, φ_i , at the center of the box. This yields

$$\varphi(P) = - \oint_{\Sigma} \frac{\partial \varphi}{\partial n_i} \frac{1}{2\pi r} d\Sigma + \sum_{i=1}^N \varphi_i \iint_{\Sigma_i} \frac{\partial}{\partial n_i} \left(\frac{1}{2\pi r} \right) d\Sigma_i + \sum_{l=1}^{2NV} \varphi_l W_l \quad 6.18$$

where, in the last term, the index l covers only the boxes in contact with the trailing edge and

$$W_l = \pm \int_{\Delta y_l} J_w dy_l \quad 6.19$$

where the upper (lower) sign is used for the upper (lower) side of the wing.

By satisfying this equation at the centers $P^{(k)}$ of the boxes, one obtains

$$\varphi_k = b_k + \sum_{i=1}^N c_{ki} \varphi_i + \sum_{i=1}^N w_{ki} \varphi_i \quad 6.20$$

with

$$b_k = \oint_{\Sigma} \frac{\partial \varphi}{\partial n_i} \frac{1}{2\pi r_k} d\Sigma \quad 6.21$$

$$c_{ki} = \iint_{\Sigma_i} \frac{\partial}{\partial n_i} \left(\frac{1}{2\pi r_k} \right) d\Sigma_i \quad 6.22$$

where

$$r_k = |P^{(k)} - P_1| = \left[(x^{(k)} - x_1)^2 + (y^{(k)} - y_1)^2 + (z^{(k)} - z_1)^2 \right]^{\frac{1}{2}} \quad 6.23$$

is the distance of the dummy point of integration P_1 from the center $P^{(k)}$ of the element k . Finally,

$$w_{ki} = W_i \Big|_{P=P^{(k)}} \quad 6.24$$

for the boxes in contact with the trailing edge and

$$w_{\kappa i} = 0 \quad 6.25$$

otherwise. Equation 6.20 can be rewritten as

$$\sum_{i=1}^N a_{\kappa i} \varphi_i = b_{\kappa} \quad 6.26$$

with

$$a_{\kappa i} = \delta_{\kappa i} - c_{\kappa i} - w_{\kappa i} \quad 6.27$$

where $\delta_{\kappa i}$ is the Kronecker delta. Eq. 6.26 is the equation which yields the solution of the problem.

6.5. Limiting Behavior for Zero Thickness

As mentioned above, the formulation described thus far becomes singular in the case of zero thickness. This is shown clearly by the fact that, for lifting surface (in the plane $z_1 = 0$). In this case, Eq. 6.1 reduces to

$$2\pi\varphi_u = - \iint_{\Sigma^{(u)}} (\varphi_u - \varphi_l) \frac{\partial}{\partial z} \left(\frac{1}{r} \right)_{z=0} dx, dy, \quad 6.28$$

and

$$2\pi\varphi_l = + \iint_{\Sigma^{(u)}} (\varphi_u - \varphi_l) \frac{\partial}{\partial z} \left(\frac{1}{r} \right)_{z=0} dx, dy, \quad 6.29$$

where $\Sigma^{(u)}$ is the portion of the plane $z_1 = 0$ (upper side) which contains the wing and the wake. By adding and subtracting Eqs. 6.28 and 6.29, one obtains

$$\varphi_u + \varphi_l = 0 \quad 6.30$$

and

$$2\pi \Delta\psi + \iint_{\Sigma^{(u)}} \Delta\psi \frac{\partial}{\partial z} \left(\frac{1}{r} \right)_{z=0} dx_1 dy_1 \quad 6.31$$

This implies that (since, as well known, there exists a nontrivial solution $\Delta\psi \neq 0$) the operator shown in Eq. 6.31 is singular.

Hence, one can expect that the numerical procedure also has a singular behavior. In order to show that this is indeed the case, consider a symmetric wing with angle of attack α and thickness ratio τ , and let τ go to zero. In this case, Eq. 6.21 shows that

$$\lim_{\tau \rightarrow 0} b_k = 0 \quad 6.32$$

In order to simplify the discussion, the numbering of the boxes is assumed to be such that the odd (even) numbers correspond to boxes in the upper (lower) surface and that the box in opposite position to the upper box i , has the number $i + 1$ (see Fig. 7). For simplicity, upper box i and lower box $i + 1$ will be called "opposite boxes".

With this numbering, it is easy to show that, according to Eq. 6.22,

$$\lim_{\tau \rightarrow 0} [c_{ki}] = \begin{bmatrix} \begin{array}{ccc|ccc} 0 & -1 & 0 & 0 & 1 & 0 & 0 \\ -1 & 0 & 1 & 0 & 0 & 1 & 0 \\ 0 & 0 & 1 & 0 & -1 & 0 & 1 \\ 0 & 0 & -1 & 0 & 1 & 0 & 0 \\ \hline & & & & & & \end{array} & \begin{array}{ccc} 1 & 0 & 0 \\ 0 & 0 & 0 \\ 0 & 0 & 0 \\ 0 & 0 & 0 \\ \hline & & & & & & \end{array} \\ \begin{array}{ccc|ccc} & & & & & & \\ & & & & & & \\ & & & & & & \\ & & & & & & \\ \hline & & & & & & \end{array} & \begin{array}{ccc} 1 & 0 & 0 \\ 0 & 0 & 0 \\ 0 & 0 & 0 \\ 0 & 0 & 0 \\ \hline & & & & & & \end{array} \end{bmatrix} \quad 6.33$$

In other words, all the coefficients c_{ki} are equal to zero except for the ones relating opposite boxes, which assume the value -1. Furthermore, the coefficients w_{ki} are equal to zero. Hence, Eq. 6.26 in the limit, as τ goes to zero, reduces to

$$\begin{bmatrix} \begin{array}{|c|c|c|} \hline 1 & 1 & 0 \\ \hline 1 & 1 & 0 \\ \hline 0 & 0 & 1 \\ \hline 0 & 0 & 1 \\ \hline \end{array} & \begin{array}{|c|c|c|} \hline 0 & 0 & 0 \\ \hline 0 & 0 & 0 \\ \hline 0 & 0 & 0 \\ \hline 0 & 0 & 0 \\ \hline \end{array} \\ \hline \begin{array}{|c|c|c|} \hline 0 & 0 & 0 \\ \hline 0 & 0 & 0 \\ \hline 0 & 0 & 0 \\ \hline 0 & 0 & 0 \\ \hline \end{array} & \begin{array}{|c|c|c|} \hline 1 & 1 & 1 \\ \hline 1 & 1 & 1 \\ \hline 1 & 1 & 1 \\ \hline 1 & 1 & 1 \\ \hline \end{array} \end{bmatrix} \{ \varphi_i \} = 0 \quad 6.34$$

This equation can have nontrivial solution since the determinant is equal to zero.

Note that this result implies that zero thickness wings (lifting surface theory) are more difficult to deal with than finite thickness wings.

However, this shows also that, by using the method proposed here, one may encounter numerical complication due to the fact that, for very thin wings, the determinant is close to zero and hence, one may encounter strong elimination of significant figures. This implies that one has to be very accurate in the evaluation of the coefficients

c_{ki} and b_k .

It may be of interest to analyze the order of magnitude of the different terms of Eq. 6.26: by writing Eq. 6.26 as

$$\{\varphi_i\} = [a_{ki}]^{-1} \{b_k\} \quad 6.35$$

and noting that

$$\{\varphi_i\} = O(1) \quad 6.36$$

$$\{b_k\} = O(\tau) \quad 6.37$$

one obtains

$$[a_{ki}]^{-1} = O\left(\frac{1}{\tau}\right) \quad 6.38$$

In order to establish the practical limits of the applicability of the method, Eq. 6.26 has been solved numerically for very small values of τ . The results are presented in Section 7.

6.6. Generalization to Unsteady Subsonic Flow

In this subsection, the formulation presented above is generalized to cover steady and unsteady subsonic flow. As shown in Appendix C, great simplification is obtained if the generalized Prandtl-Glauert transformation

$$\begin{aligned} x_0 &= \frac{x}{\beta} \\ y_0 &= y \\ z_0 &= z \\ t_0 &= a_\infty \beta t \end{aligned} \quad 6.39$$

is introduced. Following the same procedure used in Subsection C.3.2, by using Eq. 6.39, neglecting nonlinear terms, Eq. 3.32 reduces to

$$\begin{aligned}
 4\pi E \varphi = & - \oint_{\Sigma^T} [\nabla_0 S \cdot \nabla_0 \varphi - \beta^2 \frac{\partial S}{\partial t_0} \frac{\partial \varphi}{\partial t_0} \\
 & - M \frac{\partial S}{\partial t_0} \frac{\partial \varphi}{\partial x_0} - M \frac{\partial S}{\partial x_0} \frac{\partial \varphi}{\partial t_0}]^T \cdot \frac{1}{r_0} \frac{d\Sigma^T}{|\nabla_0 S^T|} \\
 & + \oint_{\Sigma^T} [\nabla_0 S \cdot \nabla_0 \left(\frac{1}{r_0}\right) - M \frac{\partial S}{\partial t_0} \frac{\partial}{\partial x_0} \left(\frac{1}{r_0}\right)]^T \cdot \varphi^T \frac{d\Sigma^T}{|\nabla_0 S^T|} \\
 & - \frac{\partial}{\partial t_0} \oint_{\Sigma^T} [\nabla_0 S \cdot \nabla_0 r_0 - M \frac{\partial S}{\partial t_0} \frac{\partial r_0}{\partial x_0} \\
 & - \frac{\partial S}{\partial t_0}]^T \cdot \varphi^T \frac{1}{r_0} \frac{d\Sigma^T}{|\nabla_0 S^T|}
 \end{aligned} \tag{6.40}$$

where

$$r_0 = \left[(x_0 - x_0)^2 + (y_0 - y_0)^2 + (z_0 - z_0)^2 \right]^{\frac{1}{2}} \tag{6.41}$$

and

$$\left[\quad \right]^{T_0} = \left[\quad \right]_{t_0 = t_0 - T_0} \tag{6.42}$$

with

$$T_0 = a_\omega \beta T = M(x_0 - x_0) + r_0 \tag{6.43}$$

Next, it is assumed that the surface is almost fixed and Eqs. 4.13 to 4.15 can be used, to yield

$$\begin{aligned}
 4\pi E \varphi = & - \oint_{\Sigma_0} \left[\frac{\partial \varphi}{\partial n_i} - M \frac{\partial S / \partial x_i}{|\nabla_0 S|} \frac{\partial \varphi}{\partial t_i} \right]^{T_0} \frac{1}{r_0} d\Sigma_0 \\
 & + \oint_{\Sigma_0} \frac{\partial}{\partial n_i} \left(\frac{1}{r_0} \right) \varphi^{T_0} d\Sigma_0 \\
 & - \oint_{\Sigma_0} \frac{\partial r_0}{\partial n_i} \frac{\partial \varphi^{T_0}}{\partial t_i} \frac{1}{r_0} d\Sigma_0
 \end{aligned} \tag{6.44}$$

Finally, neglecting terms of the same order of the nonlinear terms (which implies that $\frac{\partial \varphi}{\partial n_i}$ can be replaced by $\frac{\partial \varphi}{\partial n_i} = Q_n$) Eq. 6.44 reduces to

$$\begin{aligned}
 4\pi E \varphi = & - \oint_{\Sigma_0} Q_n^{T_0} \frac{1}{r_0} d\Sigma_0 + \oint_{\Sigma_0} \frac{\partial}{\partial n_i} \left(\frac{1}{r_0} \right) \varphi^{T_0} d\Sigma_0 \\
 & - \oint_{\Sigma_0} \frac{\partial r_0}{\partial n_i} \frac{1}{r_0} \frac{\partial \varphi^{T_0}}{\partial t_i} d\Sigma_0
 \end{aligned} \tag{6.45}$$

This is the desired equation. It may be noted that M appears only in T_0 , whereas β does not appear at all.

For steady state, Eq. 6.45 reduces to

$$4\pi E \varphi = - \oint_{\Sigma_0} Q_n \frac{1}{r_0} d\Sigma_0 + \oint_{\Sigma_0} \frac{\partial}{\partial n_i} \left(\frac{1}{r_0} \right) \varphi d\Sigma_0 \tag{6.46}$$

This shows that the same method used for incompressible flow can be used for steady compressible subsonic flow. This equation is essentially the same as Eq. 2.6.10 of Ref. 13, already discussed in Subsection 3.4.

Furthermore, for unsteady oscillating flow (as described in Subsection 4.4), combining Eqs. 4.1, 4.18 and 6.43 and 6.45 yields

$$\begin{aligned}
 4\pi E \tilde{\psi} = & - \oint_{\Sigma_0} \tilde{Q}_n \frac{1}{r_0} e^{-s_0 [M(x_0 - x_0) + r_0]} d\Sigma_0 \\
 & + \oint_{\Sigma} \frac{\partial}{\partial n_n} \left(\frac{1}{r_0} \right) \tilde{\psi} e^{-s_0 [M(x_0 - x_0) + r_0]} d\Sigma \\
 & - \oint_{\Sigma} \frac{\partial r_0}{\partial n_n} \frac{1}{r_0} \tilde{\psi} s_0 e^{-s_0 [M(x_0 - x_0) + r_0]} d\Sigma \\
 = & - \oint_{\Sigma_0} \tilde{Q}_n \frac{1}{r_0} e^{-s_0 [M(x_0 - x_0) + r_0]} d\Sigma_0 \\
 & + \oint_{\Sigma} \tilde{\psi} e^{-s_0 M(x_0 - x_0)} \frac{\partial}{\partial n_n} \left(\frac{e^{-\frac{1}{2}s_0 r_0}}{r_0} \right) d\Sigma.
 \end{aligned} \tag{6.47}$$

where

$$s_0 = \frac{s}{\beta a_\infty} \quad 6.48$$

This equation can be simplified further by introducing the functions

$$\hat{Q}_n = \tilde{Q}_n e^{-s_0 M x_0} \quad 6.49$$

$$\hat{\phi}_0 = \tilde{\phi} e^{-s_0 M x_0} \quad 6.50$$

to yield

$$\begin{aligned} 4\pi E\hat{\phi} = & - \iint_{\Sigma_0} \hat{Q}_n \frac{e^{-s_0 r_0}}{r_0} d\Sigma_0 \\ & + \iint_{\Sigma_0} \hat{\phi} \frac{\partial}{\partial n_0} \left(\frac{e^{-s_0 r_0}}{r_0} \right) d\Sigma_0 \end{aligned} \quad 6.51$$

This equation is equivalent to Eq. 4.27: the difference between the two equations is of the same order of the terms which have been neglected.

Furthermore, Eq. 6.51 shows that, by using the generalized Prandtl-Glauert transformation (Eq. 6.39) the equation relating $\hat{\phi}$ to \hat{Q}_n is completely independent of Mach number. Note however, that the contribution of the wake depends explicitly upon the Mach number, M : for, using Eq. 6.34, Eq. 5.9 reduces to

$$-\frac{1}{\rho_\infty U_\infty^2} \Delta \hat{p} = e^{-\frac{s_0 x_0}{M}} \frac{\partial}{\partial x_0} \left(e^{\frac{s_0 x_0}{M}} \Delta \hat{\phi} \right) \quad 6.52$$

where

$$\Delta \hat{p} = \Delta \tilde{p} e^{-s_0 M x}, \quad 6.53$$

which implies that, on the wake, where $\Delta p = 0$,

$$\Delta \hat{\psi} e^{\frac{s_0 x_0}{M}} = \Delta \hat{\psi}_{TE} e^{\frac{s_0 x_{0TE}}{M}} \quad 6.54$$

Note also that the only terms neglected are those in the integral which contains the boundary conditions. This is important, because, as shown in Subsection 6.5, the operator becomes singular when the thickness goes to zero. Hence, even small terms may become important when the thickness becomes small.

In conclusion, Eq. 6.5 is more suitable than Eq. 4.27 from the numerical point of view. The procedure used to solve Eq. 6.1 can be used with minor obvious modification to solve Eq. 6.51. The only complication arises from the contribution of the wake, which can be treated as described in Appendix D.

SECTION 7

NUMERICAL RESULTS

7.1. Introduction

As shown in Subsection 6.5, in the case of very thin wings, one may expect to encounter strong elimination of figures. In order to establish the limits of applicability of the proposed method, Eq. 6.26 has been solved numerically for a simple case for which numerical results are available: rectangular wing in steady subsonic flow. For the sake of simplicity, the procedure is described for incompressible flow only, since, by using the Prandtl-Glauert transformation, the steady compressible flow reduces to the incompressible one (Eq. 6.46 in Subsection 6.6).

7.2. The Geometry of the Wing

Consider a rectangular symmetric wing with thickness, h , given by

$$h = \tau c \frac{3\sqrt{3}}{2} \sqrt{\xi} (1 - \xi) \sqrt{1 - \eta^2} \quad 7.1$$

with

$$\begin{aligned} \xi &= \bar{x}/c \\ \eta &= 2\bar{y}/b \end{aligned} \quad 7.2$$

where c is the chord and b is the span, \bar{x} and \bar{y} are the cartesian coordinates of the planform at zero angle of attack (see Fig. 8) and, finally,

$$\tau = \frac{h_{max}}{c} = \frac{1}{c} h \Big|_{\substack{\xi=1/3 \\ \eta=0}} \quad 7.3$$

is the thickness ratio.

Equations 7.1 and 7.2 can be used to give the geometry of the wing in parametric form (parameters $\bar{\xi}$ and $\bar{\eta}$), at zero angle of attack, as

$$\begin{aligned} \bar{x} &= c \bar{\xi} \\ \bar{y} &= \frac{b}{2} \bar{\eta} \\ \bar{z} &= \pm \tau c \frac{3\sqrt{3}}{4} \sqrt{\bar{\xi}} (1 - \bar{\xi}) \sqrt{1 - \bar{\eta}^2} \\ &= \pm \frac{h}{2} \end{aligned} \quad 7.4$$

where the upper (lower) sign holds for the upper (lower) surface of the wing.

If the angle of the attack, α , is different from zero, the geometry of the wing is given by (See Fig. 9)

$$\begin{aligned} x &= \bar{x} \cos \alpha + \bar{z} \sin \alpha \\ y &= \bar{y} \\ z &= -\bar{x} \sin \alpha + \bar{z} \cos \alpha \end{aligned} \quad 7.5$$

For small values of τ and α , Eq. 7.5 can be approximated as

$$\begin{aligned} x &= \bar{x} \\ y &= \bar{y} \\ z &= \bar{z} - \bar{x} \alpha \end{aligned} \quad 7.6$$

Hence, the surface Σ can be written as $\pm z - \frac{h}{2} \pm \bar{x} \alpha = 0$
which implies

$$\frac{\partial S}{\partial x} = -\frac{1}{2} \frac{\partial h}{\partial \bar{x}} \pm \alpha$$

$$\frac{\partial S}{\partial y} = -\frac{1}{2} \frac{\partial h}{\partial \bar{y}} \quad 7.7$$

$$\frac{\partial S}{\partial z} = \pm 1$$

Equations 7.6 and 7.7 fully describe the geometry of the wing and enable one to evaluate the coefficients C_k and b_k .

7.3. The Numerical Procedure

The numerical procedure used to evaluate the coefficients of the equation is briefly described in the following. First, note that the wing is symmetric with respect to the plane $y = 0$. Hence, Eq. 6.26 can be rewritten as

$$\sum_{q=1}^{\hat{N}} \hat{a}_{pq} \varphi_q = \sum_{q=1}^N (\delta_{pq} - \hat{c}_{pq} - \hat{w}_{pq}) \varphi_q = b_p \quad 7.8$$

where \hat{N} is the total number of boxes on the right hand part of the wing and \hat{c}_{pq} is the influence of two boxes (in symmetric position with respect to the plane $y = 0$) on a point P^r on the right hand part of the wing,

$$\begin{aligned}
\hat{C}_{pq} &= \frac{1}{2\pi} \iint_{\Sigma_q^{(R)}} \frac{\partial}{\partial \eta_i} \left(\frac{1}{r_p} \right) d\Sigma_q^{(R)} + \frac{1}{2\pi} \iint_{\Sigma_q^{(L)}} \frac{\partial}{\partial \eta_i} \left(\frac{1}{r_p} \right) d\Sigma_q^{(L)} \\
&= \frac{1}{2\pi} \iint_{\Sigma_q^{(R)}} \left\{ \left[\frac{\partial}{\partial \eta_i} \left(\frac{1}{r_p} \right) \right]_R + \left[\frac{\partial}{\partial \eta_i} \left(\frac{1}{r_p} \right) \right]_L \right\} d\Sigma_q^{(R)}
\end{aligned} \tag{7.9}$$

with

$$\begin{aligned}
\left[\frac{\partial}{\partial \eta_i} \left(\frac{1}{r_p} \right) \right]_R &= \frac{-1}{|\nabla_i S|} \left[\frac{\partial S}{\partial x_i} (x_i - x) + \frac{\partial S}{\partial y_i} (y_i - y) + \frac{\partial S}{\partial z_i} (z_i - z) \right] \left(\frac{1}{r_p^{(R)}} \right)^3 \\
\left[\frac{\partial}{\partial \eta_i} \left(\frac{1}{r_p} \right) \right]_L &= \frac{-1}{|\nabla_i S|} \left[\frac{\partial S}{\partial x_i} (x_i - x) + \frac{\partial S}{\partial y_i} (y_i + y) + \frac{\partial S}{\partial z_i} (z_i - z) \right] \left(\frac{1}{r_p^{(L)}} \right)^3
\end{aligned} \tag{7.10}$$

where

$$\begin{aligned}
r_p^{(R)} &= \left[(x_i - x^{(p)})^2 + (y_i - y^{(p)})^2 + (z_i - z^{(p)})^2 \right]^{1/2} \\
r_p^{(L)} &= \left[(x_i - x^{(p)})^2 + (y_i + y^{(p)})^2 + (z_i - z^{(p)})^2 \right]^{1/2}
\end{aligned} \tag{7.11}$$

and all the other quantities are evaluated on the right hand part of the wing; similar expressions hold for \hat{w}_{pq} .

Second, note that $\partial S / \partial x_i$, and $\partial S / \partial y_i$ are infinite at the leading edge and the tip of the wing, respectively. Hence, it is convenient to use a nonuniform mesh for the definition of the boxes (smaller boxes in the neighborhood of the leading edge and tip, larger boxes in

the neighborhood of the trailing edge and root). This is accomplished by introducing the transformation

$$\begin{aligned}\bar{\xi} &= \bar{X}^2 & (0 \leq \bar{X} \leq 1) \\ \bar{\eta} &= 1 - (1 - \bar{Y})^2 & (0 \leq \bar{Y} \leq 1)\end{aligned}\quad 7.12$$

and using boxes of constant sizes $\Delta \bar{X}$, $\Delta \bar{Y}$ in the plane \bar{X}, \bar{Y} :

$$\begin{aligned}\Delta \bar{X} &= 1 / NX \\ \Delta \bar{Y} &= 1 / NY\end{aligned}\quad 7.13$$

where NX and NY are the number of boxes in direction \bar{X} and \bar{Y} respectively. In other words, the center of the box (m, n) is given by (see Fig. 10)

$$\begin{aligned}\bar{X}_m^{(c)} &= (m - \frac{1}{2}) \Delta \bar{X} & m = 1, \dots, NX \\ \bar{Y}_n^{(c)} &= (n - \frac{1}{2}) \Delta \bar{Y} & n = 1, \dots, NY\end{aligned}\quad 7.14$$

whereas, its boundaries are given by

$$\begin{aligned}\bar{X}_m^{(M)} &\leq \bar{X} \leq \bar{X}_m^{(P)} \\ \bar{Y}_n^{(M)} &\leq \bar{Y} \leq \bar{Y}_n^{(P)}\end{aligned}\quad 7.15$$

with

$$\begin{aligned}\bar{X}_m^{(M)} &= \bar{X}_m^{(c)} - \frac{\Delta \bar{X}}{2} = (m-1) \Delta \bar{X} \\ \bar{X}_m^{(P)} &= \bar{X}_m^{(c)} + \frac{\Delta \bar{X}}{2} = m \Delta \bar{X}\end{aligned}\quad 7.16$$

$$\bar{\gamma}_n^{(M)} = \bar{\gamma}_n^{(C)} - \frac{\Delta \bar{\gamma}}{2} = (n-1) \Delta \bar{\gamma}$$

$$\bar{\gamma}_n^{(P)} = \bar{\gamma}_n^{(C)} + \frac{\Delta \bar{\gamma}}{2} = n \Delta \bar{\gamma}$$

Note that, for each couple of values m and n , there are two boxes, one on the upper and one on the lower side of the wing: hence, the total number of boxes on the right hand part of the wing is

$$\hat{N} = 2 \cdot NX \cdot NY \quad 7.17$$

Third, the coefficients b_p are evaluated as

$$b_p = \sum_{q=1}^{\hat{N}} \iint_{\Sigma_q} \frac{\partial S}{\partial x_1} \frac{1}{2\pi} \left(\frac{1}{r_p^{(u)}} + \frac{1}{r_p^{(d)}} \right) \frac{d\Sigma_q}{|\nabla_1 S|} \quad 7.18$$

where Σ_q are the same boxes used for the evaluation of c_{pq} . This procedure is particularly convenient because it yields very accurate results and is very little time consuming, since most of the operations required are needed anyway for the evaluation of the coefficients c_{pq} .

Fourth, it should be noted that the emphasis here is on very thin wings. Hence, it is feasible to approximate each surface element Σ_q with its tangent plane at the center of the element; the boundary of the element is still given by Eq. 7.15. In this case, the integrals can be evaluated analytically. This is shown in Appendix E for the more general case of trapezoidal element, which is needed, for instance, in the case of swept or delta wings.

Finally, since only very thin wings are considered here, the pressure coefficient, given by Eq. 1.18, is evaluated as

$$C_p = -2 \frac{\partial \phi}{\partial x} = -2 \frac{\partial \phi}{\partial \bar{x}} \frac{\partial \bar{x}}{\partial x} \quad 7.19$$

$$= -\frac{1}{c \bar{x}} \frac{\partial \phi}{\partial \bar{x}}$$

where $\partial \phi / \partial \bar{x}$ is evaluated by central finite differences. Note that $\partial \phi / \partial \bar{x}$ is finite whereas $\partial \phi / \partial x$ is infinite at the leading edge. This is one of the advantages of using the transformation given by Eq. 7.12.

7.4. Numerical Results

In order to compare this method with experimental and lifting surface results, the rectangular wing considered in Refs. 18 and 19, for which

$$\begin{aligned} \alpha &= 5^\circ \\ b/c &= 3 \\ M &= .24 \end{aligned} \quad 7.20$$

is investigated here. Analysis of the thickness effect (presented in Subsection 7.4.1) shows that the solution obtained by employing a thickness ratio $\tau = .001$ is a good representation of the zero thickness solution. Furthermore, analysis of the convergence (presented in Subsection 7.4.2) shows that using $NX = NY = 7$ (that is $\hat{N} = 98$) is sufficient for the convergence. The results obtained with $\tau = .001$ and $NX = NY = 7$ are shown in Fig. 11 and 12 where the

distribution of the potential ϕ over the wing and the lift distribution

$$C_l = -\Delta c_p = c_{p_l} - c_{p_u} \quad 7.21$$

respectively, are presented in threedimensional form.

It may be noted that the diagram of $\Delta\phi$ is flat in the neighborhood of the root of the wing and the trailing edge (more precisely $\partial\Delta\phi/\partial y = 0$ at the root and $\partial\Delta\phi/\partial x = 0$ at the trailing edge). Similarly, the diagram of c_l is flat in the neighborhood of the root (more precisely $\partial c_l/\partial y = 0$ at the root). Hence, the values of $\Delta\phi$ and c_l at the center of the boxes in contact with the root (root boxes values) and the value of $\Delta\phi$ at the trailing edge boxes will be considered in the following in order to discuss the effect of the thickness and the convergence.

7.4.1. Thickness Effect

In order to analyze the thickness effect*, the problem has been solved for four values of the thickness ratio,

$\tau = .1, .01, .001$ and $.0001$ respectively. In all these cases, the number of boxes in both x and y direction is $NX = NY = 4$. Hence, the total number of boxes (for upper and lower side of the right half of the wing) is $\hat{N} = 32$ (i.e., Eq. 6.26 is a system of 32 equations and 32 unknowns). For the value $\tau = .001$, no message indicating strong elimination of figures was given, whereas, for the

*This is not an analysis of the thickness effect on the real solution (since that would depend upon nonlinear terms) but only the examination of the effect of decreasing thickness on the numerical process.

value $\tau = .0001$, a message indicating an elimination of significant figures higher than the prescribed tolerance at the 19th step was obtained.*

Hence, only the cases $\tau = .1, .01$ and $.001$ are presented here. The values of $\Delta\varphi$ at the centers of the trailing edges boxes and the root boxes are shown in Figs. 13 and 14, respectively, whereas, the lift distribution $C_l = -\Delta c_p$ at the root boxes, is shown in Fig. 15. The results indicate that the solution converges to a zero-thickness solution and that the solution for $\tau = .001$ is a good approximation for the zero thickness solution.

Note that, according to Eq. 6.6

$$\sum_{q=1}^{\infty} q_q = \frac{1}{2\pi} \sum_{q=1}^{\infty} \iint_{\Sigma_q} \frac{\partial}{\partial n_i} \left(\frac{1}{r_p} \right) d\Sigma_q = -\frac{1}{2\pi} \oint_{\Sigma} d\Omega = -1 \quad 7.22$$

since the point from which the solid angle is evaluated is on the surface Σ . This equation is poorly satisfied on the leading edge and the tip where the approximation of the surface element with its tangent plane is poorer. The

*For the solution of Eq. 6.26, the standard IBM SUBROUTINE GELG has been used. The value of the tolerance (which is compared to the ratio between the pivot at the n-th step and the initial step) was chosen to be $TOL = .001$.

poorest values of $\sum_q C_{pq}$ at "tip or leading edge boxes", are given in Table 7.1, column 1, whereas the poorer value for the "internal boxes" (not at the leading edge nor at the tip) are given in column 2.

TABLE 7.1

τ	1	2
.1	.76946	.98986
.01	.96247	.99899
.001	.99625	.99990
.0001	.99960	.99999

Table 7.1 indicates that the approximation of the surface elements with its tangent plane is not satisfactory for the "tip or leading edge boxes" for the case $\tau = .1$. A more sophisticated analysis, which evaluates the error (difference between integral on the tangent plane and integral on the real surface element) by Gaussian numerical quadrature formulae is now being analyzed.*

* Note that the use of \bar{X} and \bar{Y} See Eq. 7.12) as variables of integration eliminates the singularity of the integrands at the leading edge and the tip.

7.4.2. Convergence

In order to study the convergence of the solutions, the case $\tau = .001$ was solved for $NX = NY = 4, 5, 6$ and 7 , respectively. The value of $\Delta\varphi$ at the root and trailing edge boxes are shown in Fig. 16 and 17 respectively, whereas, the values of the lift distribution $c_l = -\Delta c_p$ at the root boxes are shown in Fig. 18.

The results show that the solution is convergent very fast and that the case 4×4 is sufficient for an accurate analysis. The computer time employed on the IBM 360/50 available at the Boston University Computing Center, are given in Table 7.2.

TABLE 7.2

Number of Boxes	Computing Time Sec.
4 x 4 x 2	22.2
5 x 5 x 2	60.4
6 x 6 x 2	129.9
7 x 7 x 2	259.9

7.5. Comparison with Existing Results

In order to evaluate the accuracy of the method, the results shown in Fig. 12 are compared to the one obtained

in Ref. 19.

For convenience, three vertical sections of the three-dimensional diagram presented in Fig. 12, are plotted in Fig. 19. The three sections correspond to values of $\bar{\eta} = .5$, $.7$ and $.9$ respectively.

In order to evaluate the comparison, the following factors should be emphasized. First, this test case was considered in order to verify the applicability of the method in the worst possible conditions (very thin wings with thickness ratio $\tau = 1/1000$). Second, the numerical procedure was chosen for its flexibility (i.e., possibility of applying it to very general geometrics) and not for its accuracy. Furthermore, it should be noted that the comparison should not be made with the experiments, but rather with the lifting surface theory, since the thickness ratio, $\tau = .001$ is considered here, is very small. Finally, it may be concluded that the results obtained here are in surprisingly excellent agreement with the ones presented in Ref. 19.

Note that the case $\tau = .1$ (which represents a realistic value of the thickness ratio) is only partially satisfactory, because Eq. 7.22 is poorly satisfied. Hence, a comparison with the experiments is not attempted here. As mentioned above, a more accurate procedure to evaluate the coefficients c_{pq} and b_p (in this procedure, the surface elements are not

necessarily planar with straight boundaries) is now under investigation. Preliminary results are in good agreement with the ones presented here (Ref. 20).

On the opposite end of the range of the thickness ratio (the case $\tau = .0001$) strong elimination of significant figure was obtained (see Subsection 7.4.1). However, note that this value of the thickness ratio is much too small to be of any practical interest. Furthermore, despite the elimination of figures, the results obtained were very close to the ones for $\tau = .001$. In conclusion, there is no limitation of the method (at least for cases of practical interest) due to the singular limiting behavior (for zero thickness) described in Subsection 6.5. It should be remarked again that finite thickness wings can be treated in a simpler fashion than zero-thickness wings.

Finally, it should be emphasized that, once the values are known, the potential ϕ and the pressure coefficient c_p can be evaluated at any point of the field. For, by using the same procedure applied to derive Eq. 6.18 (with $E = 1$ instead of $E = 1/2$), Eq. 6.1 can be approximated as

$$\begin{aligned} \phi = & -\frac{1}{4\pi} \oint_{\Sigma} \frac{\partial \phi}{\partial n_i} \frac{1}{r} d\Sigma + \frac{1}{4\pi} \sum_{i=1}^N \phi_i \iint_{\Sigma_i} \frac{\partial}{\partial n_i} \left(\frac{1}{r} \right) d\Sigma_i \\ & + \frac{1}{2} \sum_{l=1}^{2M} \phi_l w_l \end{aligned} \quad 7.23$$

Similarly

$$C_p = -2 \frac{\partial \varphi}{\partial x} = \frac{1}{2\pi} \oint_{\Sigma} \frac{\partial \varphi}{\partial n_i} \frac{\partial}{\partial x} \left(\frac{1}{r} \right) d\Sigma$$

7.24

$$- \frac{1}{2\pi} \sum_{i=1}^N \varphi_i \iint_{\Sigma_i} \frac{\partial}{\partial n_i} \frac{\partial}{\partial x} \left(\frac{1}{r} \right) d\Sigma_i - \sum_{i=1}^{2M} \varphi_i \frac{\partial w_i}{\partial x}$$

Note that these expressions can be evaluated by using the same trapezoidal elements described in Appendix E: the coefficients to be used in Eq. 7.24 are simply the derivative with respect to x of the coefficient given in Appendix E. Furthermore, if the point is on the surface Σ , Eq. 7.23 and 7.24 are still valid if coefficients are evaluated in the limit sense and the value of E is maintained equal to one.

Finally, note that the lift and the moment coefficients can be evaluated as

$$C_L = \frac{1}{c b} \int_{-b/2}^{b/2} dy_1 \int_0^c c_i dx_1 = \frac{4}{c b} \int_0^{b/2} \Delta \varphi_{TE} dy_1$$

7.25

$$C_M = \frac{1}{c^2 b} \int_{-b/2}^{b/2} dy_1 \int_0^c c_i x_1 dx_1 = \frac{2}{c^2 b} \int_{-b/2}^{b/2} dy_1 \int_0^c \Delta \varphi_{TE} x_1 dx_1$$

$$= \frac{4}{c^2 b} \int_{-b/2}^{b/2} \left(\left[\Delta \varphi x_1 \right]_0^c - \int_0^c \Delta \varphi dx_1 \right) dy_1$$

$$= \frac{4}{c^2 b} \int_{-b/2}^{b/2} c \Delta \varphi_{TE} dy_1 - \frac{4}{c^2 b} \int_{-b/2}^{b/2} dy_1 \int_0^c \Delta \varphi dx_1$$

7.26

Similar relations can be used for evaluating the generalized forces.

C - 2

SECTION 8

DISCUSSION

8.1. General Comments

As mentioned in Subsection 1.1, lifting surface theories have two main disadvantages. First, they are complicated from the numerical point of view (singularity of the integrands and, especially for unsteady state, complication of the kernel function). Second, they cannot be easily generalized to study complex configurations and motions. The formulation presented here is an attempt to reduce these disadvantages. The numerical simplicity of the proposed formulation, in comparison to the steady and (especially) unsteady lifting surface theory, is apparent from Sections 6 and 7. Note that a sufficiently accurate pressure evaluation requires only 22 seconds of computing time on an IBM 360/50 (see Subsection 7.4.2). The second point, applicability to complex configurations and motions, is discussed in the next subsection.

8.2. Applicability of the Method

The main advantage of the method proposed here is the fact that it can be used to solve a large variety of problems. for which the lifting surface theories can be used only in a very unsatisfactory way. It should be noted that the method, although classic, (as shown in

Section 5, the lifting surface theories can be obtained as a limiting case of the present formulation when the thickness goes to zero) has never been developed to its full generality.

Note also, that the method is valid for both subsonic and supersonic flow. The procedure described for the subsonic flow can be used for the supersonic one. However, for supersonic trailing edges, the procedure is simpler, since the wake has no contribution on the body.

In order to appreciate the extent of the applicability of the method, it might be convenient to consider a few typical examples.

A simple, but interesting application of this method is the evaluation of the aerodynamic forces acting on wings of finite thickness. The importance of thickness effects in the prediction of flutter boundaries has been shown by Yates and Bland.²¹ It should be noted that, in the proposed formulation, the nonlinear effect of the thickness might be included in a very systematic and natural way, by using singular perturbation methods mentioned in Section 4.

More importantly, the method can be used to solve more complicated problems, since it is formulated for arbitrary geometries and motions. The arbitrariness of the geometry implies that even complete configurations (wing, body, tail) can be studied, including wing-tail

wake interference effects. Even more detailed configurations, like tanks at the wing tips can be analyzed without any increase of difficulty.

On the other hand, the arbitrariness of the motion implies that problems which cannot be examined with lifting-surface theory, can now be solved, although the solution is rather complicated. Typical examples are: curved trajectories, accelerated motion, and roll (which is particularly important for practical applications). Other problems like gust response (and indicial motions in general) can be solved, in a relatively easy way, by making use of the generalized formulation, derived in Appendix F , which includes the effects of arbitrary initial conditions. It may be noted that damped oscillatory motion, which is important in predicting the degree of stability of linear systems, as well as arbitrary periodic motions do not offer more difficulty than the simply harmonic motion.

A particularly interesting problem is the evaluation of the aerodynamic pressure on the blades of a helicopter in forward flight in which both geometry and motion are extremely complicated. These examples show the applicability of the proposed formulation in solving problems involving complicated configurations having arbitrary motions.

It is of interest to mention that, by making use of

the method of images, described in Ref. 11, the present formulation can easily be extended to study the motion in the presence of an infinite rigid planar wall which acts like a plane of symmetry: this corresponds to the practical problem of motion in the vicinity of the ground (ground effect). Also, using the method of images, the problem of flow inside a rigid circular duct can be studied, as well as the slightly more complicated flow inside a duct of rectangular section.¹¹ These cases correspond to the important problem of accounting for the effect of the walls of a wind tunnel. In summary, with the method of images, the proposed method can be extended to study the ground effects and the effect of the wind-tunnel walls on the experimental results.

It may be worth noting again that the formulation reduces to appropriate formulae in the particular cases considered in Appendix A. Also, the lifting surface theories can be derived as a limiting case of this formulation.

SECTION 9

CONCLUDING REMARKS

A general theory of steady and unsteady, compressible aerodynamic flow around a lifting body having arbitrary shape and motion has been developed. The theory is based upon the classical Green function method. This yields an integral-differential representation of the velocity potential. For the important practical case of small perturbation, if the control point is on the surface of the body, the representation reduces to an integral differential equation relating the potential on the surface to its normal derivative. In particular, for small harmonic oscillations around a rest configuration, one obtains a two-dimensional Fredholm integral equation of second type. This formulation reduces properly to lifting surface theories and other classical results. The question of uniqueness was examined and it was found that, for thin wings, although the operator becomes singular as the thickness approaches zero, good numerical results can be obtained even for thickness ratio, $\tau = .001$.

In conclusion, the formulation developed here can be used for efficient numerical solution of a large variety of problems for which no satisfactory methods are available. Hence, the method should be more convenient than existing ones, even for very simple problems, as the rectangular wing in steady subsonic flow presented here.

REFERENCES

1. Garrick, I. E., "Nonsteady Wing Characteristics," High Speed Aerodynamics and Jet Propulsion, Vol. 7, Section F, Princeton University Press, 1957.
2. Ashley, H., Widnall, S., and Landahl, M. T., "New Directions in Lifting Surface Theory," AIAA J., Vol. 3, No. 1, Jan. 1965, pp. 3-16.
3. Landahl, M. T. and Stark, V. J. E., "Numerical Lifting-Surface Theory -- Problems and Progress," AIAA J., Vol. 6, No. 11, Nov. 1968, pp. 2049-2060.
4. Albano, E. and Rodden, W. P., "A Doublet-Lattice Method for Calculating Lift Distribution on Oscillating Surfaces in Subsonic Flows," AIAA J., Vol. 7, No. 2, Feb. 1969, pp. 279-285.
5. Baals, D. D., Robins, A. W. and Harris, R. V., Jr., "Aerodynamic Design Integration of Supersonic Aircraft," Journal of Aircraft, Vol. 7, No. 5, Sept. - Oct. 1970, pp. 385-394.
6. Djojodihardjo, R. H. and Widnall, S. E., "A Numerical Method for the Calculation of Nonlinear Unsteady Lifting Potential Flow Problems," AIAA J., Vol. 7, No. 10, Oct. 1969, pp. 2001-2009.
7. Schwartz, L., Theorie des Distributions, Hermann, Paris, 1966, pp. 13-61.

8. Watkins, C. E., Runyan, H. S. and Woolston, D. S.,
"On the Kernel Function of the Integral Equation
Relating the Lift and Downwash Distributions of Os-
cillating Finite Wings in Subsonic Flow," NACA Report
1234, 1955. (Supercedes NACA TN 3131).
9. Davies, D. E., "Calculation of Unsteady Generalized
Airforces on a Thin Wing Oscillating Harmonically in
Subsonic Flow", A.R.C., R.M. 3409, 1963 (Replaces
R.A.E. Rep. No. Structures 290- A.R.C. 25 323).
10. Garrick, I. E. and Rubinow, S. I., "Theoretical Study
of Air Forces on an Oscillating or Steady Thin Wing
in a Supersonic Main Stream", NACA TN 1383, 1947.
11. Morse, P. M. and Feshbach, H., Methods of Theoretical
Physics, McGraw-Hill, N.Y., 1953, pp. 791-856.
12. Smirnov, V. I., A Course of Higher Mathematics, Vol.II,
Addison-Wesley Publ. Co., Reading, 1964, pp. 600-603.
13. Ward, G. N., Linearized Theory of Steady High-Speed
Flow, University Press, Cambridge, 1955.
14. Yates, E. C. Jr., "Flutter and Unsteady Lift Theory',
in Performance and Dynamics of Aerospace Vehicles,
NASA SP. 258, 1971, pp. 289-374.
15. Watkins, C. E. and Berman, J. H., "On the Kernel
Function of the Integral Equation Relating Lift and
Downwash Distributions of Oscillating Wings in Super-
sonic Flow", NACA Rep. 1257, 1956 (Supercedes NACA
TN 3438).

16. Pines, S., Dugundji, J. and Neuringer, J., "Aero-dynamic Flutter Derivatives for a Flexible Wing With Supersonic and Subsonic Edges", J. Aero. Sciences, Vol. 22, No. 10, Oct. 1955, pp. 693-700.
17. Smirnov, A. I., A Course of Higher Mathematics, Vol. IV, Addison-Wesley Publ. Co., Reading, 1964, pp. 568-630.
18. Lessing, H. C., Troutman, J. C. and Menees, G. P., "Experimental Determination of the Pressure Distribution on a Rectangular Wing Oscillating in the First Bending Mode for Mach Numbers from 0.24 to 1.30," NASA TN D-344, 1960.
19. Cunningham, A. M. Jr., "An Efficient, Steady Subsonic Collocation Method for Solving Lifting-Surface Problems," J. Aircraft, Vol. 8, No. 3, March 1971, pp. 168-176.
20. Chiuchiolo, E.A., "Steady Incompressible Potential Flow Around Lifting Bodies Immersed in a Fluid", Boston Univ., Department of Aerospace Engineering, Master Thesis, 1974.
21. Yates, E. C. Jr. and Bland, S. R., "Comparative Evaluation of Methods for Predicting Flutter and Divergence of Unswept Wings of Finite Span," NASA TN D-2051, 1963.
22. Lighthill, M.J., Introduction to Fourier Analysis and Generalized Function, University Press, Cambridge, 1964.
23. Watson, G. N., A Treatise on the Theory of Bessel Functions, Second Ed., The MacMillan Co., 1948.

24. Van Dyke, M., Perturbation Methods in Fluid Mechanics, Academic Press, 1964, pp. 59-68.
25. Ashley, H., and Rodden, W.P., "Wing-Body Aerodynamic Interaction," Annual Review of Fluid Mechanics, Vol. 4, 1972, pp. 431-472.
26. Haviland, J.K., "Downwash-Velocity Potential Method for Lifting Surfaces," AIAA J., Vol. 9, No. 11, Nov. 1971, pp. 2268-2269.
27. Lamb, Sir H., Hydrodynamics, 6th Ed., Dover, N.Y., 1945, pp. 58-61.
28. Hess, J.L., and Smith, A.M.O., "Calculation of Potential Flow About Arbitrary Bodies", Progress in Aeronautical Sciences , Vol. 8, Pergamon Press, N.Y., 1966.
29. Hess, J.L., "Calculation of Potential Flow About Arbitrary Three-Dimensional Lifting Bodies", Douglas Report MDC-J5679-01, October 1972.

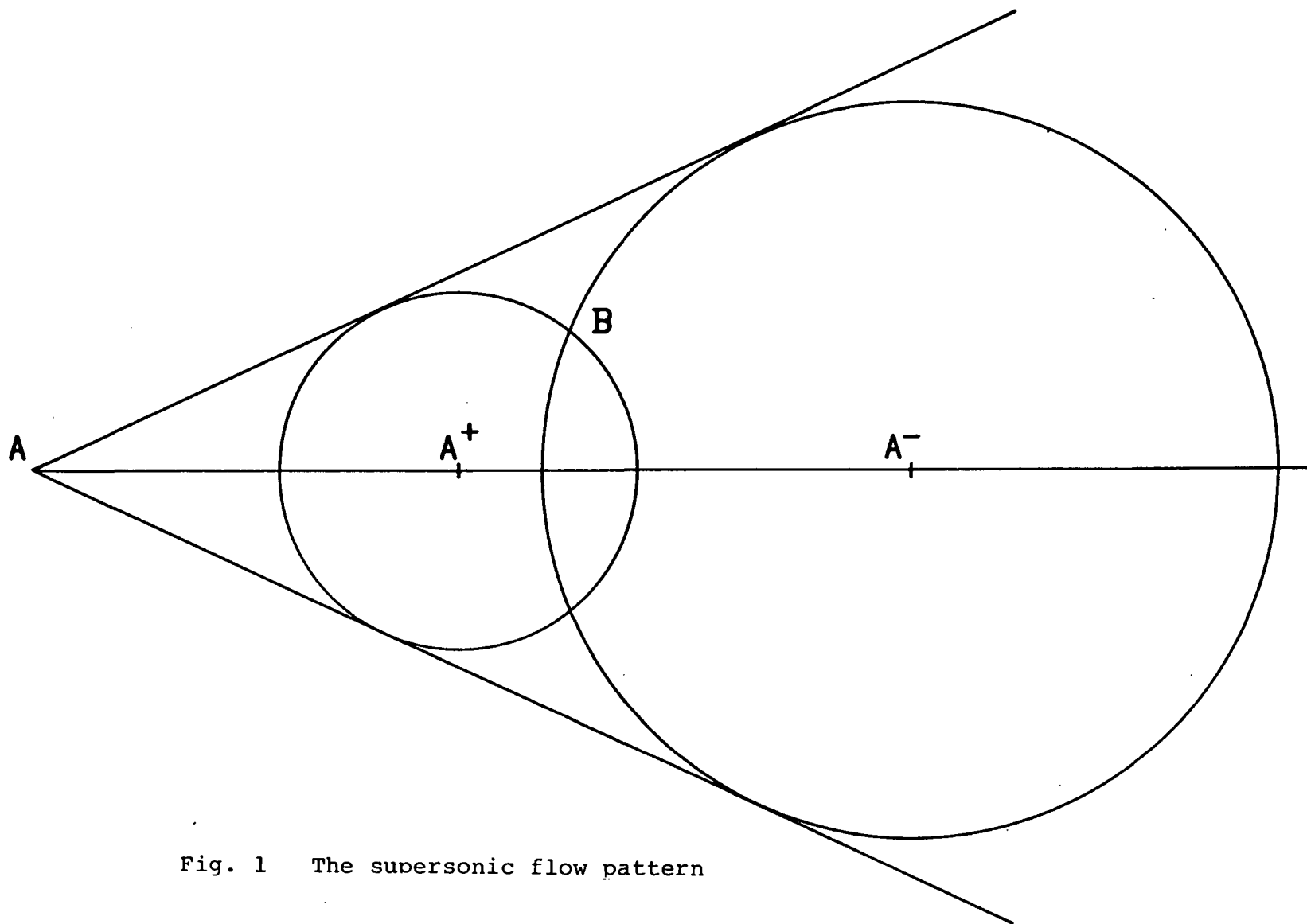


Fig. 1 The supersonic flow pattern

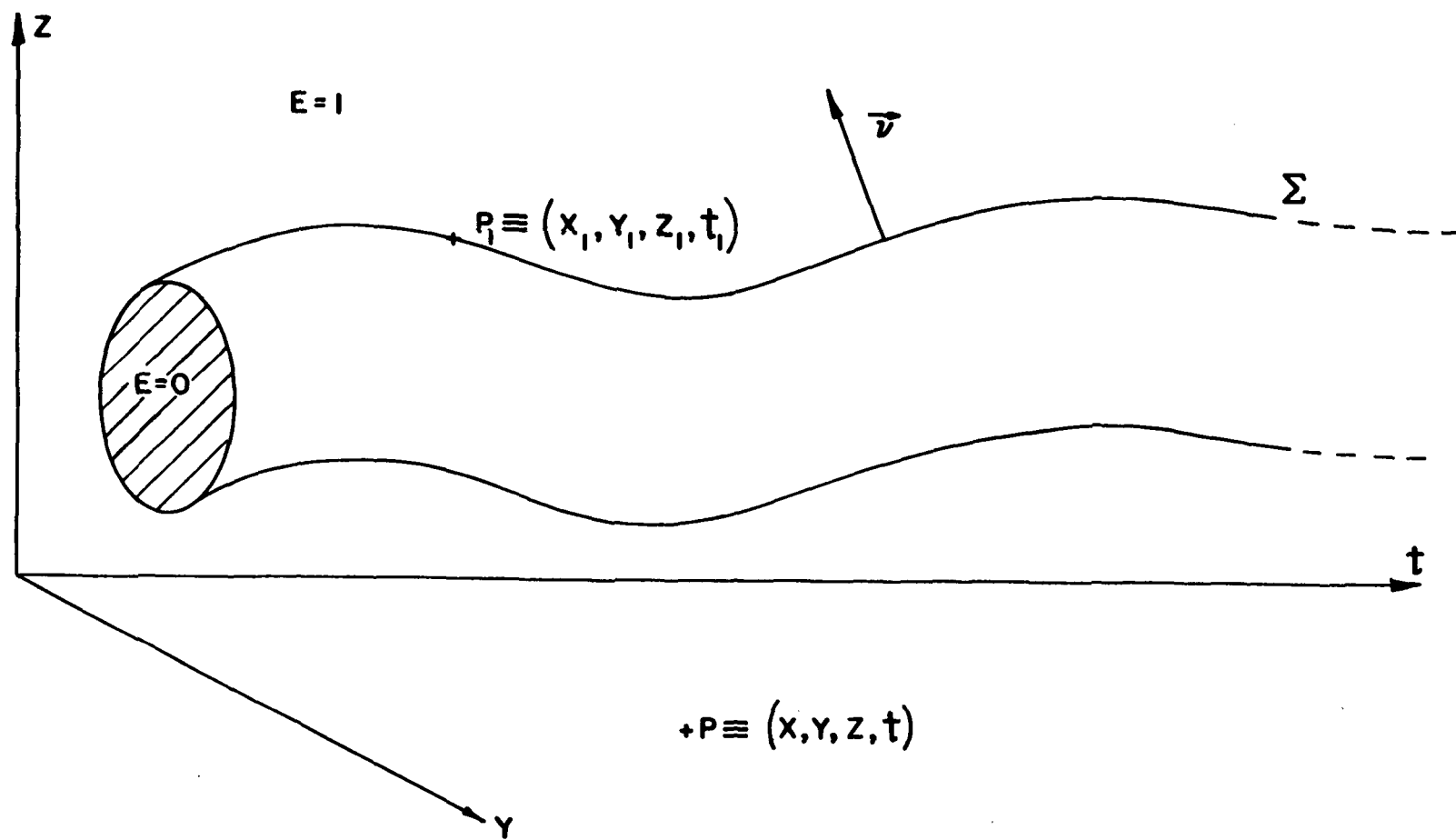


Fig. 2 The hypersurface Σ

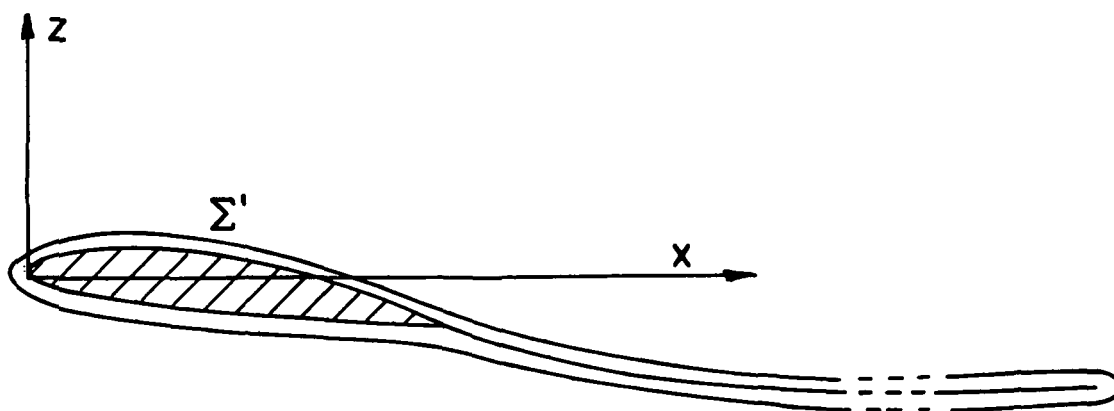


Fig. 3a The surface Σ'

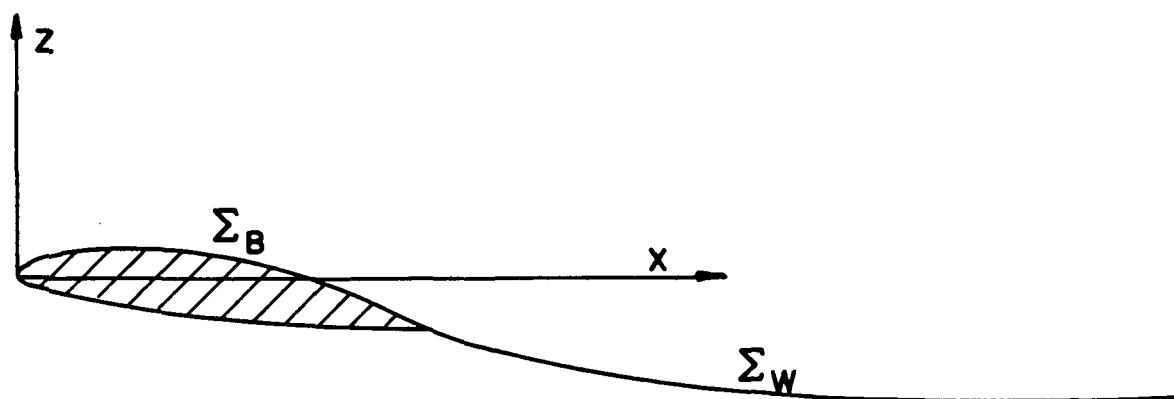


Fig. 3b The surfaces Σ_B and Σ_W

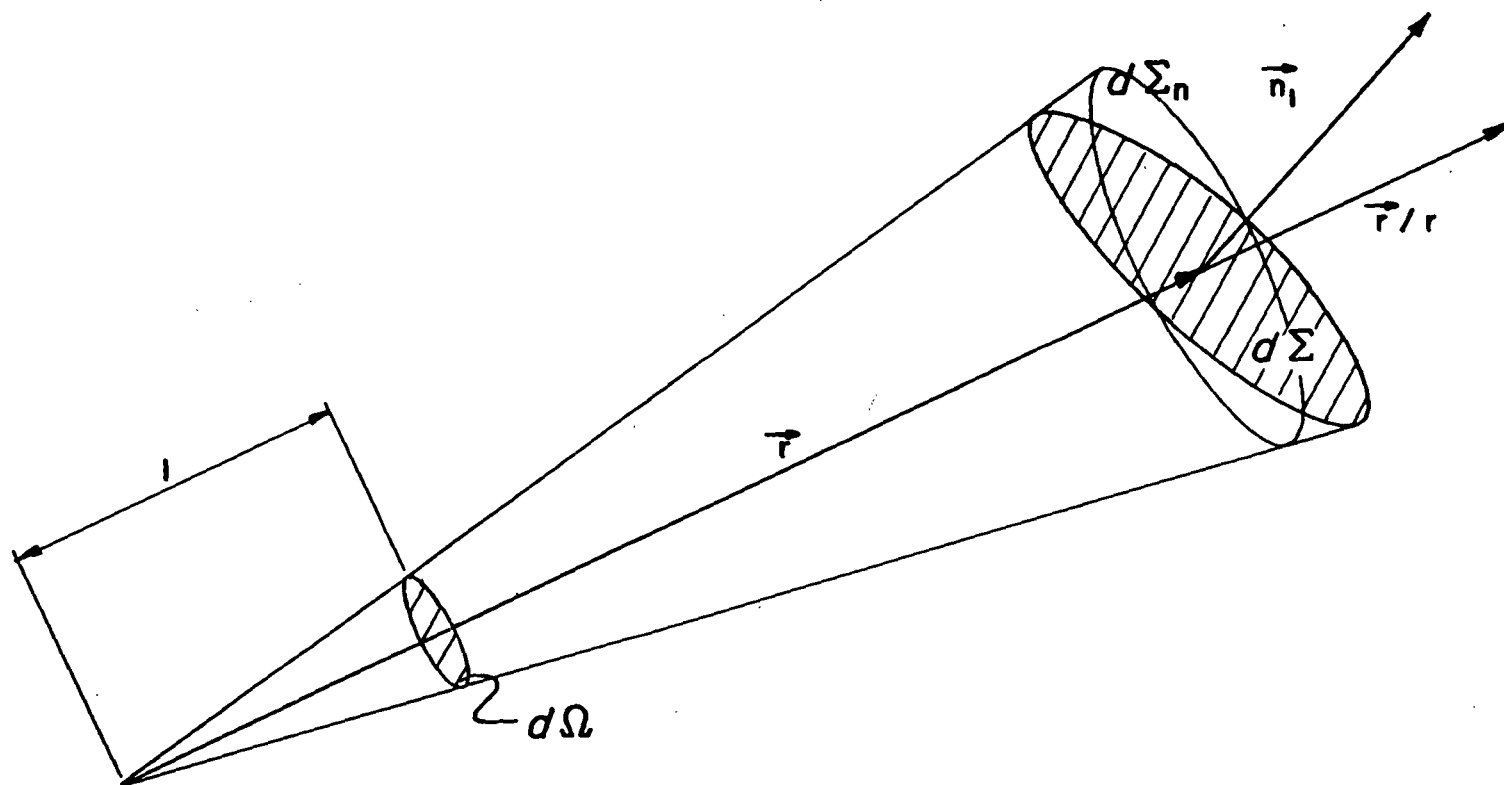


Fig. 4 Solid angle Ω

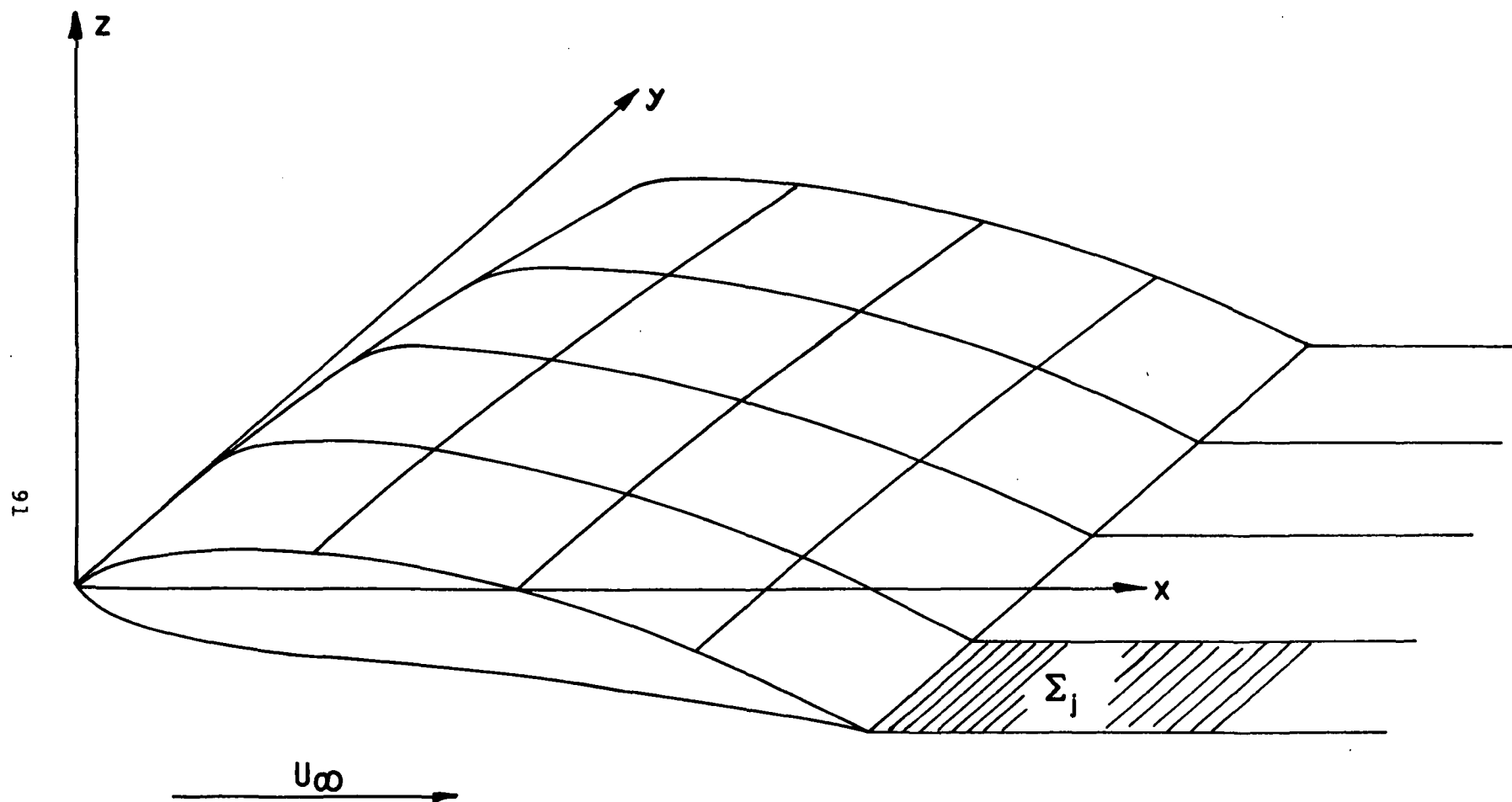


Fig. 5 Treatment of the wake

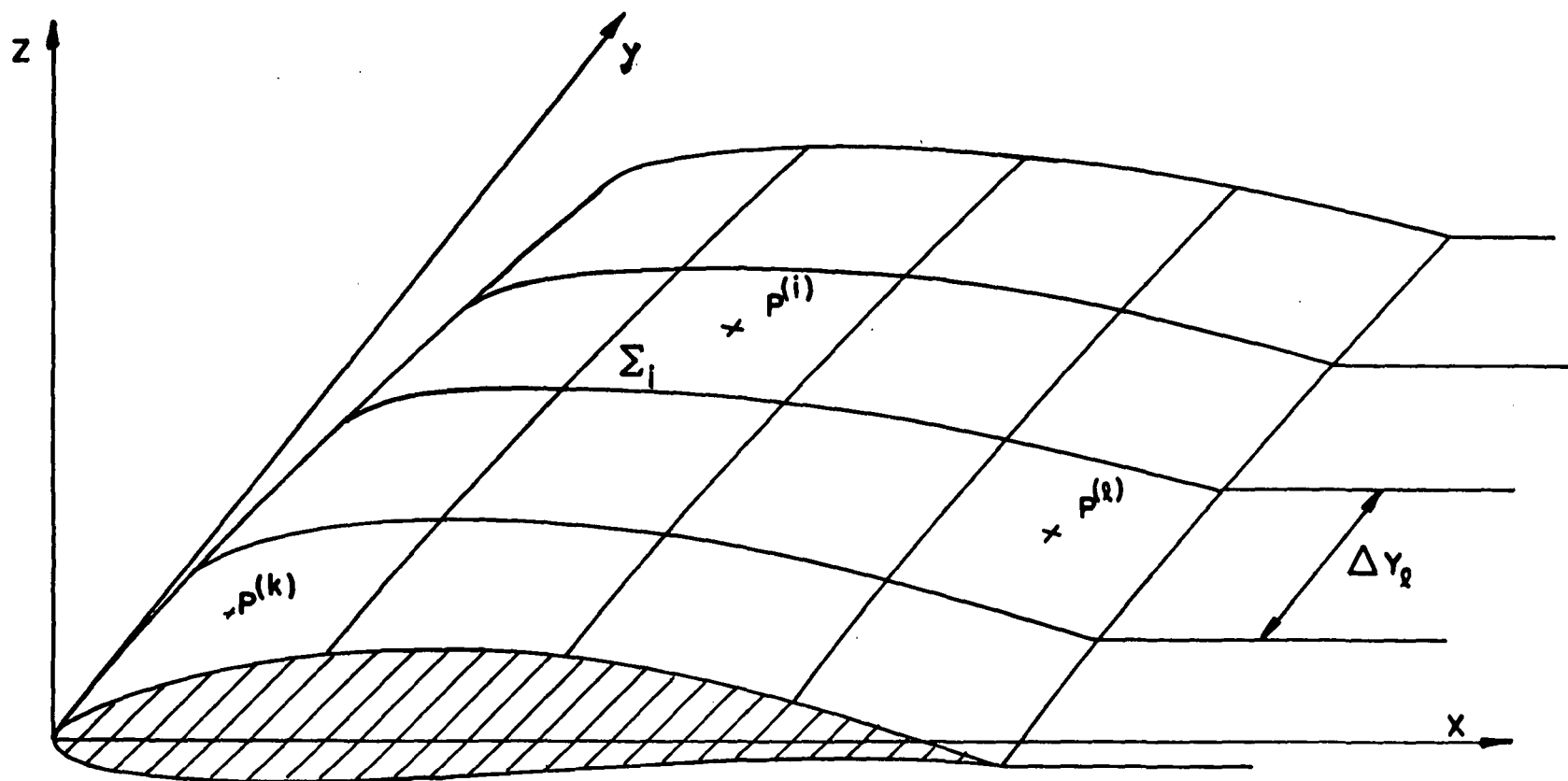


Fig. 6 Boxes and control points

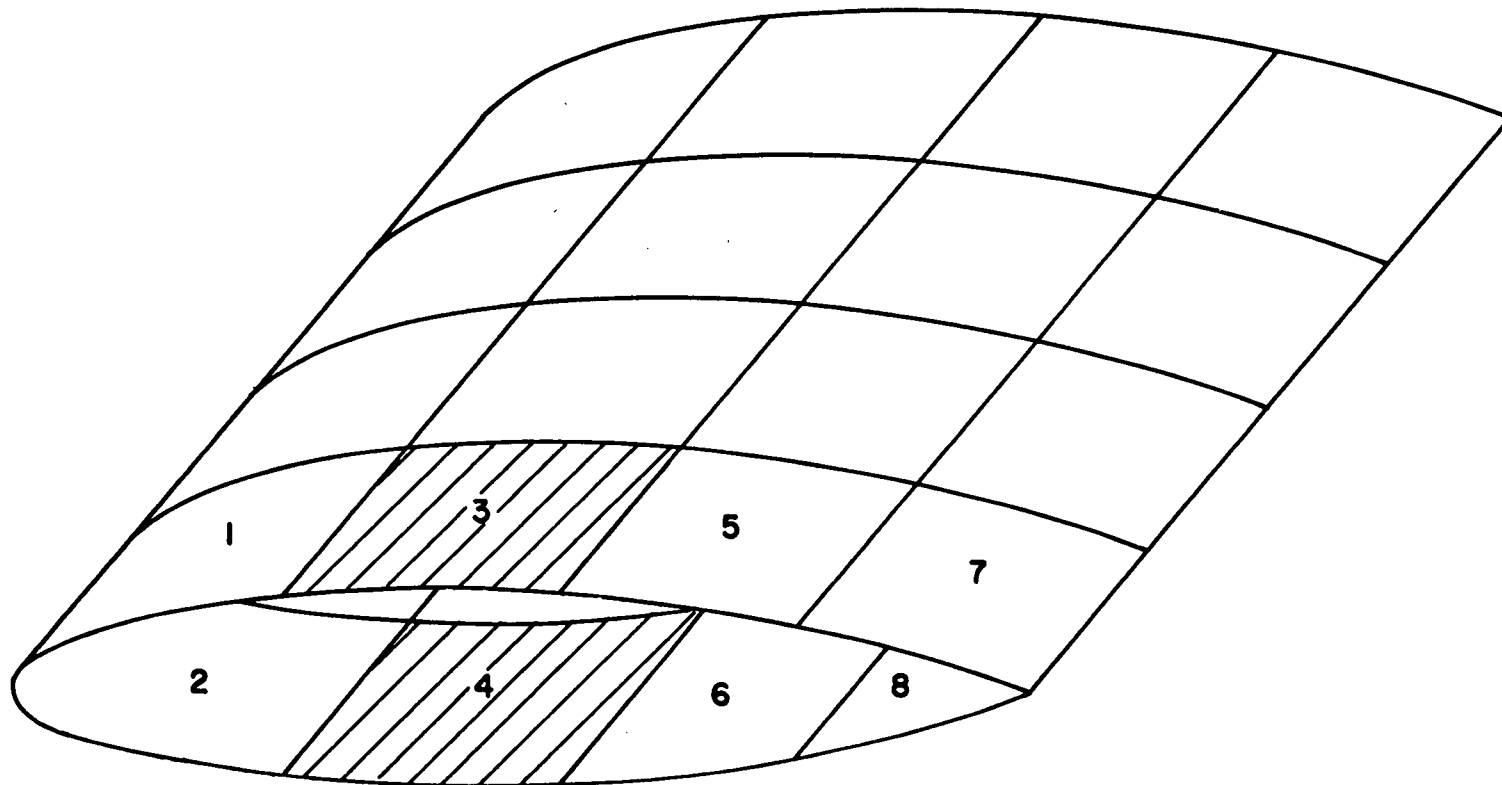


Fig. 7 Definition of opposite boxes

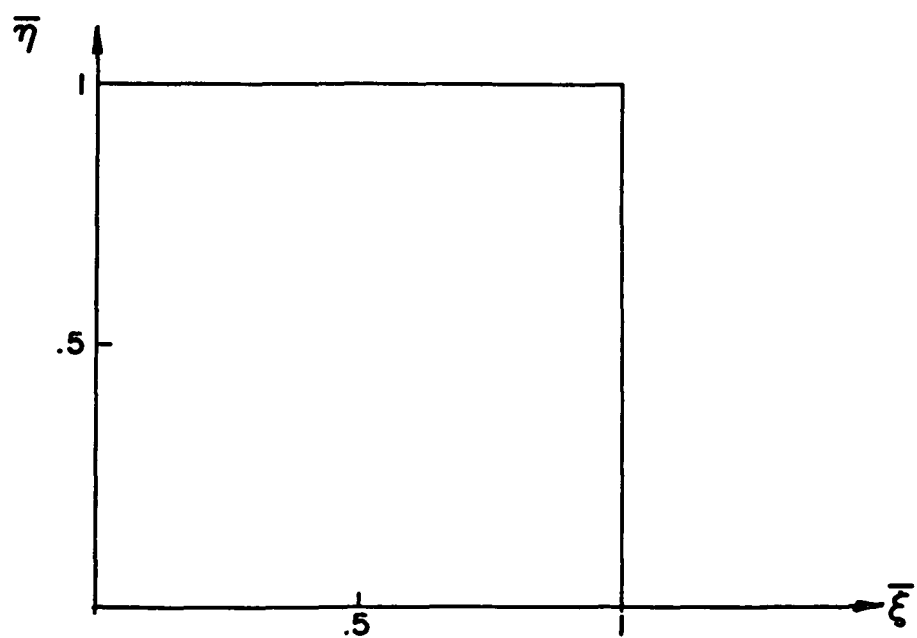
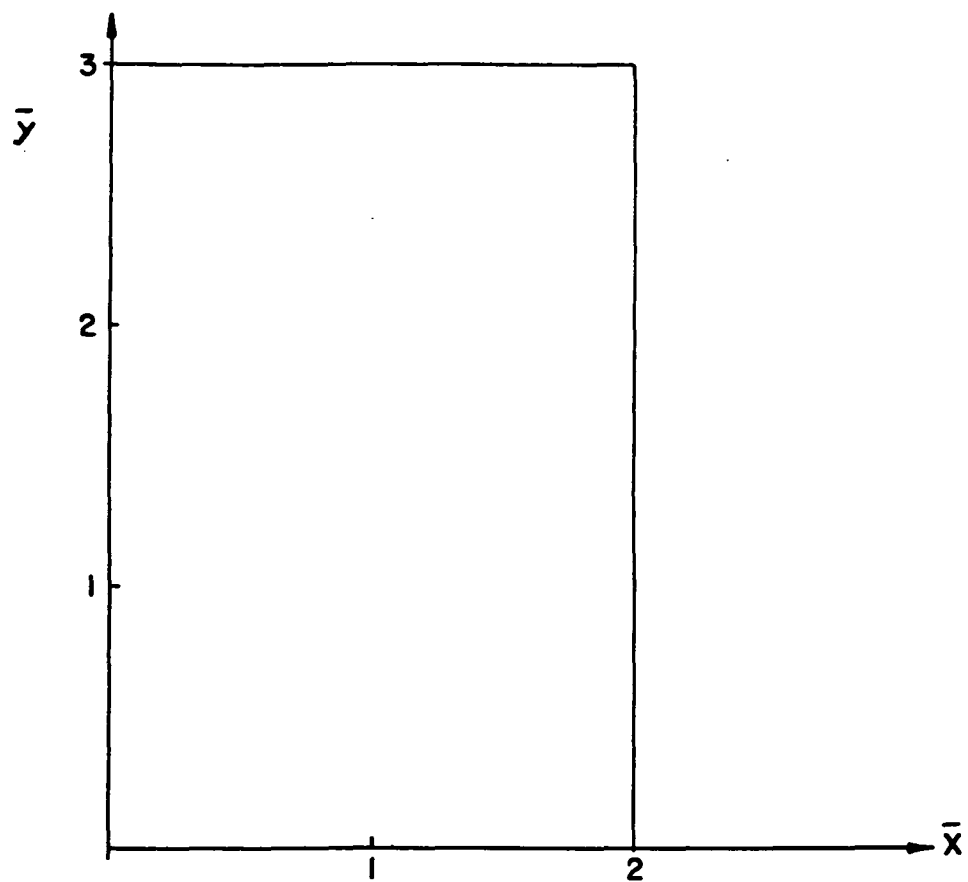


Fig. 8 Transformation $(\bar{x}, \bar{y}) \rightarrow (\bar{\xi}, \bar{\eta})$

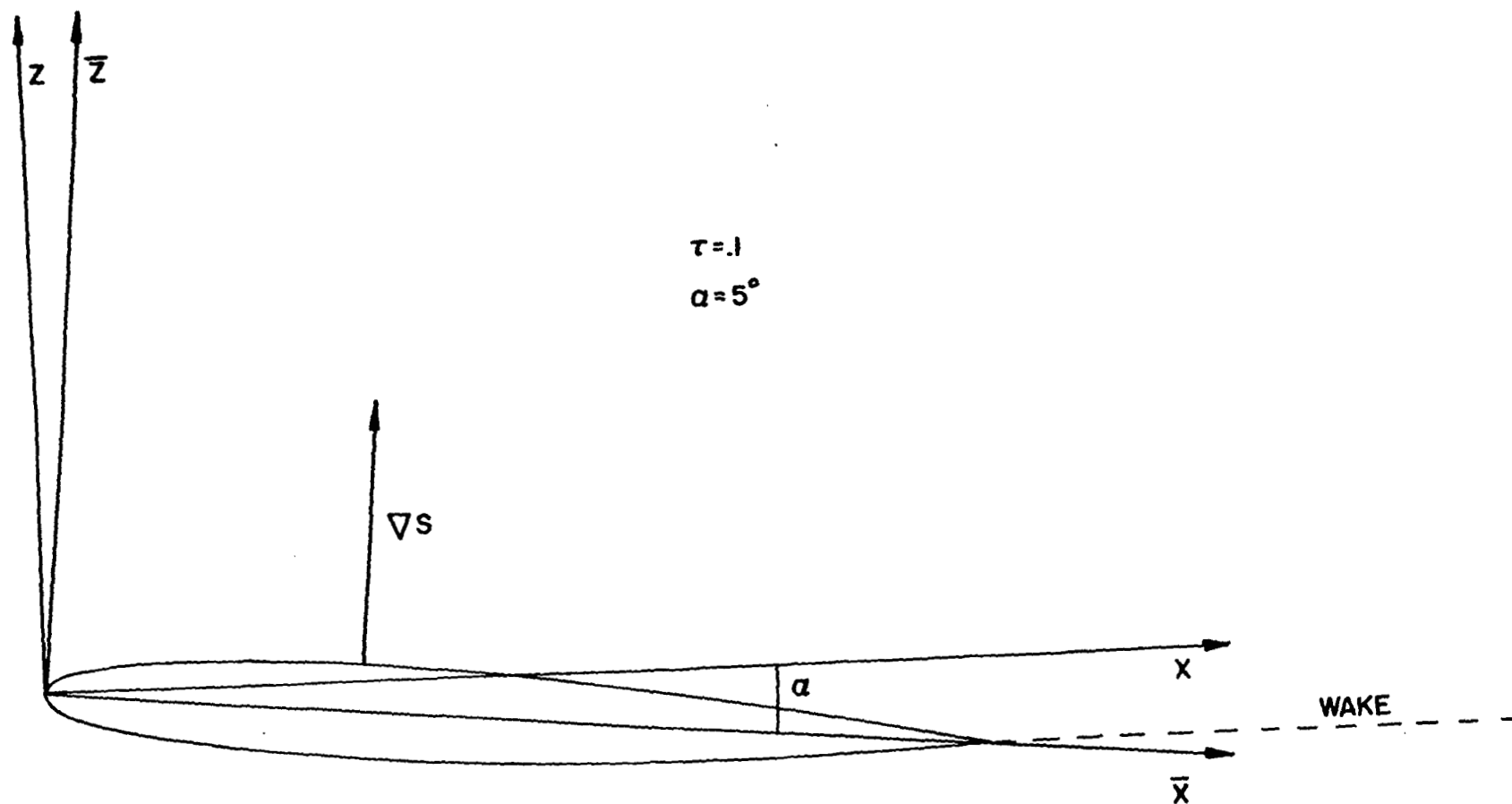


Fig. 9 Geometry of the problem

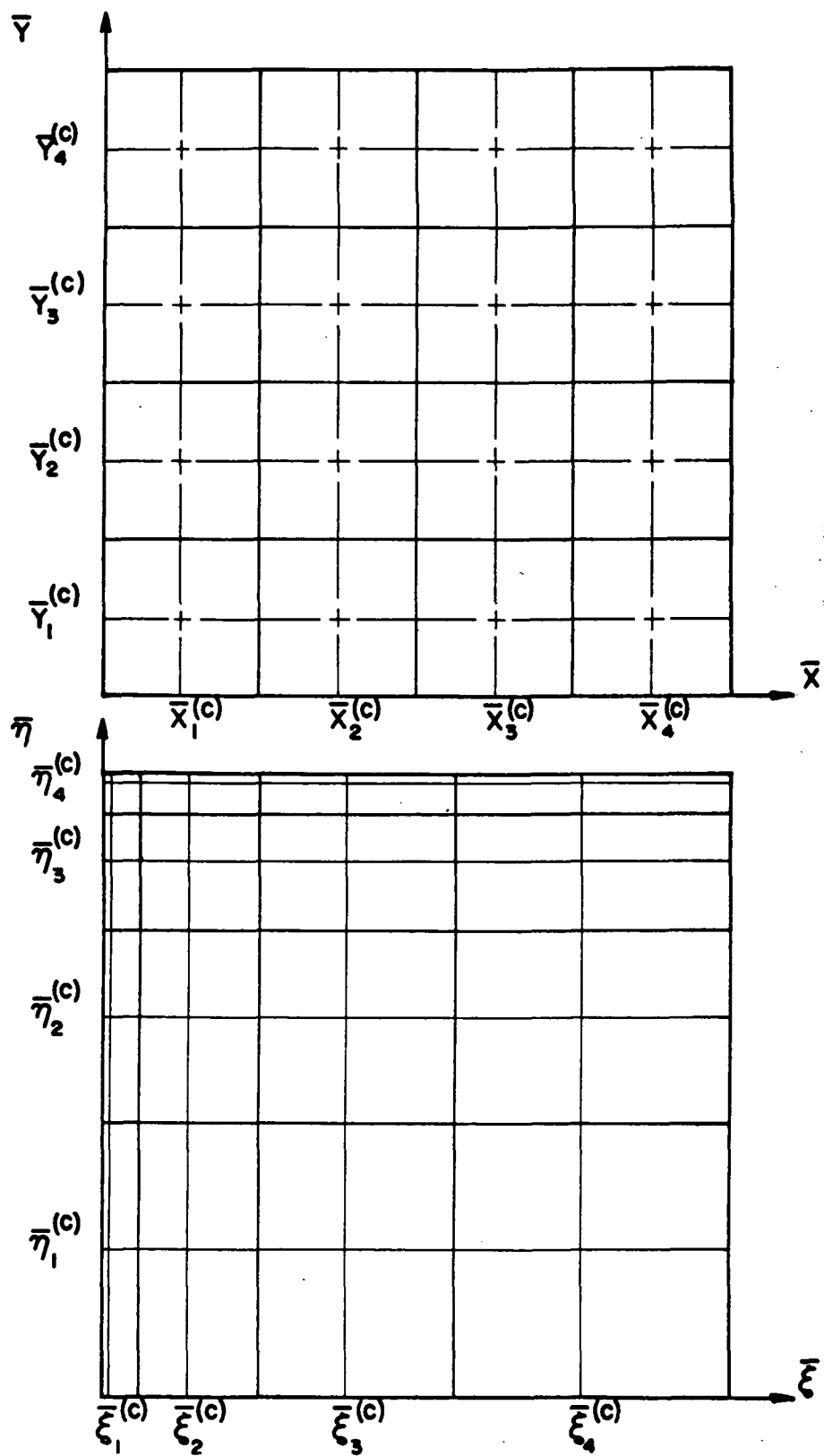


Fig. 10 Transformation $(\bar{\xi}, \bar{\eta}) \rightarrow (\bar{X}, \bar{Y})$

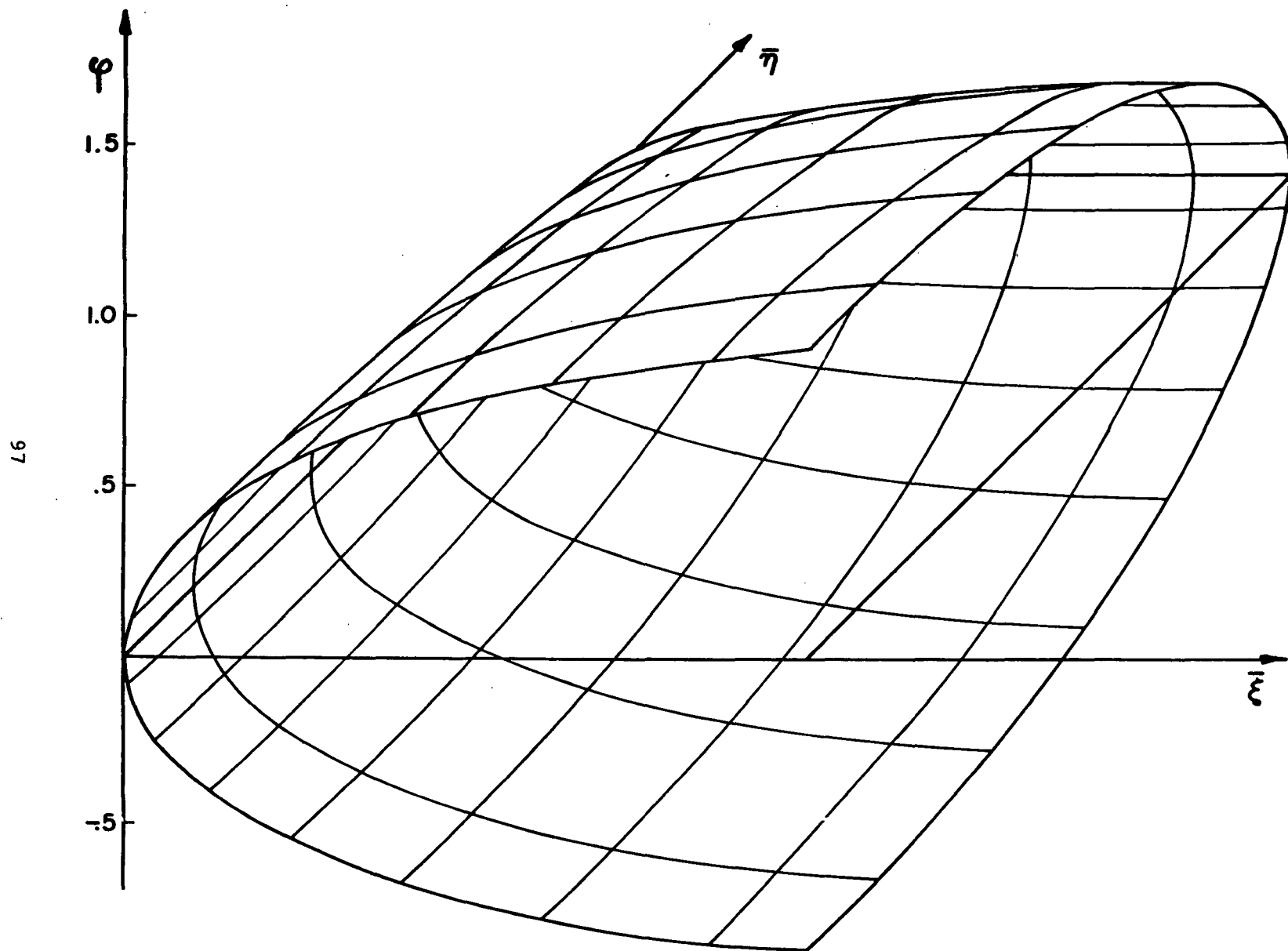


Fig. 11 Potential distribution for a rectangular wing with aspect ratio $b/c = 3$, angle of attack $\alpha = 5^\circ$ and Mach number $M = .24$

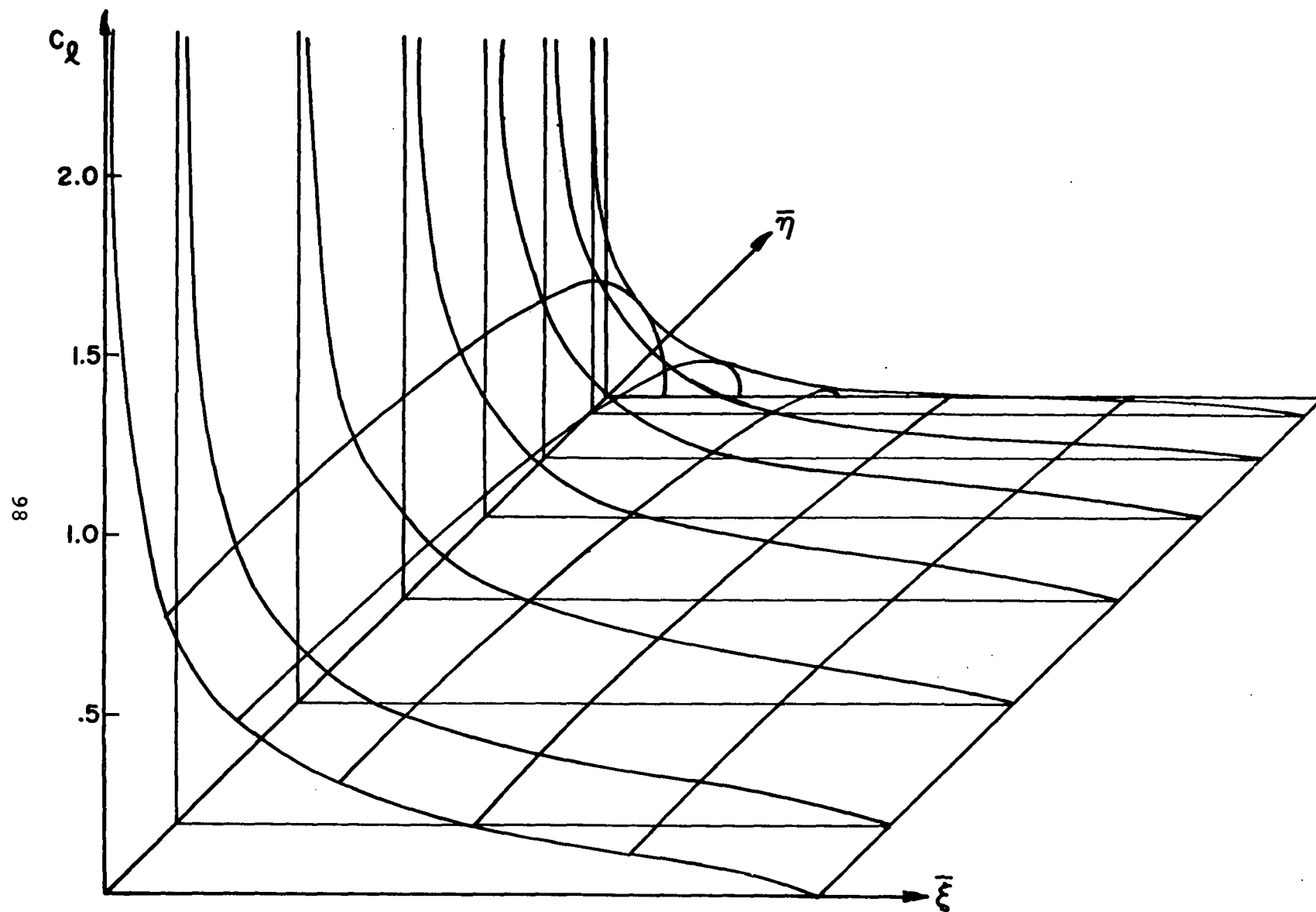


Fig. 12 Lift coefficient distribution for a rectangular wing with aspect ratio $b/c = 3$, angle of attack $\alpha = 5^\circ$ and Mach number $M = .24$

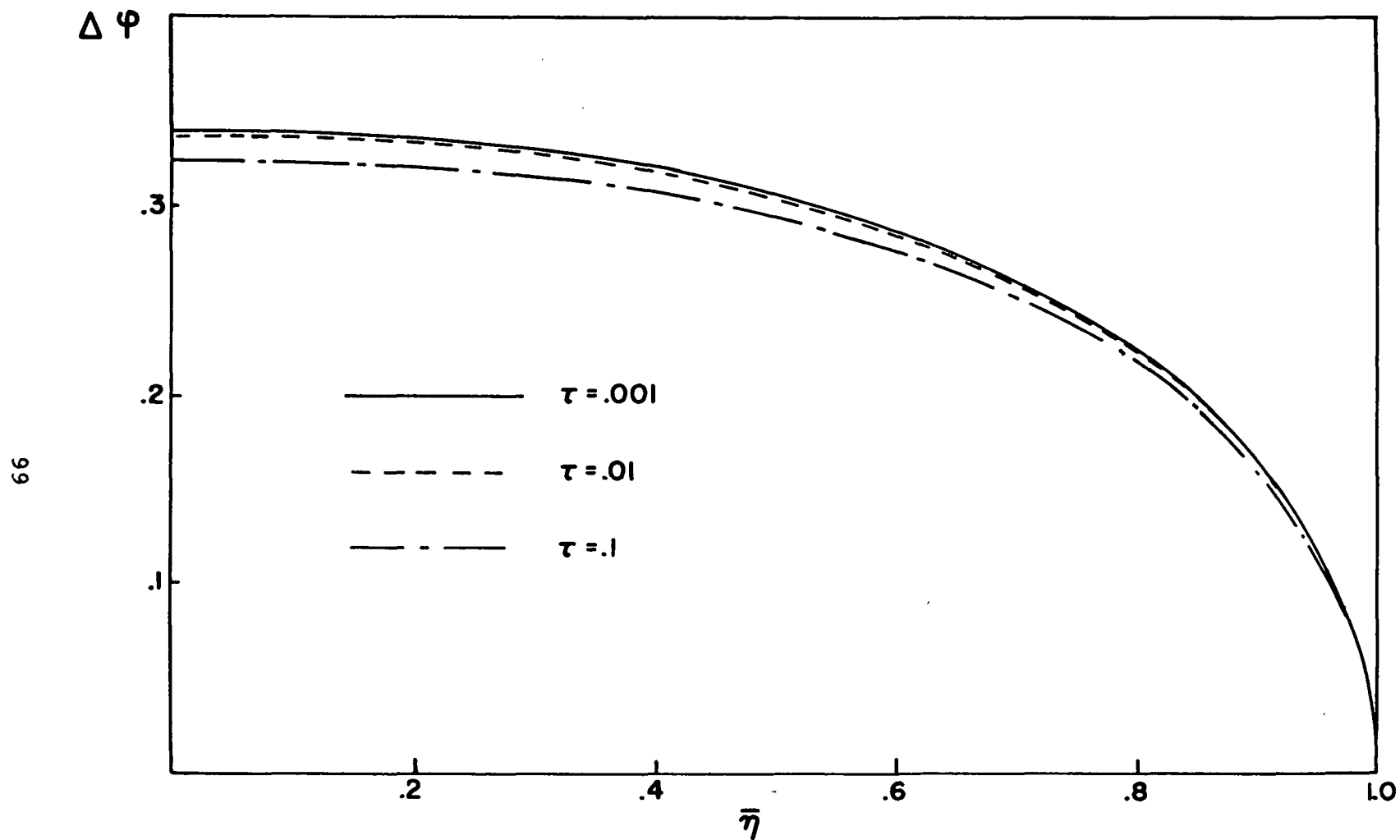


Fig. 13 Effect of decreasing thickness on the numerical scheme: Potential difference at the trailing edge boxes for $NX = NY = 4$ and different values of the thickness ratio, τ , for a rectangular wing with aspect ratio $b/c = 3$, angle of attack $\alpha = 5^\circ$ and Mach number $M = .24$

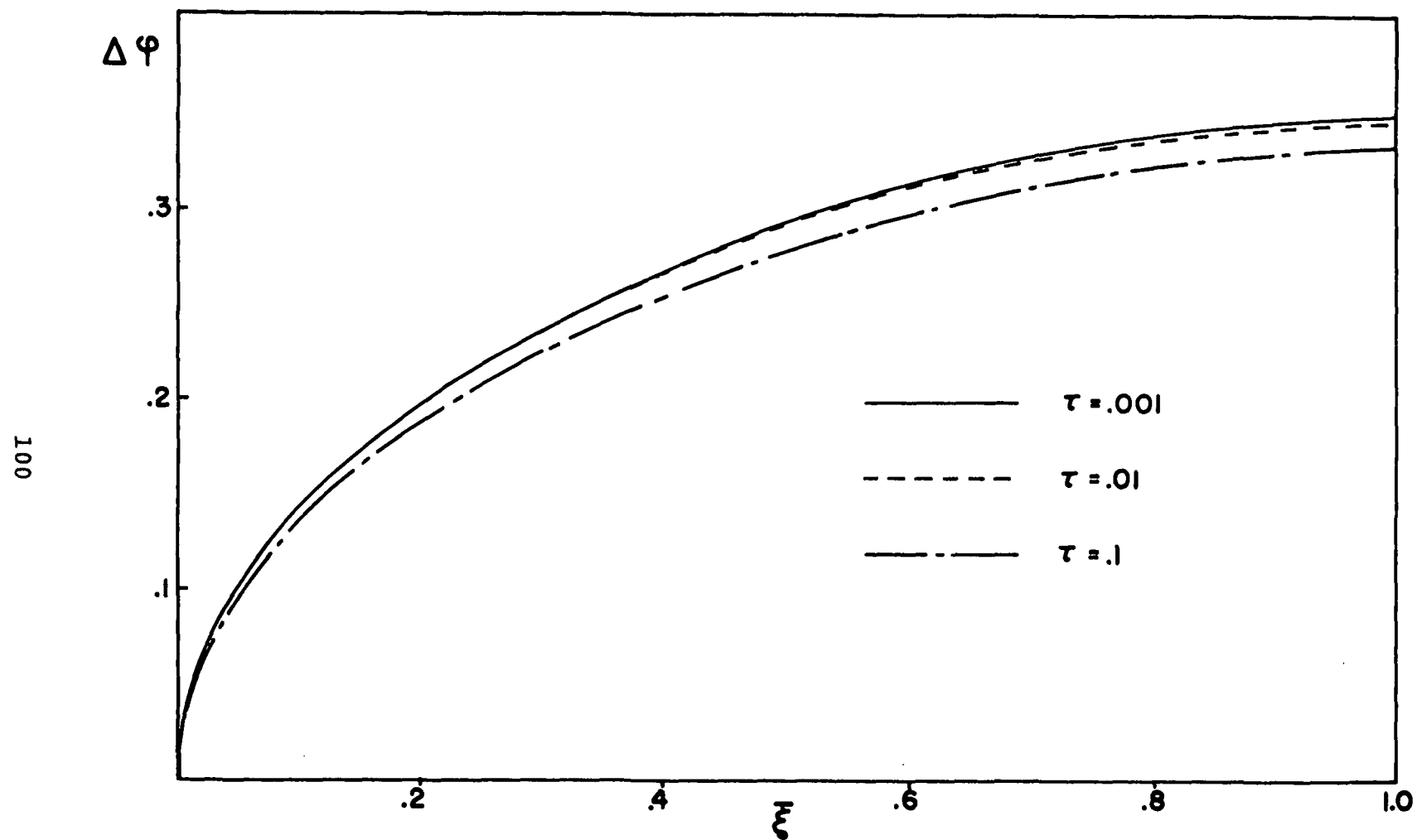


Fig. 14 Effect of decreasing thickness on the numerical scheme: Potential difference at the root boxes for $NX = NY = 4$ and different values of the thickness ratio, τ , for a rectangular wing with aspect ratio $b/c = 3$, angle of attack $\alpha = 5^\circ$ and Mach number $M = .24$

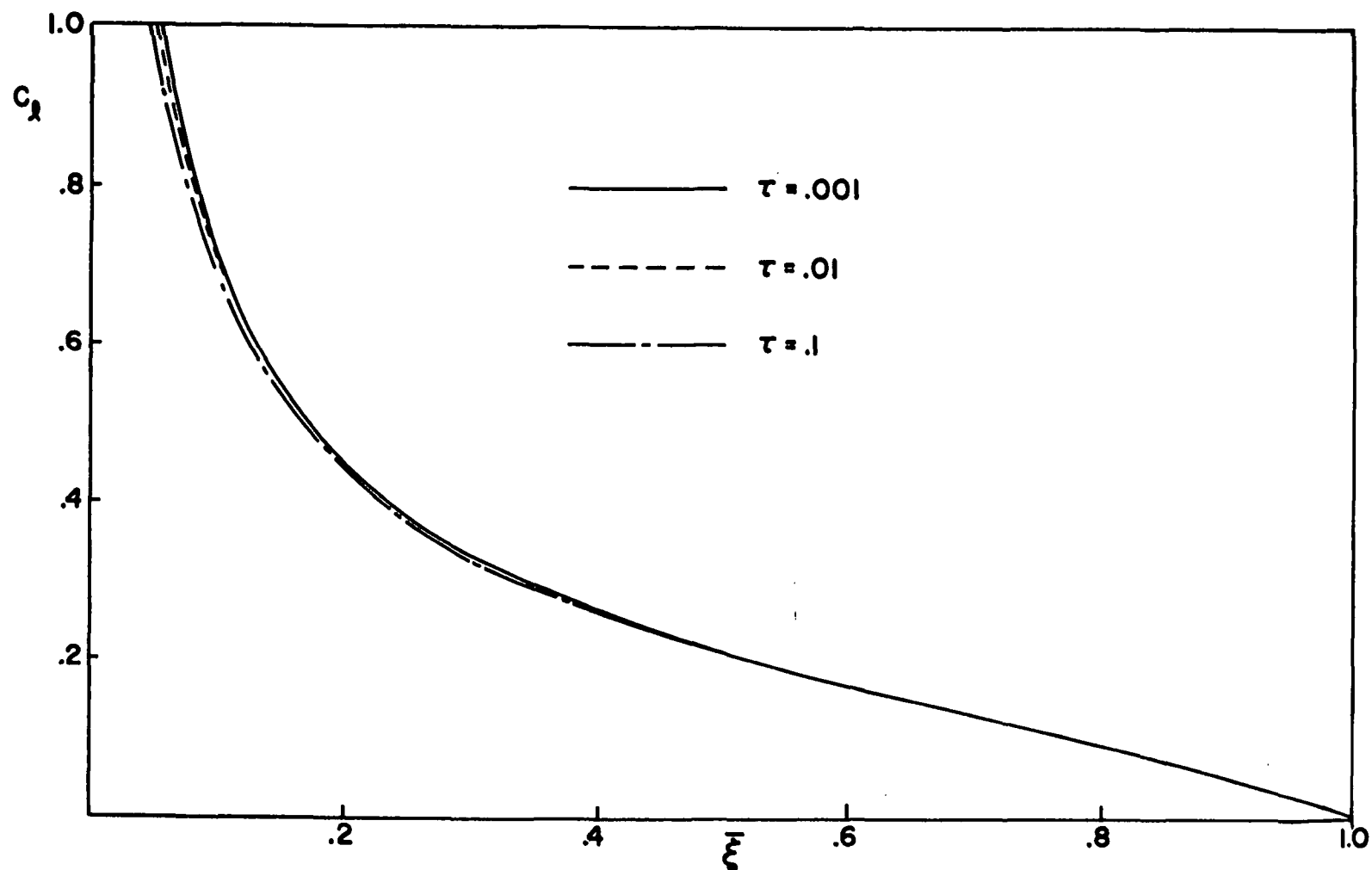


Fig. 15 Effect of decreasing thickness on the numerical scheme: Lifting pressure coefficient at the root boxes for $NX = NY = 4$ and different values of the thickness ratio, τ , for a rectangular wing with aspect ratio $b/c = 3$, angle of attack $\alpha = 5^\circ$ and Mach number $M = .24$

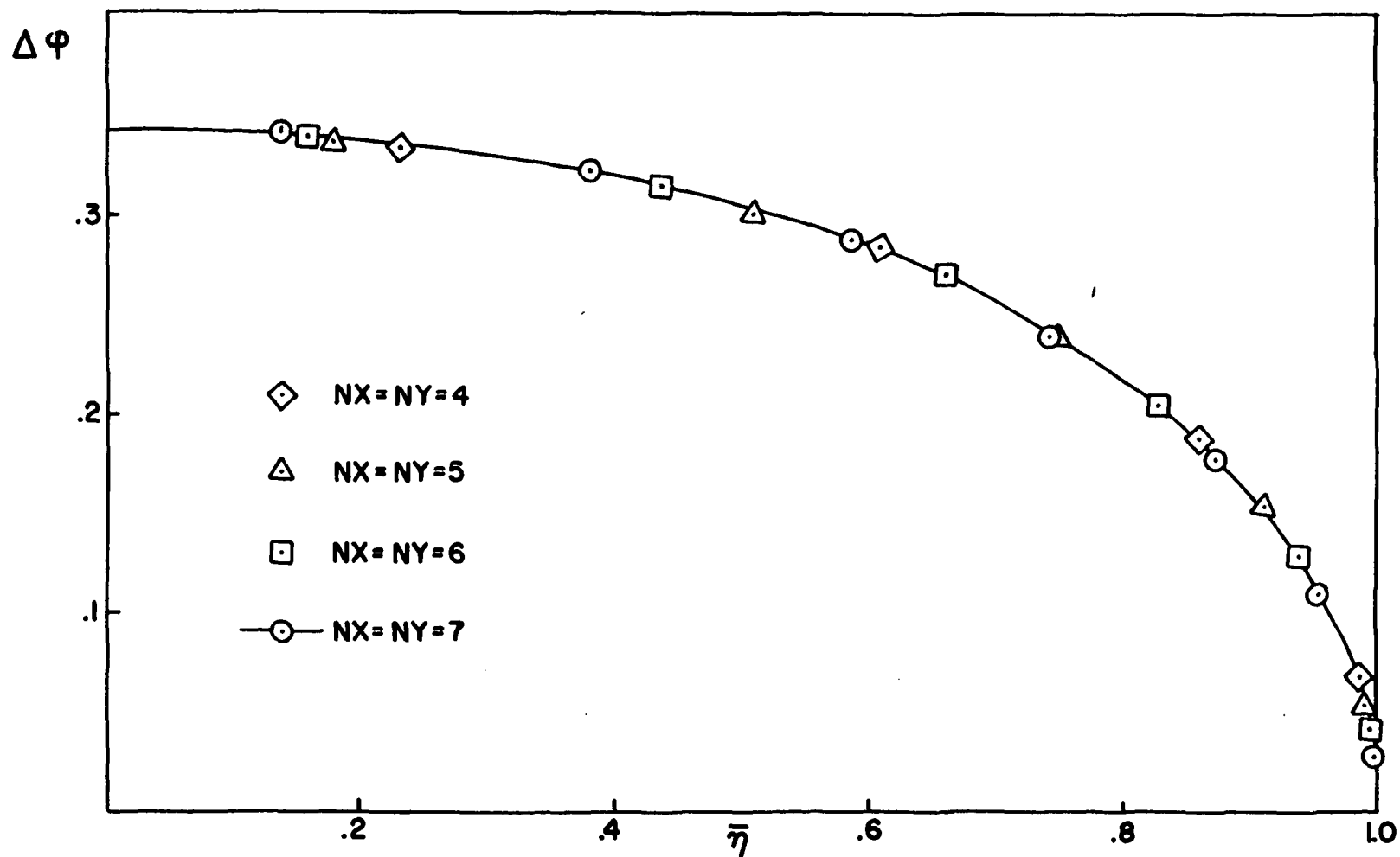


Fig. 16 Potential difference at trailing edge boxes for thickness ratio $\tau = .001$ and different values of NX and NY for a rectangular wing with aspect ratio $b/c = 3$, angle of attack $\alpha = 5^\circ$ and Mach number $M = .24$

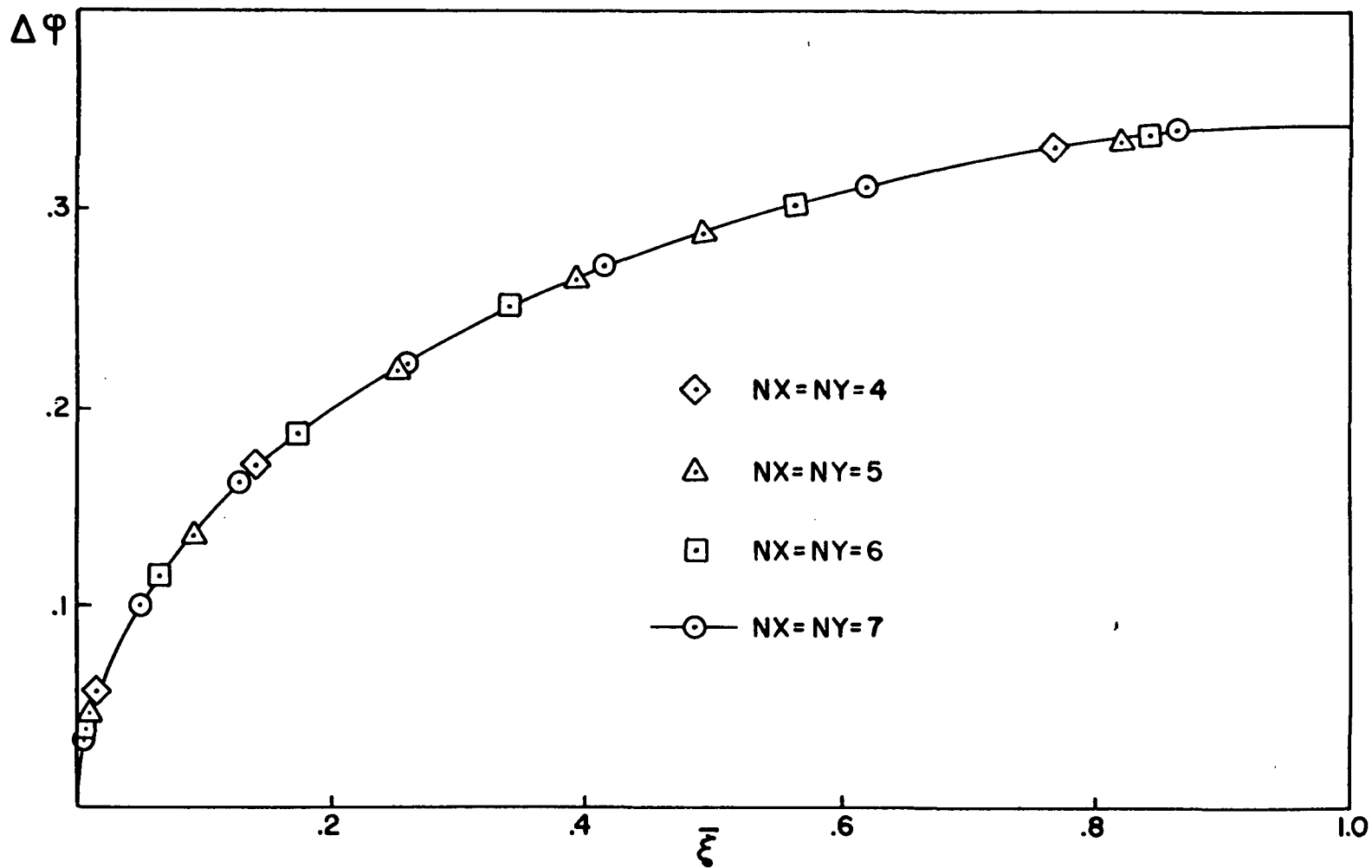


Fig. 17 Potential difference at the root boxes for thickness ratio $\tau = .001$ and different values of NX and NY for a rectangular wing with aspect ratio $b/c = 3$, angle of attack $\alpha = 5^\circ$ and Mach number $M = .24$

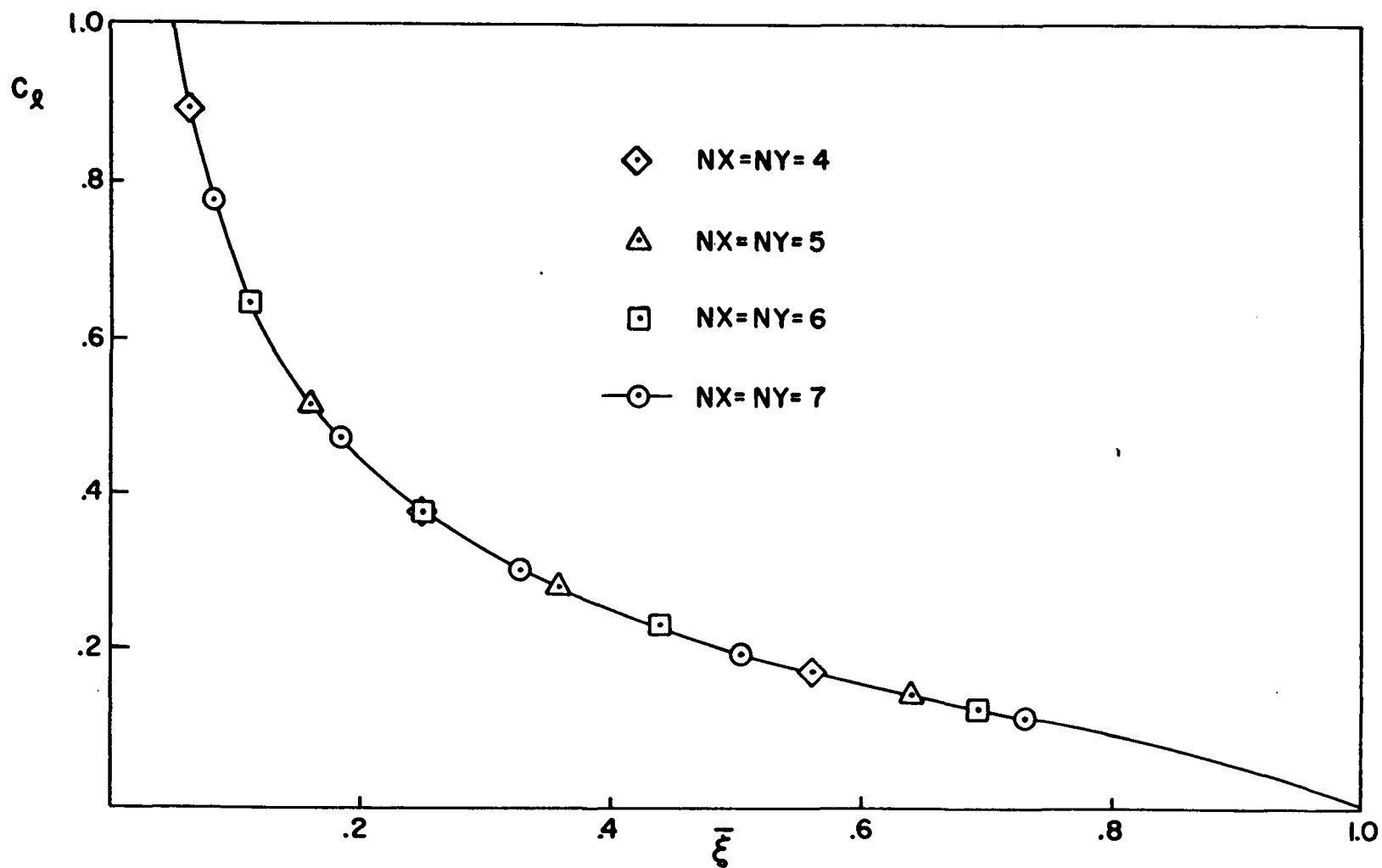


Fig. 18 Lifting pressure coefficient at root boxes for thickness ratio $\tau = .001$ and different values of NX and NY for a rectangular wing with aspect ratio $b/c = 3$, angle of attack $\alpha = 5^\circ$ and Mach number $M = .24$

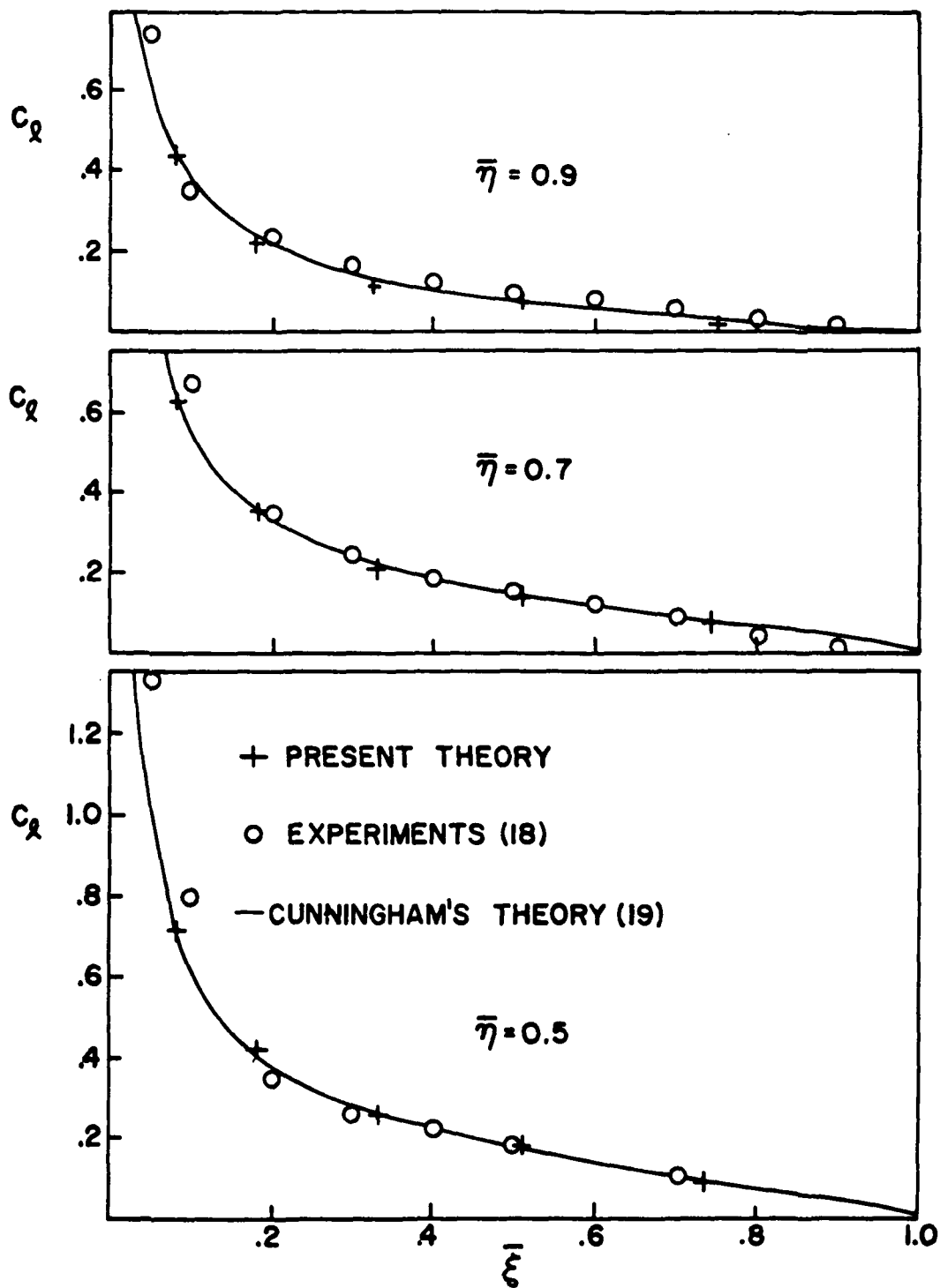


Fig. 19 Comparison with existing results for a rectangular wing with aspect ratio $b/c = 3$, angle of attack $\alpha = 5^\circ$ and Mach number $M = .24$

APPENDIX A

TWO FUNDAMENTAL FORMULAE

In Subsection 3.3, the formulae

$$\int_{-\infty}^{\infty} \int_{-\infty}^{\infty} f \delta_{\Sigma} \delta_{\tau} dV_1 dt_1 = \oint_{\Sigma^{\tau}} f^{\tau} \frac{|\nabla S|^{\tau}}{|\nabla S^{\tau}|} d\Sigma^{\tau} \quad A.1$$

and

$$\int_{-\infty}^{\infty} \int_{-\infty}^{\infty} f \delta_{\Sigma} \frac{\partial \delta_{\tau}}{\partial t_1} dV_1 dt_1 = - \frac{\partial}{\partial t} \oint_{\Sigma^{\tau}} f^{\tau} \frac{|\nabla S|^{\tau}}{|\nabla S^{\tau}|} d\Sigma^{\tau} \quad A.2$$

were used (see Eqs. 3.25 and 3.26) to derive the generalized Huygens' Principle. In this Appendix, it is shown that A.1 and A.2 are valid for any "good function", as defined by Lighthill.²² The concept used in the following is very similar to the one introduced in Ref. 22.

In order to prove Eq. A.1, it is convenient to assume the "surface distribution", δ_{Σ} , as the limiting case of volume distribution in a thin layer of the four-dimensional space (with constant infinitesimal thickness, ϵ') surrounding the surface $S(x, y, z, t) = 0$. This is equivalent to the classical procedure of defining a surface integral (which is connected to the distribution δ_{Σ} , see Eq. 3.7) as a limiting case of a volume integral. Thus define

A.3

where the "layer function" L (similar to the function E defined by Eq. 3.1 is defined by

$$\begin{aligned} L &= 1 && \text{inside the layer} \\ &= 0 && \text{outside the layer} \end{aligned} \quad \text{A.4}$$

More precisely, the function L has the value one for the points (x'_1, y'_1, z'_1, t'_1) such that

$$\frac{1}{|Q_1 S|} \left| \frac{\partial S}{\partial x_1} (x'_1 - x_1) + \frac{\partial S}{\partial y_1} (y'_1 - y_1) + \frac{\partial S}{\partial z_1} (z'_1 - z_1) + \frac{\partial S}{\partial t_1} (t'_1 - t_1) \right| < \frac{\epsilon'}{2} \quad \text{A.5}$$

In Eq. A.5, all the derivatives of S are evaluated on the surface Σ . Furthermore (x'_1, y'_1, z'_1, t'_1) is a point in the direction of the normal, \vec{v} , to the surface Σ at the point (x_1, y_1, z_1, t_1) . Note that, by definition,

$$S(x_1, y_1, z_1, t_1) = 0 \quad \text{A.6}$$

Combining Eqs. A.3 and A.5 yields

$$\iiint_{-\infty}^{\infty} \delta_{\Sigma} \delta_T dV'_1 dt'_1 = \lim_{\epsilon' \rightarrow 0} \frac{1}{\epsilon'} \iiint_{-\infty}^{\infty} L \delta_T dV'_1 dt'_1 \quad \text{A.7a}$$

Performing the time integration yields

$$\iiint_{-\infty}^{\infty} \delta_{\Sigma} \delta_T dV'_1 = \lim_{\epsilon' \rightarrow 0} \frac{1}{\epsilon'} \iiint_{-\infty}^{\infty} L^T L^T dV'_1 \quad \text{A.7b}$$

The integrand is different from zero only for the points of the layer of the three-dimensional space for which $L^T = 1$. More precisely, the integrand is different from zero for the points for which Eq. A.5 is satisfied with $t_1' = t - T'$ and $t_1 = t - T$; that is, for the points for which

$$\frac{1}{|\nabla S|^T} \left| \left[\frac{\partial S}{\partial x_1} \right]^T (x_1' - x_1) + \left[\frac{\partial S}{\partial y_1} \right]^T (y_1' - y_1) + \left[\frac{\partial S}{\partial z_1} \right]^T (z_1' - z_1) - \left[\frac{\partial S}{\partial t_1} \right]^T (T' - T) \right| < \frac{\epsilon'}{2} \quad \text{A.8}$$

Note that the thickness of the layer is infinitesimal, and thus neglecting higher order terms, $T' - T$ can be expressed as

$$T' - T = \frac{\partial T}{\partial x_1} (x_1' - x_1) + \frac{\partial T}{\partial y_1} (y_1' - y_1) + \frac{\partial T}{\partial z_1} (z_1' - z_1) \quad \text{A.9}$$

where the derivatives are evaluated on the surface

Combining Eqs. A.8 and A.9 yields

$$\begin{aligned} \frac{1}{|\nabla S|^T} \left| \left[\frac{\partial S}{\partial x_1} - \frac{\partial S}{\partial t_1} \frac{\partial T}{\partial x_1} \right]^T (x_1' - x_1) + \left[\frac{\partial S}{\partial y_1} - \frac{\partial S}{\partial t_1} \frac{\partial T}{\partial y_1} \right]^T (y_1' - y_1) \right. \\ \left. + \left[\frac{\partial S}{\partial z_1} - \frac{\partial S}{\partial t_1} \frac{\partial T}{\partial z_1} \right]^T (z_1' - z_1) \right| < \frac{\epsilon'}{2} \quad \text{A.10} \end{aligned}$$

or

$$\frac{1}{|\nabla S^T|} \left| \frac{\partial S^T}{\partial x_1} (x_1' - x_1) + \frac{\partial S^T}{\partial y_1} (y_1' - y_1) + \frac{\partial S^T}{\partial z_1} (z_1' - z_1) \right| < \frac{|\nabla S|^T}{|\nabla S^T|} \frac{\epsilon'}{2} \quad \text{A.11}$$

where S^T is given by Eq. 3.28. Thus, the layer in which the integrand is different from zero, is a layer surrounding the surface Σ^T of equation $S^T = 0$; the thickness of the layer is given by

$$\varepsilon'' = \frac{|\nabla S|^T}{|\nabla S^T|} \varepsilon' \quad \text{A.12}$$

Hence, performing the integration through the thickness and taking the limit, Eq. A.7 reduces to the desired Eq. A.1.

Next, in order to prove Eq. A.2, consider $\partial \delta_T / \partial t$, as a limit of the incremental ratio. Then

$$\begin{aligned} & \iiint_{-\infty}^{\infty} f \delta_z \frac{\partial \delta_T}{\partial t} dv, dt, \\ &= \lim_{\Delta t \rightarrow 0} \frac{1}{\Delta t} \left[\iiint_{-\infty}^{\infty} f \delta_z \delta(t_1 + \Delta t - t + \tau) dv, dt, - \iiint_{-\infty}^{\infty} f \delta_z \delta(t_1 - t + \tau) dv, dt, \right] \quad \text{A.13} \end{aligned}$$

By using Eq. A.1 and performing the limit operation, Eq. A.13 reduces to the desired Eq. A.2.

APPENDIX B

REDUCTION TO ELEMENTARY CASES

In this Appendix, it is shown how classical results can be obtained as particular cases of Eq. 3.32.

B.1. Huygens' Principle

The problem related to the Huygens' principle is a particular case of the one considered here, the differences being that

- 1) The velocity of the undisturbed flow is equal to zero
- 2) The surface is assumed fixed in time
- 3) The nonlinear terms are zero

Mathematically speaking, these differences can be expressed as

$$\begin{aligned} U_{\infty} &= 0 \quad (M=0) \\ \partial S / \partial t &= 0 \\ F &= 0 \end{aligned} \quad \text{B.1}$$

Note that, according to Eq. B.1

$$\frac{dS}{dt} = \frac{\partial S}{\partial t} + U_{\infty} \frac{\partial S}{\partial x} = 0 \quad \text{B.2}$$

Combining Eqs. 3.32, B.1 and B.2 yields

$$4\pi E\varphi = - \oint_{\Sigma} \nabla_1 S \cdot [\nabla_1 \varphi]^+ \frac{1}{r} \frac{1}{|\nabla_1 S|} d\Sigma \quad \text{B.3}$$

$$\begin{aligned}
& + \oint_{\Sigma} \nabla_S \cdot \nabla_i \left(\frac{1}{r} \right) [\varphi]^+ \frac{1}{|\nabla_i S|} d\Sigma \\
& - \oint_{\Sigma} \nabla_S \cdot \nabla_i \left(\frac{r}{a_0} \right) \left[\frac{\partial \varphi}{\partial t} \right]^+ \frac{1}{|\nabla_i S|} d\Sigma
\end{aligned}$$

where

$$\left[\quad \right]^+ = \left[\quad \right]_{t_i = t - \frac{r}{a_0}} \quad \text{B.4}$$

and

$$r = \left[(x - x_i)^2 + (y - y_i)^2 + (z - z_i)^2 \right]^{\frac{1}{2}} \quad \text{B.5}$$

Note that

$$\vec{n}_i = \frac{\nabla_i S}{|\nabla_i S|} \quad \text{B.6}$$

is the outward normal, directed from the region $E = 0$ to the region $E = 1$. Thus, Eq. B.3 reduces to

$$\begin{aligned}
\bar{E} \varphi = & - \oint_{\Sigma} \left[\frac{\partial \varphi}{\partial n_i} \right]^+ \frac{1}{4\pi r} d\Sigma + \oint_{\Sigma} \frac{\partial}{\partial n_i} \left(\frac{1}{4\pi r} \right) [\varphi]^+ d\Sigma \\
& - \frac{1}{a_0} \oint_{\Sigma} \frac{\partial r}{\partial n_i} \left[\frac{\partial \varphi}{\partial t_i} \right]^+ \frac{1}{4\pi r} d\Sigma
\end{aligned} \quad \text{B.7}$$

which is the well known Kirchhoff formula which is the mathematical expression of Huygens' principle (see Refs. 11 and 12 in which the opposite convention on the definition of the normal is used).

B.2. Integral Representation of Solution of Poisson's Equation

The differences between Poisson's equation and the case considered here are:

- 1) No time dependence
- 2) $M = 0$

Then Eq. 3.32 reduces to the classical result¹²

$$E\varphi = - \oint_{\Sigma} \left[\frac{\partial \varphi}{\partial n_i} \frac{1}{4\pi r} - \varphi \frac{\partial}{\partial n_i} \left(\frac{1}{4\pi r} \right) \right] d\Sigma$$

$$- \iiint_V F \frac{1}{4\pi r} dV,$$
B.8

In particular, for $F = 0$ (Laplace's equation) Eq. B.8 reduces to the well known formula

$$E\varphi = - \oint_{\Sigma} \left[\frac{\partial \varphi}{\partial n_i} \frac{1}{4\pi r} - \varphi \frac{\partial}{\partial n_i} \left(\frac{1}{4\pi r} \right) \right] d\Sigma$$
B.9

B.3. Poisson's Formula

In Appendix F, it is shown how Eq. 3.32 can be used in order to derive the contribution of the initial conditions. Here it is shown that for $M = 0$, the contribution of the initial conditions reduces to the well known Poisson formula, that is, the solution of the wave equation with given initial conditions. The contribution of the initial conditions is derived in Appendix F and is given by Eq. F.2. For $U_0 = 0$, one obtains $r_\beta = r$, $T = \frac{1}{a_\infty} r$ and

Eq. F.2 reduces to

$$\varphi_{1.c.} = \frac{1}{4\pi a_s} \oint_{\Sigma^+} \left(\frac{\partial \varphi}{\partial t_1} \right)^+ \frac{d\Sigma^+}{r^2} + \frac{1}{4\pi a_s} \frac{\partial}{\partial t} \oint_{\Sigma^+} \varphi^+ \frac{d\Sigma^+}{r^2} \quad \text{B.10}$$

where $\Sigma^+ = t - T$ is the spherical surface of equation

$$r = a_s t \quad \text{B.11}$$

By using Eq. B.11, Eq. B.10 may be rewritten as

$$\varphi_{1.c.} = \frac{t}{4\pi} \oint \left(\frac{\partial \varphi}{\partial t_1} \right)_{t=0} d\Omega + \frac{1}{4\pi} \frac{\partial}{\partial t} \left[t \oint (\varphi)_{t=0} d\Omega \right] \quad \text{B.12}$$

where $d\Omega = d\Sigma^+/r^2$. Equation B.12 is the well known Poisson formula¹².

APPENDIX C

THE VALUE OF THE FUNCTION E ON THE SURFACE

C.1. Introduction

Consider Eq. 3.32: neglecting the nonlinear terms ($F = 0$) Eq. 3.32 gives a representation of the potential φ , anywhere in the volume, in terms of the values of φ and $\frac{\partial \varphi}{\partial n}$ on the surface of the body. The values of $\partial \varphi / \partial n$ on the surface of the body are given by the boundary conditions but the values of φ are not known. In order to solve the problem, it is thus necessary to obtain first the values of φ on the surface. This can be done by letting the point P of the volume V approach a point P_* of the surface. Then Eq. 4.9, with $F = 0$, yields

$$\begin{aligned}
 4\pi E \varphi(P_*, t) &= \lim_{P \rightarrow P_*} \left\{ - \oint_{\Sigma^T} \left[\nabla_i S \cdot \nabla_i \varphi - \frac{1}{a_\omega^2} \frac{dS}{dt_i} \frac{d\varphi}{dt_i} \right]^T \frac{1}{r_p} \frac{d\Sigma^T}{|\nabla_i S^T|} \right. \\
 &+ \oint_{\Sigma^T} \left[\nabla_i S \cdot \nabla_i \left(\frac{1}{r_p} \right) - \frac{1}{a_\omega^2} \frac{dS}{dt_i} \frac{d}{dt_i} \left(\frac{1}{r_p} \right) \right]^T \varphi^T \frac{d\Sigma^T}{|\nabla_i S^T|} \\
 &\left. - \frac{\partial}{\partial t} \oint_{\Sigma^T} \left[\nabla_i S \cdot \nabla_i T - \frac{1}{a_\omega^2} \frac{dS}{dt_i} \left(1 + U_\omega \frac{\partial T}{\partial x_i} \right) \right]^T \frac{\varphi^T}{r_p} \frac{d\Sigma^T}{|\nabla_i S^T|} \right\} \quad \text{C.1}
 \end{aligned}$$

In this Appendix, it is shown that, in the limit, Eq. 4.9 is still valid if the definition of the function E is generalized as follows

$$\begin{aligned} E &= 1 && \text{outside } \Sigma \\ E &= 1/2 && \text{on } \Sigma \\ E &= 0 && \text{inside } \Sigma \end{aligned} \quad \text{C.2}$$

By letting $P \rightarrow P_*$, the integrands become singular in the neighborhood of P_* . Thus, it is convenient to separate the contribution of a small neighborhood* of P_* , which will be indicated as Σ_ϵ . Thus, Eq. 3.32 can be rewritten as

$$\begin{aligned} 4\pi E \varphi &= - \iint_{\Sigma^T - \Sigma_\epsilon^T} \left[\nabla_1 S \cdot \nabla_1 \varphi - \frac{1}{a_\infty^2} \frac{dS}{dt_1} \frac{d\varphi}{dt_1} \right]^T \frac{1}{r_\rho} \frac{d\Sigma^T}{|\nabla_1 S^T|} \\ &+ \iint_{\Sigma^T - \Sigma_\epsilon^T} \left[\nabla_1 S \cdot \nabla_1 \left(\frac{1}{r_\rho} \right) - \frac{1}{a_\infty^2} \frac{dS}{dt_1} \frac{d}{dt_1} \left(\frac{1}{r_\rho} \right) \right]^T \varphi^T \frac{d\Sigma^T}{|\nabla_1 S^T|} \\ &- \frac{\partial}{\partial t} \iint_{\Sigma^T - \Sigma_\epsilon^T} \left[\nabla_1 S \cdot \nabla_1 T - \frac{1}{a_\infty^2} \frac{dS}{dt_1} \left(1 + U_\infty \frac{\partial T}{\partial x_1} \right) \right]^T \frac{\varphi^T}{r_\rho} \frac{d\Sigma^T}{|\nabla_1 S^T|} \\ &+ \delta_\epsilon \end{aligned} \quad \text{C.3}$$

The neighborhood Σ_ϵ is a small circular surface element, with center P_ and radius ϵ .

where δ_ϵ is the contribution of the neighborhood of P_* , given by

$$\begin{aligned} \delta_\epsilon = & - \iint_{\Sigma_\epsilon^T} \left[\nabla_i S \cdot \nabla_i \varphi - \frac{1}{a_\infty^2} \frac{dS}{dt_i} \frac{d\varphi}{dt_i} \right]^T \frac{1}{r_\beta} \frac{d\Sigma^T}{|\nabla_i S^T|} \\ & + \iint_{\Sigma_\epsilon^T} \left[\nabla_i S \cdot \nabla_i \left(\frac{1}{r_\beta} \right) - \frac{1}{a_\infty^2} \frac{dS}{dt_i} \frac{d}{dt_i} \left(\frac{1}{r_\beta} \right) \right]^T \varphi^T \frac{d\Sigma^T}{|\nabla_i S^T|} \\ & - \frac{\partial}{\partial t} \iint_{\Sigma_\epsilon^T} \left[\nabla_i S \cdot \nabla_i T - \frac{1}{a_\infty^2} \frac{dS}{dt_i} \left(1 + U_\infty \frac{\partial T}{\partial x_i} \right) \right]^T \frac{\varphi^T}{r_\beta} \frac{d\Sigma^T}{|\nabla_i S^T|} \end{aligned} \quad \text{C.4}$$

In order to simplify the discussion of the limit of J_ϵ as $P \rightarrow P_*$, the steady incompressible case is considered first. The results are then extended to the unsteady compressible subsonic case. The supersonic case is now under consideration.

C.2. Steady Incompressible Flow

For steady incompressible flow, Eq. C.3 and C.4 reduce to

$$4\pi E \varphi = - \iint_{\Sigma - \Sigma_\epsilon} \frac{\partial \varphi}{\partial n_i} \frac{1}{r} d\Sigma + \iint_{\Sigma - \Sigma_\epsilon} \varphi \frac{\partial}{\partial n_i} \left(\frac{1}{r} \right) d\Sigma + \delta_\epsilon \quad \text{C.5}$$

and

$$\delta_\epsilon = - \iint_{\Sigma_\epsilon} \frac{\partial \varphi}{\partial n_i} \frac{1}{r} d\Sigma + \iint_{\Sigma_\epsilon} \varphi \frac{\partial}{\partial n_i} \left(\frac{1}{r} \right) d\Sigma \quad \text{C.6}$$

The analysis of δ_ϵ is highly simplified by using local coordinate X, Y, Z , with Z normal to the tangent plane (directed from $E = 0$ to $E = 1$). Then, separating terms of order ϵ , Eq. C.6 reduces to*

$$\begin{aligned} \delta_\epsilon = & - \left(\frac{\partial \varphi}{\partial Z_1} \right)_* \iint_{X_1^2 + Y_1^2 < \epsilon^2} \frac{1}{\sqrt{X_1^2 + Y_1^2 + Z^2}} dX_1 dY_1 \\ & - \varphi_* \iint_{X_1^2 + Y_1^2 < \epsilon^2} \frac{\partial}{\partial Z} \frac{1}{\sqrt{X_1^2 + Y_1^2 + Z^2}} dX_1 dY_1 + O(\epsilon) \end{aligned} \quad \text{C.7}$$

where the subscript $*$ indicates evaluation at P_* . By using polar coordinate

$$\begin{aligned} R &= \sqrt{X_1^2 + Y_1^2} \\ \theta &= \tan^{-1} \frac{Y_1}{X_1} \end{aligned} \quad \text{C.8}$$

one obtains

$$\begin{aligned} \delta_\epsilon = & - 2\pi \left(\frac{\partial \varphi}{\partial Z_1} \right)_* \int_0^\epsilon \frac{1}{\sqrt{R^2 + Z^2}} R dR \\ & - 2\pi \varphi_* \int_0^\epsilon \frac{\partial}{\partial Z} \frac{1}{\sqrt{R^2 + Z^2}} R dR + O(\epsilon) \end{aligned} \quad \text{C.9}$$

*Note that $X = Y = 0, Z_1 = 0$ and $\frac{\partial}{\partial Z_1} \Big|_{Z_1=0} = - \frac{\partial}{\partial Z} \Big|_{Z=0}$

Noting that

$$\frac{1}{Z} \frac{\partial}{\partial Z} \left(\frac{1}{\sqrt{R^2 + Z^2}} \right) = - (R^2 + Z^2)^{-\frac{3}{2}} = \frac{1}{R} \frac{\partial}{\partial R} \left(\frac{1}{\sqrt{R^2 + Z^2}} \right) \quad \text{C.10}$$

Equation C.9 becomes

$$\begin{aligned} \delta_\epsilon &= -2\pi \left(\frac{\partial \varphi}{\partial Z_1} \right)_* \left[\sqrt{R^2 + Z^2} \right]_0^\epsilon \\ &\quad - 2\pi \varphi_* Z \left[\frac{1}{\sqrt{R^2 + Z^2}} \right]_0^\epsilon + O(\epsilon) \end{aligned} \quad \text{C.11}$$

Finally, by letting P go to P_* , (that is, $Z \rightarrow 0$), one obtains

$$\begin{aligned} \lim_{P \rightarrow P_*} \delta_\epsilon &= \lim_{Z \rightarrow 0} \left[-2\pi \left(\frac{\partial \varphi}{\partial Z_1} \right)_* \left(\sqrt{\epsilon^2 + Z^2} - |Z| \right) \right. \\ &\quad \left. - 2\pi \varphi_* Z \left(\frac{1}{\sqrt{\epsilon^2 + Z^2}} - \frac{1}{|Z|} \right) \right] + O(\epsilon) \\ &= \left[-2\pi \left(\frac{\partial \varphi}{\partial Z_1} \right)_* \epsilon + 2\pi \varphi_* \frac{Z}{|Z|} \right] + O(\epsilon) \\ &= \pm 2\pi \varphi_* + O(\epsilon) \end{aligned} \quad \text{C.12}$$

where the upper (lower) sign holds for $Z > 0$ ($Z < 0$), that is, when P originates outside (inside) the surface Σ ; correspondingly, the function E assumes the value $E = 1$ ($E = 0$).

Finally, using this result in Eq. C.4, one obtains

$$4\pi \left(E \mp \frac{1}{2}\right) \varphi_* = - \iint_{\Sigma - \Sigma_\epsilon} \frac{\partial \varphi}{\partial n_1} \frac{1}{r_*} d\Sigma + \iint_{\Sigma - \Sigma_\epsilon} \varphi \frac{\partial}{\partial n_1} \frac{1}{r_*} d\Sigma + o(\epsilon) \quad \text{C.13}$$

Note that, in both cases (P inside or outside Σ),

$$\begin{aligned} E_* &= E \mp \frac{1}{2} = 1 - \frac{1}{2} = \frac{1}{2} \\ &= 0 + \frac{1}{2} = \frac{1}{2} \end{aligned} \quad \text{C.14}$$

Furthermore, r_* is the distance between the dummy point, P_1 , and the control point (on the surface Σ), P_* . Hence, by letting ϵ go to zero, Eq. C.13 yields

$$4\pi E_* \varphi_* = - \oint_{\Sigma} \frac{\partial \varphi}{\partial n_1} \frac{1}{r_*} d\Sigma + \oint_{\Sigma} \varphi \frac{\partial}{\partial n_1} \left(\frac{1}{r_*}\right) d\Sigma \quad \text{C.15}$$

It should be emphasized that the limit $\epsilon \rightarrow 0$ is now performed with P on the surface Σ . This implies that the contribution of Σ_ϵ is now of order ϵ . In order to clarify this point, consider the quantity

$$\begin{aligned}
I_{\epsilon_0}^{\epsilon} &= \int_{\epsilon_0}^{\epsilon} \frac{\partial}{\partial Z} \left(\frac{1}{\sqrt{R^2 + Z^2}} \right) R dR \\
&= \left[\frac{Z}{\sqrt{R^2 + Z^2}} \right]_{\epsilon_0}^{\epsilon} = \frac{Z}{\sqrt{\epsilon^2 + Z^2}} - \frac{Z}{\sqrt{\epsilon_0^2 + Z^2}}
\end{aligned}
\tag{C.16}$$

and note that

$$\lim_{Z \rightarrow 0} \left\{ \lim_{\epsilon \rightarrow 0} I_{\epsilon_0}^{\epsilon} \right\} = \lim_{Z \rightarrow 0} \left\{ \frac{Z}{\sqrt{\epsilon^2 + Z^2}} - \frac{Z}{|Z|} \right\} = \text{sign}(Z)
\tag{C.17}$$

whereas

$$\lim_{\epsilon \rightarrow 0} \left\{ \lim_{Z \rightarrow 0} I_{\epsilon_0}^{\epsilon} \right\} = \lim_{\epsilon \rightarrow 0} 0 = 0
\tag{C.18}$$

The difference between these two limits is due to the fact that, in the limit (as $Z \rightarrow 0$), the integrand of $I_{\epsilon_0}^{\epsilon}$ behaves like a Dirac delta function and hence, its contribution for a domain which excludes the singular point is zero.

It may be worth noting that, in Eq. C.12, the sequence of limits indicated in Eq. C.17 must be performed, whereas in Eq. C.15, the one indicated in Eq. C.18 must be used.

Finally, it is shown that the results obtained here

are equivalent to the definition of E given by Eq. C.2:
 note that for steady incompressible flow, Eq. 4.9, with
 $F = 0$, yields

$$4\pi E\varphi = - \oint_{\Sigma} \frac{\partial \varphi}{\partial n_1} \frac{1}{r} d\Sigma + \oint_{\Sigma} \varphi \frac{\partial}{\partial n_1} \left(\frac{1}{r} \right) d\Sigma \quad \text{C.19}$$

Note that Eq. C.19 must be used if P is outside or inside the surface, whereas Eq. C.15 must be used if P is on the surface. However, by comparing Eqs. C.15 and C.19, it is easily seen that Eq. 19 is valid everywhere (outside, inside and on the surface Σ), if the convention is made that E is given by Eq. C.2.

C.3. Unsteady Compressible Subsonic Flow

In order to simplify the analysis of unsteady subsonic flow, it is convenient first to analyze Eq. C.4 with the nonrestrictive assumption that the frame of reference is connected with the undisturbed air; this implies that

$$U_{\infty} = 0 \quad M = 0 \quad \beta = 1 \quad \text{C.20}$$

This is considered in Subsection C.3.1. The general case is discussed in Subsection C.3.2.

C.3.1. Frame of Reference with $U_\infty = 0$

With the assumption C.20,* Eq. C.4 reduces to

$$\begin{aligned} \delta_\epsilon = & - \iint_{\Sigma_\epsilon^T} \left[\nabla_1 S \cdot \nabla_1 \varphi - \frac{1}{a_\infty^2} \frac{\partial S}{\partial t_1} \frac{\partial \varphi}{\partial t_1} \right]^T \frac{1}{r} \frac{d\Sigma^T}{|\nabla_1 S^T|} \\ & + \iint_{\Sigma_\epsilon^T} \left[\nabla_1 S \cdot \nabla_1 \left(\frac{1}{r} \right) \right]^T \varphi^T \frac{d\Sigma}{|\nabla_1 S^T|} \\ & - \frac{\partial}{\partial t} \iint \left[\nabla_1 S \cdot \nabla_1 T - \frac{1}{a_\infty^2} \frac{\partial S}{\partial t_1} \right]^T \frac{\varphi^T}{r} \frac{d\Sigma}{|\nabla_1 S^T|} \end{aligned} \quad \text{C.21}$$

where, according to Eqs. 2.38 and C.20,

$$T = \frac{r}{a_\infty} \quad \text{C.22}$$

In order to examine Eq. C.21, it is convenient to introduce a time shift so that $t \equiv 0$. Furthermore, let P_* be a point located on the surface at $t = 0$; then it is convenient to consider a frame of reference with origin at P_* and Z axis directed along the normal to the surface of the body (Fig. C.1).

* Note that, strictly speaking, this assumption makes Eq. 1.3 meaningless. Hence, this section should be considered as a mathematical introduction to Subsection C.3.2. Physically meaningful results can be obtained if φ is replaced by ϕ in this whole Subsection.

Thus, the equation of the body is given by

$$S = Z_1 - \bar{f}(X_1, Y_1, t_1) = 0 \quad C.23$$

with

$$\begin{aligned} \bar{f}(0, 0, 0) &= 0 \\ \frac{\partial \bar{f}}{\partial X_1}(0, 0, 0) &= 0 \\ \frac{\partial \bar{f}}{\partial Y_1}(0, 0, 0) &= 0 \end{aligned} \quad C.24$$

but, in general

$$\frac{\partial \bar{f}}{\partial t_1}(0, 0, 0) = \bar{c} \neq 0 \quad C.25$$

By using a Taylor series expansion and neglecting higher order terms, Eq. C.23 reduces to

$$S = Z_1 - \bar{c} t_1 = 0 \quad C.26$$

where Eqs. C.24 and C.25 have been used. Eq. C.26 shows that \bar{c} is the velocity of the surface of the body at $P = P_*$ and $t = 0$. Hence, in an infinitesimal neighborhood of P_* , the surface S^T is given by

$$\begin{aligned} S^T &= Z_1 - \bar{c} t + \frac{\bar{c}}{a_w} \sqrt{X_1^2 + Y_1^2 + (Z_1 - Z)^2} \\ &= Z_1 - \bar{c} t + \frac{\bar{c}}{a_w} \sqrt{R^2 + (Z_1 - Z)^2} = 0 \end{aligned} \quad C.27$$

with

$$R = \sqrt{X_1^2 + Y_1^2} \quad \text{C.28}$$

Next, it is important to note that, for $P = P_*$ (i.e., $Z = 0$ and $t = 0$), the surface Σ^T does not have a tangent plane in P_* , but rather a tangent cone. In order to see this, consider the normal to Σ_ϵ^T given by $\nabla_1 S^T / |\nabla_1 S^T|$ where, according to Eq. C.27

$$\nabla_1 S^T = \vec{K} + \frac{\vec{e}}{a_w} \nabla_1 \sqrt{R^2 + Z_1^2} \quad \text{C.29}$$

where \vec{K} is a unit vector in direction Z . Equation C.29 shows that the surface $\Sigma^T = 0$ has the shape of a cone in an infinitesimal neighborhood, Σ_ϵ^T , of P_* . For, Eq. C.29 can be rewritten as

$$\nabla_1 S^T = \vec{K} + \vec{H} \quad \text{C.30}$$

with

$$\vec{H} = \frac{\vec{e}}{a_w} \nabla_1 \sqrt{R^2 + Z_1^2} \quad \text{C.31}$$

In Eq. C.30, \vec{K} is constant whereas \vec{H} is directed along the tangent to the surface Σ_ϵ^T . Note that $\vec{K} + \vec{H}$ is directed along the normal to Σ_ϵ^T . This configuration is sketched in Fig. C.2 where \vec{K} and \vec{H} are shown at two points, P_1' and P_1'' , in the neighborhood of P_* .

In order to analyze the contribution δ_ϵ it is convenient to use polar coordinates in the plane $\tilde{\Sigma}_\epsilon^T$,

defined as the plane normal to \vec{K} at the point P_* . Note, however, that for $Z = 0$, the surface Σ^T is a hyperboloid with axis parallel to \vec{K} .

Noting that

$$\frac{d\Sigma^T}{|\nabla S^T|} = \frac{d\tilde{\Sigma}^T}{|\partial S^T / \partial Z_1|} = \frac{2\pi R dR}{1 + \frac{\bar{\epsilon}}{a_*} \frac{Z_1}{r}} \quad \text{C.32}$$

and that the first integral in Eq. C.21, as well as T , is of order ϵ , Eq. C.21 reduces to

$$\begin{aligned} \delta_\epsilon &= \left[\varphi(P_*, t) \iint_{\Sigma_\epsilon^T} \vec{K} \cdot \nabla \left(\frac{1}{r} \right) \frac{d\Sigma^T}{|\vec{K} + \vec{H}|} \right. \\ &\quad \left. - \frac{1}{a_*} \frac{\partial}{\partial t} \left\{ \varphi(P_*, t) \iint_{\Sigma_\epsilon^T} \left(\vec{K} \cdot \nabla r - \frac{\bar{\epsilon}}{a_*} \right) \frac{1}{r} \frac{d\Sigma^T}{|\vec{K} + \vec{H}|} \right\} \right]_{t=0} + O(\epsilon) \quad \text{C.33} \\ &= \left[-\varphi(P_*, t) \int_0^\epsilon \frac{Z_1 - Z}{r^3} \frac{2\pi R dR}{1 + \frac{\bar{\epsilon}}{a_*} \frac{Z_1}{r}} \right. \\ &\quad \left. - \frac{1}{a_*} \frac{\partial}{\partial t} \left\{ \varphi(P_*, t) \int_0^\epsilon \left(\frac{Z_1 - Z}{r} - \frac{\bar{\epsilon}}{a_*} \right) \frac{1}{r} \frac{2\pi R dR}{1 + \frac{\bar{\epsilon}}{a_*} \frac{Z_1}{r}} \right\} \right]_{t=0} + O(\epsilon) \end{aligned}$$

In order to evaluate the integrals, it is convenient to use, as variable of integration, the variable

$$\tilde{Z}_1 = Z_1 - \bar{c} t \quad \text{C.34}$$

Note that, according to Eq. C.27

$$\tilde{Z}_1 = -\frac{\bar{c}}{a_\infty} r = -\frac{\bar{c}}{a_\infty} \sqrt{R^2 - (\tilde{Z}_1 - \tilde{Z})^2} \quad \text{C.35}$$

where

$$\tilde{Z} = Z - \bar{c} t \quad \text{C.36}$$

Note that, according to Eq. C.27

$$\left(1 + \frac{\bar{c}}{a_\infty} \frac{Z_1}{r}\right) dZ_1 = -\frac{\bar{c}}{a_\infty} \frac{R}{r} dR \quad \text{C.37}$$

By using Eqs. C.35 and C.37, Eq. C.33 reduces to*

$$\begin{aligned} \delta_\varepsilon &= \left[-2\pi \varphi(p_*, t) \int_{\tilde{Z}_1(0)}^{\tilde{Z}_1(\varepsilon)} \frac{\tilde{Z}_1 - \tilde{Z}}{\left(-\frac{a_\infty^3}{\bar{c}^3} \tilde{Z}_1^3\right)} \frac{a_\infty^2}{\bar{c}^2} \tilde{Z}_1 d\tilde{Z}_1 \right. \\ &\quad \left. - \frac{1}{a_\infty} \frac{\partial}{\partial t} \left\{ 2\pi \varphi(p_*, t) \int_{\tilde{Z}_1(0)}^{\tilde{Z}_1(\varepsilon)} \left(\frac{\tilde{Z}_1 - \tilde{Z}}{\left(-\frac{a_\infty}{\bar{c}} \tilde{Z}_1\right)} - \frac{\bar{c}}{a_\infty} \right) \frac{1}{\left(-\frac{a_\infty}{\bar{c}} \tilde{Z}_1\right)} \frac{a_\infty^2}{\bar{c}^2} \tilde{Z}_1 d\tilde{Z}_1 \right\} \right]_{t=0} + O(\varepsilon) \\ &= \left[2\pi \varphi(p_*, t) \frac{\bar{c}}{a_\infty} \int_{\tilde{Z}_1(0)}^{\tilde{Z}_1(\varepsilon)} \frac{\tilde{Z}_1 - \tilde{Z}}{\tilde{Z}_1^2} d\tilde{Z}_1 \right] \end{aligned}$$

* Using Eq. C.32, C.35 and C.37, it is easy to show that, as anticipated, the first integral in Eq. C.21 is indeed of order ε .

$$\begin{aligned}
& + \frac{1}{a_w} \frac{\partial}{\partial t} \left\{ 2\pi \varphi(p_*, t) \int_{\tilde{Z}_1(0)}^{\tilde{Z}_1(\epsilon)} \frac{\tilde{Z}}{\tilde{Z}_1} d\tilde{Z}_1 \right\} \Big|_{t=0} + O(\epsilon) \\
& = \left[2\pi \varphi(p_*, t) \frac{\bar{c}}{a_w} \left[\ln \tilde{Z}_1 + \frac{\tilde{Z}}{\tilde{Z}_1} \right]_{\tilde{Z}_1(0)}^{\tilde{Z}_1(\epsilon)} + \frac{1}{a_w} \frac{\partial}{\partial t} \left\{ 2\pi \varphi(p_*, t) \tilde{Z} \left[\ln \tilde{Z}_1 \right]_{\tilde{Z}_1(0)}^{\tilde{Z}_1(\epsilon)} \right\} \right]_{t=0} + O(\epsilon) \\
& = 2\pi \varphi(p_*, 0) \frac{1}{a_w} \left[\bar{c} \ln \tilde{Z}_1(\epsilon) - \bar{c} \ln \tilde{Z}_1(0) + \bar{c} \frac{\tilde{Z}}{\tilde{Z}_1(\epsilon)} - \bar{c} \frac{\tilde{Z}}{\tilde{Z}_1(0)} \right]_{t=0} \\
& \quad + 2\pi \varphi(p_*, 0) \frac{1}{a_w} \left[\frac{\partial \tilde{Z}}{\partial t} (\ln \tilde{Z}_1(\epsilon) - \ln \tilde{Z}_1(0)) - \frac{\tilde{Z}}{\tilde{Z}_1(\epsilon)} \frac{\partial \tilde{Z}_1(\epsilon)}{\partial t} - \frac{\tilde{Z}}{\tilde{Z}_1(0)} \frac{\partial \tilde{Z}_1(0)}{\partial t} \right]_{t=0} \\
& \quad + 2\pi \frac{\partial \varphi(p_*, 0)}{\partial t} \frac{1}{a_w} \left[\tilde{Z} \ln \tilde{Z}_1(\epsilon) - \tilde{Z} \ln \tilde{Z}_1(0) \right]_{t=0} + O(\epsilon)
\end{aligned} \tag{C.38}$$

where $\tilde{Z}_1(R)$ is obtained by solving Eq. C.25 with respect to \tilde{Z}_1 . This yields

$$\tilde{Z}_1 = - \frac{\Gamma}{1-\Gamma^2} \left[\Gamma \tilde{Z} + \sqrt{\tilde{Z}^2 + (1-\Gamma^2)R} \right] \tag{C.39}$$

with $\Gamma = \bar{c}/a_w$. Hence

$$\begin{aligned}
\tilde{Z}_1(0) &= - \frac{\Gamma}{1-\Gamma^2} \left[\Gamma + \text{sign}(\tilde{Z}) \right] \tilde{Z} \\
\tilde{Z}_1(\epsilon) &= - \frac{\Gamma}{1-\Gamma^2} \left[\Gamma \tilde{Z} + \sqrt{\tilde{Z}^2 + (1-\Gamma^2)\epsilon^2} \right]
\end{aligned} \tag{C.40}$$

and

$$\begin{aligned} \frac{1}{a_w} \frac{\partial \tilde{Z}_1(0)}{\partial t} &= \frac{\Gamma^2}{1-\Gamma^2} \left[\Gamma + \text{sign}(\tilde{Z}) \right] \\ \frac{1}{a_w} \frac{\partial \tilde{Z}_1(\epsilon)}{\partial t} &= \frac{\Gamma^2}{1-\Gamma^2} \left[\Gamma + \frac{\tilde{Z}}{\sqrt{\tilde{Z}^2 + (1-\Gamma^2)\epsilon^2}} \right] \end{aligned} \quad \text{C.41}$$

since, according to C.36

$$\frac{1}{a_w} \frac{\partial \tilde{Z}}{\partial t} = - \frac{\tilde{c}}{a_w} = -\Gamma \quad \text{C.42}$$

Combining Eqs. C.38, C.40, C.41 and C.42 yields

$$\begin{aligned} \delta_c &= 2\pi \varphi(p_*, 0) \frac{1}{a_w} \left[\frac{\tilde{Z}}{\tilde{Z}_1(\epsilon)} \left(\tilde{c} + \frac{\partial \tilde{Z}_1(\epsilon)}{\partial t} \right) - \frac{\tilde{Z}}{\tilde{Z}_1(0)} \left(\tilde{c} + \frac{\partial \tilde{Z}_1(0)}{\partial t} \right) \right]_{t=0} \\ &+ 2\pi \frac{\partial \varphi}{\partial t}(p_*, 0) \frac{1}{a_w} \left[\tilde{Z} \ln \frac{\tilde{Z}_1(\epsilon)}{\tilde{Z}_1(0)} \right]_{t=0} \end{aligned} \quad \text{C.43}$$

Note that

$$\begin{aligned} \frac{1}{a_w} \left[\tilde{c} + \frac{\partial \tilde{Z}_1(\epsilon)}{\partial t} \right] &= \frac{\Gamma}{1-\Gamma^2} \left[1 + \frac{\Gamma \tilde{Z}}{\sqrt{\tilde{Z}^2 + (1-\Gamma^2)\epsilon^2}} \right] \\ &= \frac{\Gamma}{1-\Gamma^2} \frac{\sqrt{\tilde{Z}^2 + (1-\Gamma^2)\epsilon^2} + \Gamma \tilde{Z}}{\sqrt{\tilde{Z}^2 + (1-\Gamma^2)\epsilon^2}} = - \frac{\tilde{Z}_1(\epsilon)}{\sqrt{\tilde{Z}^2 + (1-\Gamma^2)\epsilon^2}} \end{aligned} \quad \text{C.44}$$

and

$$\begin{aligned} \frac{1}{a_w} \left[\tilde{c} + \frac{\partial \tilde{Z}_1(0)}{\partial t} \right] &= \frac{\Gamma}{1-\Gamma^2} \left[1 + \Gamma \text{sign}(\tilde{Z}) \right] \\ &= - \text{sign}(\tilde{Z}) \frac{\tilde{Z}_1(0)}{\tilde{Z}} \end{aligned} \quad \text{C.45}$$

Finally, combining Eqs. C.43 to C.45 yields (note that, for $t = 0$, $\tilde{z}_1 = z_1$ and $\tilde{z} = z$)

$$\begin{aligned} \delta_\epsilon = 2\pi \varphi(p_*, 0) \left[\frac{Z}{|Z|} - \frac{Z}{\sqrt{Z^2 + (1-\Gamma^2)\epsilon^2}} \right] \\ + 2\pi \frac{\partial \varphi}{\partial t}(p_*, 0) \frac{1}{a_\infty} \left[Z \ln \left(\frac{\Gamma + Z/\sqrt{Z^2 + (1-\Gamma^2)\epsilon^2}}{\Gamma + Z/|Z|} \right) \right] \end{aligned} \quad \text{C.46}$$

and, by letting Z go to zero

$$\lim_{p \rightarrow p_*} \delta_\epsilon = 2\pi \varphi(p_*, 0) \operatorname{sign}(Z) + O(\epsilon) \quad \text{C.47}$$

which is identically equal to Eq. C.12. This implies that the results obtained in Subsection C.1 (in particular Eq. C.2), are valid also for unsteady compressible subsonic flow with $U_\infty = 0$. The case $U_\infty \neq 0$ is considered next.

C.3.2. Frame of Reference with $U_\infty \neq 0$

In Subsection C.3.2, it is shown that the results obtained in Subsection C.2 are valid also for unsteady compressible subsonic flow with frame of reference connected with the undisturbed air ($U_\infty = 0$). In this subsection, this last restriction is removed. In this case, noting that the first integral of Eq. C.4 is of order ϵ , and T is also of order ϵ , Eq. C.4 can be

rewritten as

$$\begin{aligned}
\delta_\varepsilon &= \iint_{\Sigma_\varepsilon^T} \left[\nabla_1 S \cdot \nabla_1 \left(\frac{1}{r_\rho} \right) - \frac{1}{a_\infty^2} \left(\frac{\partial S}{\partial t_1} + U_\infty \frac{\partial S}{\partial x_1} \right) U_\infty \frac{\partial}{\partial x_1} \left(\frac{1}{r_\rho} \right) \right]^T \varphi^T \frac{d\Sigma^T}{|\nabla_1 S^T|} \\
&\quad - \frac{\partial}{\partial t} \iint_{\Sigma_\varepsilon^T} \left[\nabla_1 S \cdot \nabla_1 T - \frac{1}{a_\infty^2} \left(\frac{\partial S}{\partial t_1} + U_\infty \frac{\partial S}{\partial x_1} \right) \left(1 + U_\infty \frac{\partial T}{\partial x_1} \right) \right]^T \frac{\varphi^T}{r_\rho} \frac{d\Sigma^T}{|\nabla_1 S^T|} \\
&= \varphi(p_*, t) \iint_{\Sigma_\varepsilon^T} \left[\nabla_1 S \cdot \nabla_1 \left(\frac{1}{r_\rho} \right) - M^2 \frac{\partial S}{\partial x_1} \frac{\partial}{\partial x_1} \left(\frac{1}{r_\rho} \right) - \frac{U_\infty}{a_\infty^2} \frac{\partial S}{\partial t_1} \frac{\partial}{\partial x_1} \left(\frac{1}{r_\rho} \right) \right] \frac{d\Sigma^T}{|\nabla_1 S^T|} \quad \text{C.48} \\
&\quad - \frac{\partial}{\partial t} \left\{ \varphi(p_*, t) \iint_{\Sigma_\varepsilon^T} \left[\nabla_1 S \cdot \nabla_1 T - M^2 \frac{\partial S}{\partial x_1} \frac{\partial T}{\partial x_1} - \frac{U_\infty}{a_\infty^2} \frac{\partial S}{\partial t_1} \frac{\partial T}{\partial x_1} \right. \right. \\
&\quad \left. \left. - \frac{1}{a_\infty} \left(\frac{\partial S}{\partial t_1} + U_\infty \frac{\partial S}{\partial x_1} \right) \right] \frac{1}{r_\rho} \frac{d\Sigma^T}{|\nabla_1 S^T|} \right\} + O(\varepsilon)
\end{aligned}$$

In order to analyze Eq. C.48, it is convenient to use the Prandtl-Glauert transformation. By using Eqs. 3.37 and 3.40, Eq. C.20 reduces to

$$\begin{aligned}
\delta_\varepsilon &= \varphi_* \iint_{\Sigma_\varepsilon^T} \left[\nabla_1 S \cdot \nabla_1 \left(\frac{1}{r_\varepsilon} \right) - \frac{U_\infty}{\beta a_\infty^2} \frac{\partial S}{\partial t_1} \frac{\partial}{\partial x_1} \left(\frac{1}{r_\varepsilon} \right) \right] \frac{d\Sigma_\varepsilon}{|\nabla_1 S^T|} \\
&\quad - \frac{\partial}{\partial t} \left\{ \varphi_* \iint_{\Sigma_\varepsilon^T} \left[\nabla_1 S \cdot \nabla_1 T - \frac{U_\infty}{\beta a_\infty^2} \frac{\partial S}{\partial t_1} \frac{\partial T}{\partial x_1} \right. \right.
\end{aligned}$$

$$- \frac{1}{a_*^2} \left(\frac{\partial S}{\partial t_1} + \frac{1}{\beta} U_* \frac{\partial S}{\partial x_{01}} \right) \left] \frac{1}{r_*} \frac{d\Sigma_0}{|V_{01} S^T|} + O(\epsilon) \quad \text{C.49}$$

with $\varphi_* = \varphi(P_*, t)$ and

$$T = \frac{1}{a_* \beta^2} \left[M(x_1 - x) + r_\beta \right] = \frac{1}{a_* \beta} \left[M(x_{01} - x_0) + r_0 \right] \quad \text{C.50}$$

Combining Eq. C.49 and C.50 and generalizing the Prandtl-Glauert transformation by introducing

$$t_* = \beta a_* t \quad \text{C.51}$$

yields

$$\begin{aligned} \delta_\epsilon = \varphi_* \iint_{\Sigma_{t_*}^T} & \left[\nabla_{01} S \cdot \nabla_{01} \left(\frac{1}{r_*} \right) - \frac{U_*}{a_*} \frac{\partial S}{\partial t_{01}} \frac{\partial}{\partial x_{01}} \left(\frac{1}{r_*} \right) \right] \frac{d\Sigma_0}{|V_{01} S^T|} \\ & - \frac{\partial}{\partial t_*} \left\{ \varphi_* \iint_{\Sigma_{t_*}^T} \left[\nabla_{01} S \cdot \nabla_{01} r_* - \frac{U_*}{a_*} \frac{\partial S}{\partial t_{01}} \frac{\partial r_*}{\partial x_{01}} - \frac{\partial S}{\partial t_{01}} \right] \frac{1}{r_*} \frac{d\Sigma_0}{|V_{01} S^T|} \right\} \quad \text{C.52} \\ & + O(\epsilon) \end{aligned}$$

This equation can be considerably simplified by noting that

$$\begin{aligned}
\nabla_{\mathbf{r}_0} S^T &\equiv \nabla_{\mathbf{r}_0} (S^T) = \left[\nabla_{\mathbf{r}_0} S - \frac{\partial S}{\partial t_0} \nabla_{\mathbf{r}_0} \vec{t} \right]^T \\
&= \left[\nabla_{\mathbf{r}_0} S - \frac{\partial S}{\partial t_0} (M \vec{i} + \nabla_{\mathbf{r}_0} \mathbf{r}_0) \right]^T \\
&= \left[\left(\nabla_{\mathbf{r}_0} S - \frac{\partial S}{\partial t_0} M \vec{i} \right) - \frac{\partial S}{\partial t_0} \nabla_{\mathbf{r}_0} \mathbf{r}_0 \right]^T \\
&= \left[\vec{D} - \frac{\partial S}{\partial t_0} \nabla_{\mathbf{r}_0} \mathbf{r}_0 \right]^T \\
&= \left[|\vec{D}| (\vec{k}_0 + \vec{H}_0) \right]^T
\end{aligned} \tag{C.53}$$

where \vec{i} is a unit vector in x_0 -direction and

$$\begin{aligned}
\vec{D}_0 &= \nabla_{\mathbf{r}_0} S - \frac{U_0}{a_0} \frac{\partial S}{\partial t_0} \vec{i} \\
\vec{k}_0 &= \vec{D}_0 / |\vec{D}_0| \\
\vec{H}_0 &= - \frac{\partial S}{\partial t_0} \nabla_{\mathbf{r}_0} \mathbf{r}_0 / |\vec{D}_0| = \bar{c}_0 \nabla_{\mathbf{r}_0} \mathbf{r}_0
\end{aligned} \tag{C.54}$$

with

$$\bar{c}_0 = - \frac{\partial S}{\partial t_0} \frac{1}{|\vec{D}_0|} \tag{C.55}$$

Note that Eqs. C.53 and C.54 are in full correspondance with Eqs. C.30 and C.31. Combining Eqs. C.52 to C.55 yields

$$\begin{aligned}
\delta_\epsilon &= \varphi_* \iint_{\Sigma_\epsilon^T} \vec{k}_0 \cdot \nabla_{\mathbf{r}_0} \left(\frac{1}{r_0} \right) \frac{d\Sigma_0^T}{|\vec{k}_0 + \vec{H}_0|} \\
&\quad - \frac{1}{a_0} \frac{\partial}{\partial t_0} \left\{ \iint_{\Sigma_\epsilon^T} (\vec{k}_0 \cdot \nabla_{\mathbf{r}_0} \mathbf{r}_0 + \frac{\bar{c}_0}{a_0}) \frac{1}{r_0} \frac{d\Sigma_0^T}{|\vec{k}_0 + \vec{H}_0|} \right\}
\end{aligned} \tag{C.56}$$

Equation C.56 is formally equal to Eq. C.33. Hence, the results obtained for $U_{\infty} = 0$ (Subsection C.3.1), are valid for the general case as well.

Finally, an important remark should be made. As shown by Eq. C.38, each of the two integrals tends to infinity as Z goes to zero. However, their difference tends to the finite value given by Eq. C.47. Hence, the numerical integration of the two integrals must be very careful.

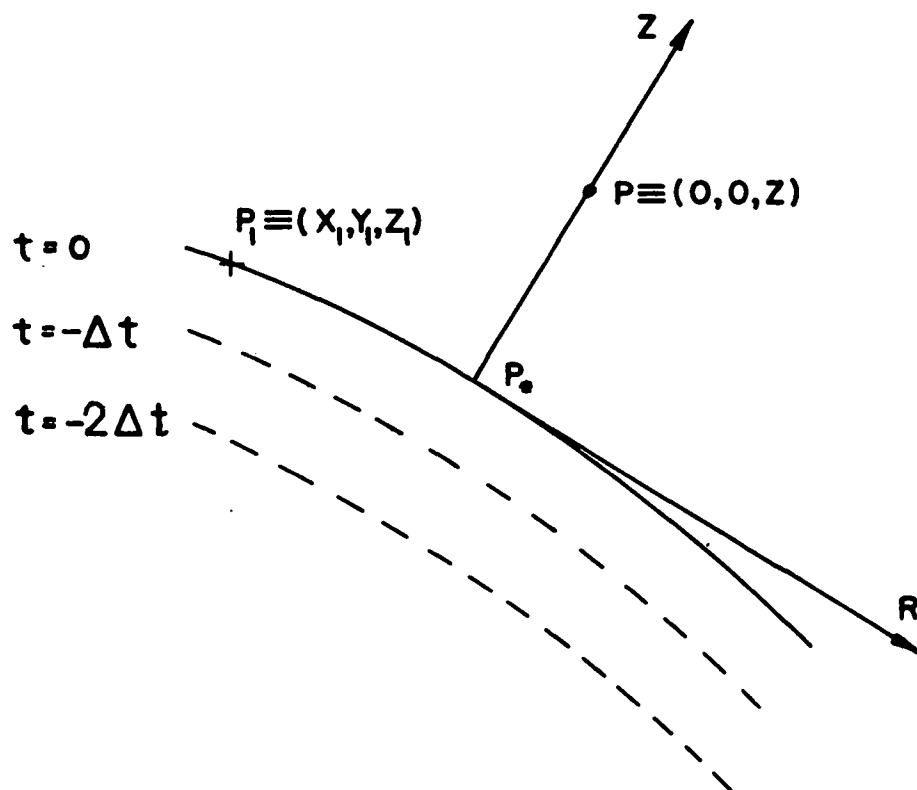


Fig. C.1 The surface Σ in the neighborhood of P_*

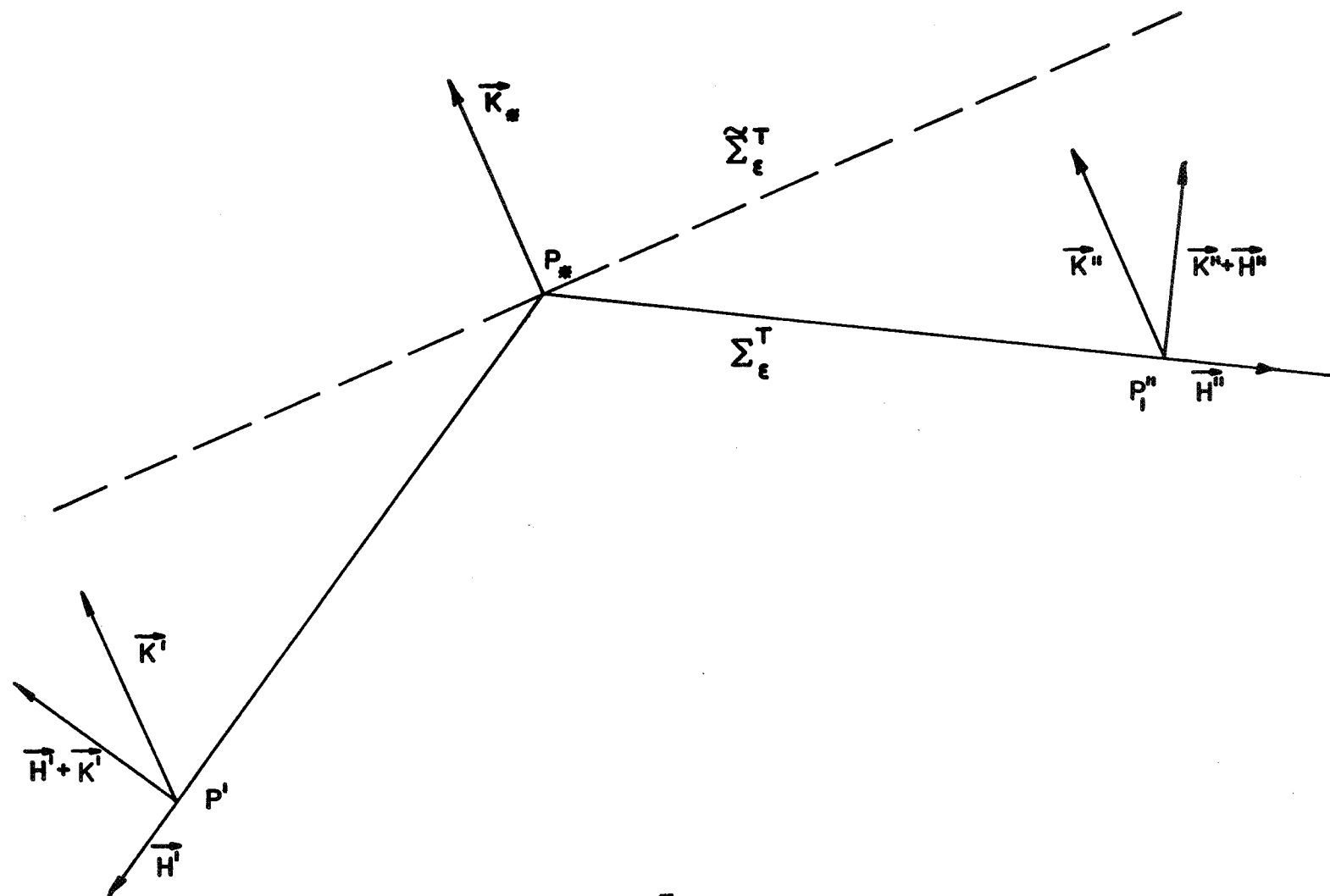


Fig. C.2 The surface Σ^T in the neighborhood of P_*

APPENDIX D

UNSTEADY WAKE AND LIFTING SURFACE THEORY KERNEL

D.1. Introduction

In this Appendix, an explicit expression for the evaluation of the unsteady wake (Subsection D.2) is given. Finally, for the sake of completeness, an explicit expression for the kernel function of the integral equation given in Ref. 8 is derived from the results obtained in this appendix.

D.2. Unsteady Subsonic Wake

In this subsection, a treatment for the wake of an oscillating wing in subsonic flow is derived. The same assumption made for the steady state wake (Subsection 6.3) is made here: the wake is approximated by straight vortex-lines, parallel to the direction of the flow, emanating from the trailing edge of the wing. For the sake of simplicity, the trailing edge is assumed to lie on the plane $x_1 = 0$.

Under this assumption, Eq. 4.19 reduces to

$$\begin{aligned}
 4\pi E \tilde{\varphi} = & - \oint_{\Sigma_B} \tilde{Q}_n e^{-i\omega T} \frac{1}{r_p} d\Sigma \\
 & + \oint_{\Sigma_B} \tilde{\varphi} \frac{\partial}{\partial n_1} \left(\frac{e^{-i\omega T}}{r_p} \right) d\Sigma + \tilde{I}_w
 \end{aligned}
 \tag{D.1}$$

with

$$\tilde{I}_w = \iint_{\Sigma_w} (\tilde{\varphi}_u - \tilde{\varphi}_l) \frac{\partial}{\partial \bar{z}_1} \left(\frac{e^{-i\omega T}}{r_\beta} \right) dx, dy, \quad D.2$$

In order to take advantage of the fact that there is no pressure jump across the wake, it is convenient to follow a procedure similar to the one outlined in Subsection 5.2.

By using Eq. 5.11, Eq. D.2 may be rewritten as

$$\begin{aligned} \tilde{I}_w &= \int_{-b/2}^{b/2} dy_1 \int_{x_{TE}}^{\infty} \frac{\partial}{\partial \bar{z}_1} \left(\frac{e^{-i\omega T}}{r_\beta} \right) \left\{ \int_{-\infty}^{x_1} \frac{-1}{\rho_\infty U_\infty^2} e^{\frac{i\omega}{U_\infty}(\lambda_2 - x_1)} \Delta \tilde{p}(\lambda_2, y) d\lambda_2 \right\} dx_1 \\ &= \int_{-b/2}^{b/2} \hat{I}_w dy_1, \end{aligned} \quad D.3$$

where

$$\begin{aligned} \hat{I}_w &= -\frac{1}{\rho_\infty U_\infty^2} \int_{x_{TE}}^{\infty} \left\{ \frac{\partial}{\partial \bar{z}_1} \left(\frac{e^{-i\omega T}}{r_\beta} \right) \int_{-\infty}^{x_1} e^{\frac{i\omega}{U_\infty}(\lambda_2 - x_1)} \Delta \tilde{p}(\lambda_2, y) d\lambda_2 \right\} dx_1 \\ &= -\frac{1}{\rho_\infty U_\infty^2} \int_{x_{TE}}^{\infty} \left\{ \frac{\partial}{\partial \bar{z}_1} \left(\frac{e^{-i\omega(T + \frac{x_1}{U_\infty})}}{r_\beta} \right) \int_{-\infty}^{x_1} e^{\frac{i\omega \lambda_2}{U_\infty}} \Delta \tilde{p}(\lambda_2, y) d\lambda_2 \right\} dx_1 \\ &= \left[\frac{1}{\rho_\infty U_\infty^2} \int_{x_1}^{\infty} \frac{\partial}{\partial \bar{z}_1} \left(\frac{e^{-i\omega(T + \frac{\lambda_1}{U_\infty})}}{r_{\lambda_1}} \right) d\lambda_1 \cdot \int_{-\infty}^{x_1} e^{\frac{i\omega \lambda_2}{U_\infty}} \Delta \tilde{p}(\lambda_2, y) d\lambda_2 \right]_{x_{TE}}^{\infty} \\ &= \frac{1}{\rho_\infty U_\infty^2} \int_{x_{TE}}^{\infty} \left\{ \int_{x_1}^{\infty} \frac{\partial}{\partial \bar{z}_1} \left(\frac{e^{-i\omega(T + \frac{\lambda_1}{U_\infty})}}{r_{\lambda_1}} \right) d\lambda_1 \cdot e^{\frac{i\omega x_1}{U_\infty}} \Delta \tilde{p}(x_1, y) \right\} dx_1. \end{aligned} \quad D.4$$

where integration by parts has been used and

$$r_{\lambda_1} = \left[(\lambda_1 - x)^2 + \beta^2 [(y_1 - y)^2 + (z_1 - z)^2] \right]^{1/2} \quad \text{D.5}$$

Eq. D.4 can be simplified considerably by noting that $\Delta \tilde{p} = 0$ on the wake: this implies that the last term is identically equal to zero. Furthermore, the upper contribution of the first term is zero because the first integral is equal to zero for $x_1 = \infty$. Finally, note that, according to Eq. 5.11

$$-\frac{1}{\rho_\infty U_\infty^2} \int_{-\infty}^{x_{TE}} e^{\frac{i\omega \lambda_1}{U_\infty}} \Delta \tilde{p}(\lambda_1, y) d\lambda_1 = e^{\frac{i\omega x_{TE}}{U_\infty}} \Delta \tilde{\varphi}(x_{TE}, y) \quad \text{D.6}$$

Hence, Eq. D.4 reduces to

$$\begin{aligned} \hat{I}_W &= e^{\frac{i\omega}{U_\infty} x_{TE}} \Delta \tilde{\varphi}(x_{TE}, y_1) \int_{x_{TE}}^{\infty} \frac{\partial}{\partial z_1} \left(\frac{e^{-i\omega(\tau + \frac{\lambda_1}{U_\infty})}}{r_{\lambda_1}} \right) d\lambda_1 \\ &= e^{\frac{i\omega}{U_\infty} (x_{TE} - x)} \Delta \tilde{\varphi}(x_{TE}, y_1) \int_{-\infty}^{x - x_{TE}} \frac{\partial}{\partial z_1} \left(\frac{e^{i\omega(\frac{\lambda}{U_\infty} - T)}}{r_\lambda} \right) d\lambda \end{aligned} \quad \text{D.7}$$

where $\lambda = x - \lambda_1$, and

$$r_\lambda = \left[\lambda^2 + \beta^2 [(y_1 - y) + (z_1 - z)^2] \right]^{1/2} \quad \text{D.8}$$

Note that, according to Eq. 2.38, with $x - x_1 = \lambda$,

$$\begin{aligned}\frac{\lambda}{U_\infty} - T &= \frac{\lambda}{U_\infty} - \frac{1}{a_\infty \beta^2} [r_\lambda - M\lambda] \\ &= \frac{1}{U_\infty \beta^2} [\lambda - Mr_\lambda]\end{aligned}\quad \text{D.9}$$

Finally, combining Eqs. D.3, D.7 and D.9 yields

$$\tilde{I}_W = \int_{-b/2}^{b/2} \Delta \tilde{\varphi}(x_{TE}, y_1) \tilde{J}_W(x_{TE}, y_1) dy_1 \quad \text{D.10}$$

with (note that $\partial/\partial z_1 = -\partial/\partial z$)

$$\tilde{J}_W(x_{TE}, y_1) = -e^{\frac{i\omega}{U_\infty}(x_{TE} - x)} \int_{-\infty}^{x - x_{TE}} \frac{\partial}{\partial z} \left[\frac{e^{\frac{i\omega}{U_\infty \beta^2}(\lambda - Mr_\lambda)}}{r_\lambda} \right] d\lambda \quad \text{D.11}$$

Note that, according to Eq. 5.15, the Kernel function of the lifting surface integral equation is given by

$$K = - \left[\frac{\partial}{\partial z} \tilde{J}_W(x_1, y_1) \right]_{z=0} \quad \text{D.12}$$

D.3. An Explicit Expression For \tilde{J}_W

In order to derive an explicit expression for \tilde{J}_W , consider the integral

$$\hat{J}_w(x_1, y_1) = \int_{-\infty}^{x-x_1} \frac{\partial}{\partial z} \left[\frac{e^{\frac{i\omega}{\beta^2 U}(\lambda - Mr_\lambda)}}{r_\lambda} \right] d\lambda$$

$$= \frac{\partial}{\partial z} \int_{-\infty}^{x-x_1} \frac{1}{r_\lambda} e^{\frac{i\omega}{\beta^2 U}(\lambda - Mr_\lambda)} d\lambda$$

D.13

In order to evaluate \hat{J}_w , consider the classical transformation

$$u = \frac{Mr_\lambda - \lambda}{\beta R} = \frac{M \sqrt{\lambda^2 + R^2} - \lambda}{\beta R}$$

D.14

with

$$R = \beta \sqrt{(y - y_1)^2 + (z - z_1)^2}$$

D.15

Note that

$$\sqrt{1+u^2} = \frac{1}{\beta R} \left[\beta^2 R^2 + M^2(\lambda^2 + R^2) - 2M\lambda \sqrt{\lambda^2 + R^2} + \lambda^2 \right]^{1/2}$$

$$= \frac{1}{\beta R} \left[(R^2 + \lambda^2) - 2M\lambda \sqrt{\lambda^2 + R^2} + M^2 \lambda^2 \right]^{1/2}$$

$$= \frac{\sqrt{\lambda^2 + R^2} - M\lambda}{\beta R}$$

D.16

and

$$\frac{du}{d\lambda} = \frac{1}{\beta R} \left[M \frac{\lambda}{\sqrt{\lambda^2 + R^2}} - 1 \right] = - \frac{\sqrt{\lambda^2 + R^2} - M\lambda}{\beta R r_\lambda} = - \frac{\sqrt{1+u^2}}{r_\lambda}$$

D.17

Hence, using the transformation D.14, Eq. D.13 becomes

$$\hat{J}_w = \frac{\partial}{\partial z} \int_{u_1}^{\infty} \frac{e^{-\frac{i\omega R}{\beta u} u}}{\sqrt{1+u^2}} du \quad D.18$$

where

$$u_1 = \frac{M \sqrt{(x-x_1)^2 + R^2} - (x-x_1)}{\beta R} \quad D.19$$

Consider the integral in Eq. D.18

$$\hat{I} = \int_{u_1}^{\infty} \frac{e^{-i\kappa u}}{\sqrt{1+u^2}} du \quad D.20$$

where

$$\kappa = \frac{\omega}{u \beta} R = \frac{\omega}{u_{\infty}} \sqrt{(y_1 - y)^2 + (z_1 - z)^2} \quad D.21$$

In order to evaluate \hat{I} it is convenient to make use of the contour integration. Consider the integral

$$\hat{I}_c = \oint_C \frac{e^{-i\kappa u}}{\sqrt{1+u^2}} du \quad D.22$$

where $C = C_1 + C_2 + C_3 + C_4 + C_5$ is the contour indicated in Fig. D.1. The point $+i$ and $-i$ are branch points:

by connecting them by the branch line shown in Fig. D.1,
the integrand can be treated as an analytic function;
thus, the Cauchy's Theorem yields that

$$\bar{I}_1 + \bar{I}_2 + \bar{I}_3 + \bar{I}_4 + \bar{I}_5 = 0 \quad D.23$$

where

$$\bar{I}_\ell = \int_{C_\ell} \frac{e^{-ixu}}{\sqrt{1+u^2}} du \quad D.24$$

On the other hand, if the radius of the circle C_4 goes to zero and the circle of C_2 goes to infinity, one obtains

$$\bar{I}_4 \rightarrow 0 \quad D.25$$

and, by the Jordan lemma

$$\bar{I}_2 \rightarrow 0 \quad D.26$$

Furthermore,

$$\bar{I}_1 \rightarrow \hat{I} \equiv \int_{u_1}^{\infty} \frac{e^{-ixu}}{\sqrt{1+u^2}} du \quad D.27$$

whereas

$$\bar{I}_5 \rightarrow \hat{I}_5 \equiv \int_{-i}^{u_1} \frac{e^{-ixu}}{\sqrt{1+u^2}} du \quad D.28$$

and finally (Ref. 23)

$$\begin{aligned}\bar{I}_3 \rightarrow \hat{I}_3 &\equiv \int_{-\infty}^{-i} \frac{e^{-ixu}}{\sqrt{1+u^2}} du = - \int_1^{\infty} \frac{e^{-xu}}{\sqrt{u^2-1}} du \\ &= - \int_0^{\infty} e^{-x \cosh \theta} d\theta = -K_0(x)\end{aligned}\quad \text{D.29}$$

where $K_0(x)$ is the modified Bessel function of second kind of zero order.

Hence, by using Eqs. D.25 to D.29, Eq. D.23 yields, in the limit

$$\hat{I} = \int_{u_1}^{\infty} \frac{e^{-ixu}}{\sqrt{1+u^2}} du = -\hat{I}_3 - \hat{I}_5 = K_0(x) + \int_{u_1}^{-i} \frac{e^{-ixu}}{\sqrt{1+u^2}} du \quad \text{D.30}$$

Next, this result can be used in Eq. D.18 to yield

$$\hat{J}_w = \frac{\partial \hat{I}}{\partial z} = -K_1(x) \frac{\partial x}{\partial z} - i \frac{\partial x}{\partial z} \int_{u_1}^{-i} \frac{u e^{-ixu}}{\sqrt{1+u^2}} du - \frac{e^{-ixu_1}}{\sqrt{1+u_1^2}} \frac{\partial u_1}{\partial z} \quad \text{D.31}$$

where the relation (Ref. 23)

$$\frac{\partial K_0(x)}{\partial x} = -K_1(x) \quad \text{D.32}$$

has been used, where K_1 is the modified Bessel function of second kind of first order, given by (Ref. 23)

$$K_1(x) = \left(\gamma + \ln \frac{x}{2}\right) I_1(x) + \frac{1}{x} - \frac{x}{2} \sum_{m=0}^{\infty} \frac{1}{m!(m+1)!} \left[\left(1 + \frac{1}{2} + \dots + \frac{1}{m+1}\right) - \frac{1}{2} \frac{1}{m+1} \right] \left(\frac{x}{2}\right)^{2m} \quad D.33$$

where $\gamma = .4772157$ is the Euler constant.

Finally, the indefinite integral

$$\hat{F}(u) = -ix \int \frac{u e^{-ixu}}{\sqrt{1+u^2}} du \quad D.34$$

is analyzed in Subsection D.4. The results are given by Eqs. D.41 to D.44. By combining Eq. D.11, D.13 and D.34, one obtains

$$\begin{aligned} \tilde{J}_w(x, y_1) &= -e^{\frac{i\omega}{U_w}(x_1-x)} \hat{J}_w(x, y_1) \\ &= -e^{\frac{i\omega}{U_w}(x_1-x)} \left\{ \frac{1}{x} \frac{\partial x}{\partial z} \left[\hat{F}(i) - \hat{F}(u_1) \right] - \frac{e^{-ixu_1}}{\sqrt{1+u_1^2}} \frac{\partial u_1}{\partial z} - K_1(x) \frac{\partial x}{\partial z} \right\} \quad D.35 \end{aligned}$$

where x is given by Eq. D.21 and

$$\frac{\partial x}{\partial z} = \frac{\omega}{\beta U_w} \frac{\partial R}{\partial z} = x \frac{1}{R} \frac{\partial R}{\partial z} = \beta^2 x \frac{z-z_1}{R^2} = \frac{\omega}{U_w} \frac{z_1-z}{\sqrt{(y-y_1)^2 + (z-z_1)^2}} \quad D.36$$

since, according to Eq. D.15

$$\frac{\partial R}{\partial z} = \beta \frac{z-z_1}{\sqrt{(y-y_1)^2 + (z-z_1)^2}} = \beta^2 \frac{z-z_1}{R} \quad D.37$$

and, finally, according to Eqs. D.16, D.19 and D.38

$$\begin{aligned}
 \frac{1}{\sqrt{1+u_1^2}} \frac{\partial u_1}{\partial z} &= \frac{1}{\sqrt{1+u_1^2}} \frac{\partial}{\partial z} \left(\frac{M \sqrt{(x-x_1)^2 + R^2} + (x_1 - x)}{\beta R} \right) \\
 &= \frac{1}{\sqrt{1+u_1^2}} \left[\frac{1}{\beta R} \frac{MR}{\sqrt{(x-x_1)^2 + R^2}} + \frac{M \sqrt{(x-x_1)^2 + R^2} + (x_1 - x)}{-\beta R^2} \right] \frac{dR}{dz} \\
 &= \frac{1}{\sqrt{1+u_1^2}} \frac{1}{\beta R^2 r_\beta} \left[MR^2 - M[(x-x_1)^2 + R^2] - (x_1 - x) r_\beta \right] \beta^2 \frac{z-z_1}{R} \quad \text{D.38} \\
 &= - \frac{1}{\sqrt{1+u_1^2}} \frac{\beta (z-z_1)}{R^3 r_\beta} \left[M(x_1 - x)^2 + r_\beta (x_1 - x) \right] \\
 &= - \frac{\beta R (x_1 - x)}{M(x_1 - x) + r_\beta} \frac{\beta (z-z_1)}{R^3 r_\beta} \left[M(x_1 - x) + r_\beta \right] = - \beta^2 \frac{(z-z_1)(x_1 - x)}{R^2 r_\beta} \\
 &= - \frac{(z-z_1)(x_1 - x)}{(y-y_1)^2 + (z-z_1)^2} \frac{1}{r_\beta}
 \end{aligned}$$

Note that, as shown in Subsection D.5 (Eq. D.63)

$$\hat{F}(-i) = - \frac{\pi}{2} \kappa I_1(\kappa) \quad \text{D.39}$$

where $I_1(\kappa)$ is the modified Bessel function of the first kind of first order (Ref. 23).

Finally, combining Eqs. D.35 to D.39 yields

$$\begin{aligned} \tilde{J}_w(x, y) = & - e^{\frac{i\omega}{U_\infty}(x-x_0)} \left\{ - \frac{\omega}{U_\infty} \frac{1}{\sqrt{(y-y_0)^2 + (z-z_0)^2}} \left[K_1 \left(\frac{\omega}{U_\infty} \sqrt{(y-y_0)^2 + (z-z_0)^2} \right) \right. \right. \\ & + \left. \frac{\pi}{2} i I_1 \left(\frac{\omega}{U_\infty} \sqrt{(y-y_0)^2 + (z-z_0)^2} \right) \right] + \frac{x_0 - x}{(y-y_0)^2 + (z-z_0)^2} \frac{e^{-\frac{i\omega}{U_\infty}[(x-x_0) + M r_p]}}{r_p} \\ & \left. - \frac{1}{(y-y_0)^2 + (z-z_0)^2} \hat{F}(u) \right\} (z-z_0) \end{aligned} \quad D.40$$

As mentioned above, an explicit expression for $F(u)$ is derived in Subsection D.4, where it is shown that

$$\hat{F}(u) = \sum_n \hat{F}_n(u) \quad D.41$$

where $\hat{F}_n(u)$ can be evaluated by using the recurrent formula

$$\hat{F}_n(u) = \frac{1}{n!} (-i)^n x^n \sqrt{1+u^2} u^{n-1} + \frac{x^2}{n(n-2)} \hat{F}_{n-2}(u) \quad D.42$$

with x given by Eq. D.21 and

$$\hat{F}_1(u) = -i x \sqrt{1+u^2} \quad D.43$$

and

$$\hat{F}_2(u) = -\frac{x^2}{2} \left[u \sqrt{1+u^2} - \ln(u + \sqrt{1+u^2}) \right] \quad D.44$$

D.4. The Kernel of the Lifting Surface Theory

In this Subsection, the results obtained thus far are used in order to derive an explicit expression for

the Kernel function of the lifting surface theory. In order to do this, it is convenient to rewrite Eq. D.40 as

$$\tilde{J}_w = -(z - z_1) \tilde{K} \quad D.45$$

where

$$\tilde{K} = e^{\frac{i\omega}{U_\infty}(x_1 - x)} \left\{ -\frac{\omega}{U_\infty} \frac{1}{\sqrt{(y - y_1)^2 + (z - z_1)^2}} K_1 + \right. \\ \left. + \frac{x_1 - x}{(y - y_1)^2 + (z - z_1)^2} \frac{e^{-\frac{i\omega}{\beta^2 U_\infty}[(x_1 - x) + M r_1]}}{r_1} + \frac{[F(-i) - F(y_1)]}{(y - y_1)^2 + (z - z_1)^2} \right\} \quad D.46$$

According to Eq. D.12

$$K_z = \frac{\partial}{\partial z} \left[(z - z_1) \tilde{K} \right]_{z_1=0} = \left[\tilde{K} + (z - z_1) \frac{\partial \tilde{K}}{\partial z} \right]_{z_1=0} \quad D.47$$

and

$$K = \lim_{z \rightarrow 0} K_z = \tilde{K} \Big|_{z=z_1=0} \\ = e^{\frac{i\omega}{U_\infty}(x_1 - x)} \left\{ -\frac{\omega}{U_\infty} \frac{1}{|y_1 - y|} K_1 \left(\frac{\omega}{U_\infty} |y_1 - y| \right) + \right. \\ \left. + \frac{x_1 - x}{|y_1 - y|^2} \frac{1}{r} e^{-\frac{i\omega}{\beta^2 U_\infty}[(x_1 - x) + M \sqrt{(x_1 - x)^2 + \beta^2 (y_1 - y)^2}]} \right. \\ \left. + \frac{1}{|y_1 - y|^2} \left[\hat{F}(-i) - \hat{F}(y_1) \right] \right\} \quad D.48$$

In order to show that this expression is equal to the one given in Ref. 8, it is sufficient to note that

$$\begin{aligned}\hat{F}(u) - \hat{F}(-i) &= \int_0^{u_1} \frac{i x u e^{-i x u}}{\sqrt{1+u^2}} du + \int_i^0 \frac{i x u e^{-i x u}}{\sqrt{1+u^2}} du \\ &= -i x \int_0^{u_1} \frac{u e^{-i x u}}{\sqrt{1+u^2}} du - i x + i x \frac{\pi}{2} \left[I_1(x) - L_1(x) \right]\end{aligned}\quad \text{D.49}$$

where Eq. D.66 has been used.

Finally, combining Eq. D.48 and D.49, yields

$$\begin{aligned}K &= e^{\frac{i\omega}{U_\omega}(x_1-x)} \left\{ -\frac{\omega}{|y_1-y|} \frac{1}{U_\omega} k_1 \left(\frac{\omega}{U_\omega} |y_1-y| \right) \right. \\ &\quad - \frac{i n \omega}{2 U_\omega} \frac{1}{|y_1-y|} \left[I_1 \left(\frac{\omega}{U_\omega} |y_1-y| \right) - L_1 \left(\frac{\omega}{U_\omega} |y_1-y| \right) \right] + i \frac{\omega}{U_\omega} \frac{1}{|y_1-y|} \\ &\quad + i \frac{\omega}{U_\omega} \frac{1}{|y_1-y|} \int_0^{\frac{x-x_1 - M \sqrt{(x_1-x)^2 + \beta^2(y_1-y)^2}}{\beta^2 |y_1-y|}} \frac{u e^{-\frac{i\omega}{U_\omega} |y_1-y| u}}{\sqrt{1+u^2}} du \\ &\quad \left. - \frac{x-x_1}{|y_1-y|^2} \frac{1}{\sqrt{(x_1-x)^2 + \beta^2(y_1-y)^2}} e^{\frac{i\omega}{\beta^2 U_\omega} \left[x-x_1 - M \sqrt{(x_1-x)^2 + \beta^2(y_1-y)^2} \right]} \right\}\end{aligned}\quad \text{D.50}$$

in agreement with Eq. D.8 given in Ref. 8.

D.5. Evaluation of the Integral \hat{F}

Consider the indefinite integral

$$\hat{F} = -ix \int \frac{u e^{-ixu}}{\sqrt{1+u^2}} du \quad \text{D.51}$$

This integral can be integrated by series as follows:

$$\hat{F} = -ix \int u \sum_{m=0}^{\infty} \frac{(-ixu)^m}{m!} \frac{1}{\sqrt{1+u^2}} du = \sum_{n=1}^{\infty} \frac{(-ix)^n}{(n-1)!} f_n \quad \text{D.52}$$

with

$$f_n = \int \frac{u^n}{\sqrt{1+u^2}} du \quad \text{D.53}$$

Note that the interchange between integration and summation signs is allowed by the uniform convergence of the series of the exponential function.

The integral given by Eq. D.53 can be evaluated by using the recurrent formula*

$$n f_n = u^{n-1} \sqrt{1+u^2} - (n-1) f_{n-2} \quad \text{D.54}$$

In particular, disregarding the constant of integration,

$$\begin{aligned} f_0 &= \int \frac{1}{\sqrt{1+u^2}} du = \ln(u + \sqrt{1+u^2}) \\ f_1 &= \int \frac{u}{\sqrt{1+u^2}} du = \sqrt{1+u^2} \end{aligned} \quad \text{D.55}$$

*Note that, for $u > 1$, f_n is divergent as n goes to infinity. However, the ratio $f_n/(n-1)!$ (where f_n is evaluated analytically) is convergent to zero.

Hence, Eq. D.52 may be written as

$$\hat{F}(u) = \sum_{n=1}^{\infty} \hat{F}_n(u) \quad \text{D.56}$$

where

$$\begin{aligned} \hat{F}_n &= \frac{(-ix)^n}{(n-1)!} f_n \\ &= (-i)^n \frac{x^n}{(n-1)!} \frac{1}{n} u^{n-1} \sqrt{1+u^2} - (-i)^n \frac{x^n}{(n-1)!} \frac{1}{n} (n-1) f_{n-1} \end{aligned} \quad \text{D.57}$$

$$= (-i)^n \frac{x^n}{n!} u^{n-1} \sqrt{1+u^2} + \frac{x^2}{n(n-2)} \frac{(-ix)^{n-2}}{(n-3)!} f_{n-2}$$

or

$$\hat{F}_n = (-i)^n \frac{x^n}{n!} u^{n-1} \sqrt{1+u^2} + \frac{x^2}{n(n-2)} \hat{F}_{n-2} \quad \text{D.58}$$

with

$$\hat{F}_1 = -ix \sqrt{1+u^2} \quad \text{D.59}$$

and

$$\hat{F}_2 = -\frac{x^2}{2} \left(u \sqrt{1+u^2} - \ln(u + \sqrt{1+u^2}) \right) \quad \text{D.60}$$

Note, in particular, that $\hat{F}_1(-i) = 0$ and

$$\hat{F}_2(-i) = \frac{x^2}{2} \ln(-i) = -\frac{x^2}{4} \pi i \quad \text{D.61}$$

Hence, $\hat{F}_n(-i) = 0$ for $n = \text{odd}$ and

$$\hat{F}_n(-i) = \frac{x^2}{n(n-2)} \hat{F}_{n-2}(-i) = -\pi i \left(\frac{x}{2}\right)^n \frac{1}{\left(\frac{n}{2}\right)! \left(\frac{n}{2}-1\right)!} \quad \text{D.62}$$

for $n = \text{even}$. Thus

$$\begin{aligned} \hat{F}(-i) &= \sum_{n=1}^{\infty} \hat{F}_n(-i) = \sum_{m=1}^{\infty} \hat{F}_{2m}(-i) = -\pi i \sum_{m=1}^{\infty} \frac{1}{m!(m-1)!} \left(\frac{x}{2}\right)^{2m} \\ &= -\pi i \frac{x}{2} \sum_{p=0}^{\infty} \frac{1}{(p+1)! p!} \left(\frac{x}{2}\right)^{2p+1} = -\pi i \frac{x}{2} I_1(x) \end{aligned} \quad \text{D.63}$$

Note also that $\hat{F}_2(0) = 0$ and

$$F_1(0) = -ix \quad \text{D.64}$$

Hence $\hat{F}_n(0) = 0$ for $n = \text{even}$ and

$$\begin{aligned} \hat{F}_n(0) &= \frac{x^2}{n(n-2)} \hat{F}_{n-2}(0) \\ &= -\pi i \left(\frac{x}{2}\right)^n \frac{1}{\Gamma(1+\frac{n}{2}) \Gamma(\frac{n}{2})} \end{aligned} \quad \text{D.65}$$

for $n = \text{odd}$ (where Γ is the Euler gamma function or factorial function). Thus

$$\begin{aligned} \hat{F}(0) &= \sum_{n=1}^{\infty} \hat{F}_n(0) = -i\pi \sum_{m=0}^{\infty} \left(\frac{x}{2}\right)^{2m+3} \frac{1}{\Gamma(m+\frac{3}{2}) \Gamma(m+\frac{5}{2})} - ix \\ &= -i\pi \frac{x}{2} L_1(x) - ix \end{aligned} \quad \text{D.66}$$

where $L_1(x)$ is the Struve function (Ref. 23).

Combining Eqs. D.63 and D.66 yields

$$\hat{F}(-i) - \hat{F}(0) = -ix \int_0^{-i} \frac{u e^{-ixu}}{\sqrt{1+u^2}} du = -\frac{\pi i}{2} [I_1(x) - L_1(x)] + ix \quad D.67$$

in agreement with the well known relation (Ref. 23)

$$\begin{aligned} \frac{\pi}{2} [I_1(x) - L_1(x)] &= x \int_0^{\pi/2} e^{-x \cos \varphi} \sin^2 \varphi d\varphi \\ &= x \int_0^1 \sqrt{1-\xi^2} e^{-x\xi} d\xi = ix \int_0^{-i} \sqrt{1+u^2} e^{-ixu} du \\ &= - \left[\sqrt{1+u^2} e^{-ixu} \right]_0^{-i} + \int_0^{-i} \frac{u e^{-ixu}}{\sqrt{1+u^2}} du \\ &= 1 + \int_0^{-i} \frac{u}{\sqrt{1+u^2}} e^{-ixu} du \end{aligned} \quad D.68$$

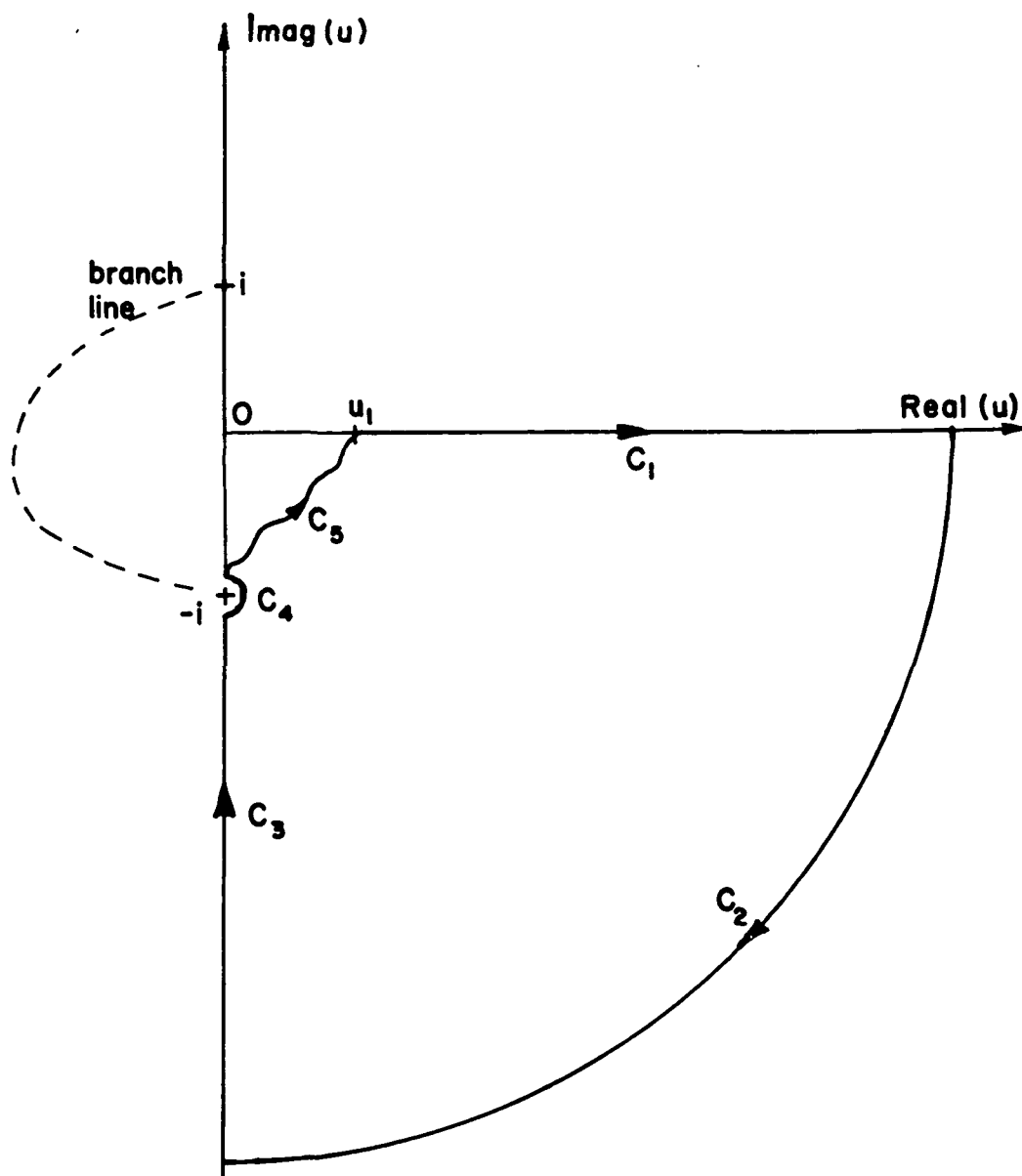


Fig. D.1 The contour of integration

APPENDIX E

SOURCES AND DOUBLETS ON A TRAPEZOIDAL ELEMENT

E.1. Trapezoidal Element

In this Appendix, the effect of the sources and doublets distributed on a trapezoidal planar element are obtained in analytic form. As mentioned in Section 6, it is of interest to consider planar elements described by the equation

$$z_i - z_{ic} = \bar{\alpha}(x_i - x_{ic}) + \bar{\beta}(y_i - y_{ic}) \quad \text{E.1}$$

where the subscript c stands for center of the element. The boundary of the projection of this element on the plane $z = 0$ are given by

$$\begin{aligned} x_{im} + d_m(y_i - y) \leq x_i \leq x_{ip} + d_p(y_i - y) \\ y_{im} \leq y_i \leq y_{ip} \end{aligned} \quad \text{E.2}$$

Equation E.2 represents a trapezoid and the element defined by Eqs. E.1 and E.2 is called trapezoidal planar element (see Fig. E.1).

E.2. Doublet Distribution

Consider first the integral of a doublet distribution of unit density over a trapezoidal planar element, given

by

$$\begin{aligned}
 \hat{I}_D &= \iint \frac{\partial}{\partial n_i} \left(\frac{1}{r} \right) d\Sigma \\
 &= - \int_{y_{im}}^{y_{ip}} dy_i \int_{x_{im}+d_m(y_i-y)}^{x_{ip}+d_p(y_i-y)} \left[\frac{\partial S}{\partial x_i} (x_i-x) + \frac{\partial S}{\partial y_i} (y_i-y) + \frac{\partial S}{\partial z_i} (z_i-z) \right] \frac{1}{r^3} dx_i \\
 &= s \int_{y_{im}}^{y_{ip}} dy_i \int_{x_{im}+d_m(y_i-y)}^{x_{ip}+d_p(y_i-y)} \left[\bar{\alpha} (x_i-x) + \bar{\beta} (y_i-y) - (z_i-z) \right] \frac{1}{r^3} dx_i
 \end{aligned}
 \tag{E.3}$$

where

$$\begin{aligned}
 s &= \frac{\partial S / \partial z_i}{|\partial S / \partial z_i|} = \begin{cases} 1 & \text{on upper surface} \\ -1 & \text{on lower surface} \end{cases}
 \end{aligned}
 \tag{E.4}$$

and use has been made of the fact that, according to

Eq. E.1

$$\begin{aligned}
 \bar{\alpha} &= - \frac{\partial S}{\partial x_i} / \frac{\partial S}{\partial z_i} \\
 \bar{\beta} &= - \frac{\partial S}{\partial y_i} / \frac{\partial S}{\partial z_i}
 \end{aligned}
 \tag{E.5}$$

It should be noted that, for trapezoidal planar elements, $\bar{\alpha}$ and $\bar{\beta}$ are constant and that, according to Eq. E.1,

$$\begin{aligned}
 \bar{\delta} &= (z_i - z) - \bar{\alpha} (x_i - x) - \bar{\beta} (y_i - y) \\
 &= (z_{ie} - z) - \bar{\alpha} (x_{ie} - x) - \bar{\beta} (y_{ie} - y)
 \end{aligned}
 \tag{E.6}$$

Thus, Eq. E.3 reduces to

$$\hat{I}_D = -s\bar{\delta} \int_{y_m}^{y_p} \frac{dy_i}{x_{ip} + d_p(y_i - y)} \frac{1}{r^3} dx_i \quad \text{E.7}$$

with

$$r = \left[(x_i - x)^2 + (y_i - y)^2 + \left(\bar{\delta} + \bar{\alpha}(x_i - x) + \bar{\beta}(y_i - y) \right)^2 \right]^{\frac{1}{2}} \quad \text{E.8}$$

This integral can be simplified considerably if the new variables are introduced:

$$\begin{aligned} \hat{\xi} &= \left[(x_i - x) + \bar{\alpha}(z_i - z) \right] (1 + \bar{\alpha}^2)^{-\frac{1}{2}} \\ \hat{\eta} &= \left[-\bar{\alpha}\bar{\beta}(x_i - x) + (1 + \bar{\alpha}^2)(y_i - y) + \bar{\beta}(z_i - z) \right] (1 + \bar{\alpha}^2)^{-\frac{1}{2}} (1 + \bar{\alpha}^2 + \bar{\beta}^2)^{-\frac{1}{2}} \\ \hat{\zeta} &= \left[-\bar{\alpha}(x_i - x) - \bar{\beta}(y_i - y) + (z_i - z) \right] (1 + \bar{\alpha}^2 + \bar{\beta}^2)^{-\frac{1}{2}} \end{aligned} \quad \text{E.9}$$

These new variables represent coordinates in a new frame of reference with origin in the point x, y, z and base vectors

$$\begin{aligned} \vec{i} &= \left\{ \begin{matrix} 1 \\ 0 \\ \bar{\alpha} \end{matrix} \right\} (1 + \bar{\alpha}^2)^{-\frac{1}{2}} \\ \vec{j} &= \left\{ \begin{matrix} -\bar{\alpha}\bar{\beta} \\ 1 + \bar{\alpha}^2 \\ \bar{\beta} \end{matrix} \right\} (1 + \bar{\alpha}^2)^{-\frac{1}{2}} (1 + \bar{\alpha}^2 + \bar{\beta}^2)^{-\frac{1}{2}} \\ \vec{k} &= \left\{ \begin{matrix} -\bar{\alpha} \\ -\bar{\beta} \\ 1 \end{matrix} \right\} (1 + \bar{\alpha}^2 + \bar{\beta}^2)^{-\frac{1}{2}} \end{aligned} \quad \text{E.10}$$

It should be noted that the vector \vec{k} is normal to the plane of the element. It is also immediately verified that \vec{i} , \vec{j} , \vec{k} are mutually orthogonal unit vectors and thus represent a (right-hand) reference system.

Note that z_1 is not an independent variable: combining Eqs. E.1 and E.9 yields

$$\begin{aligned}\hat{\xi} &= \left[(1 + \bar{\alpha}^2)(x_1 - x) + \bar{\alpha}\bar{\beta}(y_1 - y) + \bar{\alpha}\bar{\delta} \right] (1 + \bar{\alpha}^2)^{-\frac{1}{2}} \\ \hat{\eta} &= \left[(1 + \bar{\alpha}^2 + \bar{\beta}^2)(y_1 - y) + \bar{\beta}\bar{\delta} \right] (1 + \bar{\alpha}^2)^{-\frac{1}{2}} (1 + \bar{\alpha}^2 + \bar{\beta}^2)^{-\frac{1}{2}} \\ \hat{\zeta} &= \bar{\delta} (1 + \bar{\alpha}^2 + \bar{\beta}^2)^{-\frac{1}{2}}\end{aligned}\tag{E.11}$$

where $\bar{\delta}$ is a constant given by Eq. E.6.

Using $\hat{\xi}$ and $\hat{\eta}$ as new variables of integration, Eq. E.1 reduces to (note that $dx_1 dy_1 = (1 + \bar{\alpha}^2 + \bar{\beta}^2)^{-\frac{1}{2}} d\hat{\xi} d\hat{\eta}$)

$$\hat{I}_D = -s \hat{\zeta} \int_{\eta_m}^{\eta_p} d\hat{\eta} \int_{\xi_m(\eta)}^{\xi_p(\eta)} \frac{1}{\bar{\rho}^3} d\hat{\xi}\tag{E.12}$$

where $\hat{\rho}^2 = \hat{\xi}^2 + \hat{\eta}^2 + \hat{\zeta}^2$ and, according to Eq. E.11

$$\begin{aligned}\hat{\eta}_p &= \left[(1 + \bar{\alpha}^2 + \bar{\beta}^2)(y_{1,p} - y) + \bar{\beta}\bar{\delta} \right] (1 + \bar{\alpha}^2)^{-\frac{1}{2}} (1 + \bar{\alpha}^2 + \bar{\beta}^2)^{-\frac{1}{2}} \\ \hat{\eta}_m &= \left[(1 + \bar{\alpha}^2 + \bar{\beta}^2)(y_{1,m} - y) + \bar{\beta}\bar{\delta} \right] (1 + \bar{\alpha}^2)^{-\frac{1}{2}} (1 + \bar{\alpha}^2 + \bar{\beta}^2)^{-\frac{1}{2}}\end{aligned}\tag{E.13}$$

and

$$\begin{aligned}
\hat{\xi}_p(\hat{\eta}) &= \left\{ (1+\bar{\alpha}^2) \left[(x_{1p} - x) + d_p (y_i - y) \right] + \bar{\alpha} \bar{\beta} (y_i - y) + \bar{\alpha} \bar{\delta} \right\} (1+\bar{\alpha}^2)^{-\frac{1}{2}} \\
&= \left\{ (1+\bar{\alpha}^2) (x_{1p} - x) + \left[(1+\bar{\alpha}^2) d_p + \bar{\alpha} \bar{\beta} \right] (y_i - y) + \bar{\alpha} \bar{\delta} \right\} (1+\bar{\alpha}^2)^{-\frac{1}{2}} \\
&= \left\{ (1+\bar{\alpha}^2) (x_{1p} - x) + \left[(1+\bar{\alpha}^2) d_p + \bar{\alpha} \bar{\beta} \right] \frac{\hat{\eta} \sqrt{1+\bar{\alpha}^2} \sqrt{1+\bar{\alpha}^2 + \bar{\beta}^2} - \bar{\delta} \bar{\beta}}{1+\bar{\alpha}^2 + \bar{\beta}^2} + \bar{\alpha} \bar{\delta} \right\} (1+\bar{\alpha}^2)^{-\frac{1}{2}} \\
&= \left\{ (1+\bar{\alpha}^2) (x_{1p} - x) - \frac{(1+\bar{\alpha}^2) d_p + \bar{\alpha} \bar{\beta}}{1+\bar{\alpha}^2 + \bar{\beta}^2} \bar{\beta} \bar{\delta} + \bar{\alpha} \bar{\delta} \right\} (1+\bar{\alpha}^2)^{-\frac{1}{2}} + \frac{(1+\bar{\alpha}^2) d_p + \bar{\alpha} \bar{\beta}}{\sqrt{1+\bar{\alpha}^2 + \bar{\beta}^2}} \hat{\eta} \quad \text{E.14} \\
&= \left\{ (1+\bar{\alpha}^2) (x_{1p} - x) + \frac{-(1+\bar{\alpha}^2) d_p \bar{\beta} \bar{\delta} + (1+\bar{\alpha}^2) \bar{\alpha} \bar{\delta}}{(1+\bar{\alpha}^2 + \bar{\beta}^2)} \right\} (1+\bar{\alpha}^2)^{-\frac{1}{2}} + \frac{(1+\bar{\alpha}^2) d_p + \bar{\alpha} \bar{\beta}}{\sqrt{1+\bar{\alpha}^2 + \bar{\beta}^2}} \hat{\eta} \\
&= \sqrt{1+\bar{\alpha}^2} \left\{ (x_{1p} - x) + \frac{(\bar{\alpha} - d_p \bar{\beta}) \bar{\delta}}{1+\bar{\alpha}^2 + \bar{\beta}^2} \right\} + \frac{\bar{\alpha} \bar{\beta} + (1+\bar{\alpha}^2) d_p}{\sqrt{1+\bar{\alpha}^2 + \bar{\beta}^2}} \hat{\eta} \\
&= \hat{\xi}_{0p} + \hat{\xi}_{1p} \hat{\eta}
\end{aligned}$$

with

$$\begin{aligned}
\hat{\xi}_{0p} &= \sqrt{1+\bar{\alpha}^2} \left[(x_{1p} - x) + \frac{1}{1+\bar{\alpha}^2 + \bar{\beta}^2} (\bar{\alpha} - d_p \bar{\beta}) \bar{\delta} \right] \\
\hat{\xi}_{1p} &= \frac{\bar{\alpha} \bar{\beta} + (1+\bar{\alpha}^2) d_p}{\sqrt{1+\bar{\alpha}^2 + \bar{\beta}^2}} \quad \text{E.15}
\end{aligned}$$

Similarly

$$\hat{\xi}_m = \hat{\xi}_{0m} + \hat{\xi}_{1m} \hat{\eta} \quad \text{E.16}$$

with

$$\begin{aligned}\hat{\xi}_{om} &= \sqrt{1+\bar{\alpha}^2} \left[(x_{1m} - x) + \frac{1}{1+\bar{\alpha}^2+\bar{\beta}^2} (\bar{\alpha} - d_m \bar{\beta}) \bar{\delta} \right] \\ \hat{\xi}_{1m} &= \frac{\bar{\alpha} \bar{\beta} + (1+\bar{\alpha}^2) d_m}{\sqrt{1+\bar{\alpha}^2+\bar{\beta}^2}}\end{aligned}\quad \text{E.17}$$

Integrating Eq. E.12 yields

$$\begin{aligned}\hat{I}_D &= -s \hat{\xi} \int_{\hat{\eta}_m}^{\hat{\eta}_p} \left[\frac{\hat{\xi}}{\hat{\eta}^2 + \hat{\xi}^2} \frac{1}{\bar{\beta}} \right]_{\hat{\xi}=\hat{\xi}_p(\hat{\eta})}^{\hat{\xi}=\hat{\xi}_m(\hat{\eta})} d\hat{\eta} \\ &= -s \hat{\xi} \int_{\hat{\eta}_m}^{\hat{\eta}_p} \frac{\hat{\xi}_{op} + \hat{\xi}_{1p} \hat{\eta}}{\hat{\eta}^2 + \hat{\xi}^2} \left[(\hat{\xi}_{op} + \hat{\xi}_{1p} \hat{\eta})^2 + \hat{\eta}^2 + \hat{\xi}^2 \right]^{-\frac{1}{2}} d\hat{\eta} \\ &\quad + s \hat{\xi} \int_{\hat{\eta}_m}^{\hat{\eta}_p} \frac{\hat{\xi}_{om} + \hat{\xi}_{1m} \hat{\eta}}{\hat{\eta}^2 + \hat{\xi}^2} \left[(\hat{\xi}_{om} + \hat{\xi}_{1m} \hat{\eta})^2 + \hat{\eta}^2 + \hat{\xi}^2 \right]^{-\frac{1}{2}} d\hat{\eta}\end{aligned}\quad \text{E.18}$$

Consider the indefinite integral

$$\hat{I}_1 = \int \frac{\hat{\xi}_o + \hat{\xi}_1 \hat{\eta}}{\hat{\eta}^2 + \hat{\xi}^2} \left[(\hat{\xi}_o + \hat{\xi}_1 \hat{\eta})^2 + \hat{\eta}^2 + \hat{\xi}^2 \right]^{-\frac{1}{2}} d\hat{\eta} \quad \text{E.19}$$

This can be integrated by standard methods of integration; using the transformation

$$\hat{\eta} = -\frac{\hat{\xi}_o}{\hat{\xi}_1} \frac{\hat{t} - \hat{\xi}^2 \hat{\xi}_1^2 / \hat{\xi}_o^2}{\hat{t} + 1} \quad \text{E.20}$$

and integrating yields

$$\hat{I}_1 = \frac{1}{|\hat{\xi}_1|} \tan^{-1} \left\{ \frac{\hat{\xi}_o \hat{t}}{|\hat{\xi}_1| \sqrt{\hat{t}^2 + \frac{\hat{\xi}^2 \hat{\xi}_1^2}{\hat{\xi}_o^2} + \hat{\xi}_1^2 \left(1 + \frac{\hat{\xi}^2 \hat{\xi}_1^2}{\hat{\xi}_o^2} \right)}} \right\} \quad \text{E.21}$$

and, returning to the original variable, $\hat{\eta}$

$$\hat{I}_1 = \frac{1}{|\hat{\xi}|} \tan^{-1} \left\{ \frac{\hat{\xi}_0}{|\hat{\xi}|} \frac{\hat{\eta} - \frac{\hat{\xi}_1}{\hat{\xi}_0} \hat{\xi}^2}{[(\hat{\xi}_0 + \hat{\xi}_1 \hat{\eta})^2 + \hat{\eta}^2 + \hat{\xi}^2]^{1/2}} \right\} \quad \text{E.22}$$

Finally, by using Eq. E.22, Eq. E.18 reduces to

$$\hat{I}_0 = -s \frac{\hat{\xi}}{|\hat{\xi}|} \hat{I} \quad \text{E.23}$$

with

$$\begin{aligned} \hat{I} &= \tan^{-1} \left\{ \frac{\hat{\xi}_{op}}{|\hat{\xi}|} \left(\hat{\eta}_p - \frac{\hat{\xi}_{ip}}{\hat{\xi}_{op}} \hat{\xi}^2 \right) \frac{1}{\hat{\rho}_{pp}} \right\} \\ &- \tan^{-1} \left\{ \frac{\hat{\xi}_{op}}{|\hat{\xi}|} \left(\hat{\eta}_m - \frac{\hat{\xi}_{ip}}{\hat{\xi}_{op}} \hat{\xi}^2 \right) \frac{1}{\hat{\rho}_{pm}} \right\} \\ &- \tan^{-1} \left\{ \frac{\hat{\xi}_{om}}{|\hat{\xi}|} \left(\hat{\eta}_p - \frac{\hat{\xi}_{im}}{\hat{\xi}_{om}} \hat{\xi}^2 \right) \frac{1}{\hat{\rho}_{mp}} \right\} \\ &+ \tan^{-1} \left\{ \frac{\hat{\xi}_{om}}{|\hat{\xi}|} \left(\hat{\eta}_m - \frac{\hat{\xi}_{im}}{\hat{\xi}_{om}} \hat{\xi}^2 \right) \frac{1}{\hat{\rho}_{mm}} \right\} \end{aligned} \quad \text{E.24}$$

where

$$\begin{aligned} \hat{\rho}_{pp} &= [\hat{\xi}_{pp}^2 + \hat{\eta}_p^2 + \hat{\xi}^2]^{1/2} \\ \hat{\rho}_{pm} &= [\hat{\xi}_{pm}^2 + \hat{\eta}_m^2 + \hat{\xi}^2]^{1/2} \\ \hat{\rho}_{mp} &= [\hat{\xi}_{mp}^2 + \hat{\eta}_p^2 + \hat{\xi}^2]^{1/2} \\ \hat{\rho}_{mm} &= [\hat{\xi}_{mm}^2 + \hat{\eta}_m^2 + \hat{\xi}^2]^{1/2} \end{aligned} \quad \text{E.25}$$

with

$$\begin{aligned}
 \hat{\xi}_{pp} &= \hat{\xi}_{op} + \hat{\xi}_{ip} \hat{\eta}_p \\
 \hat{\xi}_{pm} &= \hat{\xi}_{op} + \hat{\xi}_{ip} \hat{\eta}_m \\
 \hat{\xi}_{mp} &= \hat{\xi}_{om} + \hat{\xi}_{im} \hat{\eta}_p \\
 \hat{\xi}_{mm} &= \hat{\xi}_{om} + \hat{\xi}_{im} \hat{\eta}_m
 \end{aligned}
 \tag{E.26}$$

E.3. Source Distribution

Finally, consider the integral of a source distribution of density $\frac{\partial S}{\partial x_i} / |\nabla S|$ over a trapezoidal planar element, given by

$$\begin{aligned}
 \hat{I}_s &= \iint \frac{1}{r} \frac{\partial S}{\partial x_i} \frac{d\Sigma}{|\nabla S|} \\
 &= \frac{\partial S / \partial x_i}{|\partial S / \partial z_i|} \int_{y_{im}}^{y_{ip}} dy_i \int_{x_{im} + d_m(y_i - y)}^{x_{ip} + d_p(y_i - y)} \frac{1}{r} dx_i
 \end{aligned}
 \tag{E.27}$$

Using the transformation introduced in the preceeding subsection yields

$$\hat{I}_s = -s \bar{\alpha} (1 + \bar{\alpha}^2 + \bar{\beta}^2)^{-\frac{1}{2}} \int_{\hat{\eta}_m}^{\hat{\eta}_p} d\hat{\eta} \int_{\hat{\xi}_m(\hat{\eta})}^{\hat{\xi}_p(\hat{\eta})} \frac{1}{\bar{\rho}} d\hat{\xi}
 \tag{E.28}$$

and, by integration

$$\begin{aligned}
 \hat{I}_s &= \frac{-s\bar{\alpha}}{(1+\bar{\alpha}^2+\bar{\beta}^2)^{\frac{1}{2}}} \int_{\hat{\eta}_m}^{\hat{\eta}_p} \left[\ln(\hat{\xi} + \sqrt{\hat{\xi}^2 + \hat{\eta}^2 + \hat{z}^2}) \right]_{\hat{\xi}=\hat{\xi}_m(\hat{\eta})}^{\hat{\xi}=\hat{\xi}_p(\hat{\eta})} d\hat{\eta} \\
 &= \frac{-s\bar{\alpha}}{(1+\bar{\alpha}^2+\bar{\beta}^2)^{\frac{1}{2}}} \left\{ \int_{\hat{\eta}_m}^{\hat{\eta}_p} \ln \left[(\hat{\xi}_{op} + \hat{\xi}_{ip} \hat{\eta}) + \sqrt{(\hat{\xi}_{op} + \hat{\xi}_{ip} \hat{\eta})^2 + \hat{\eta}^2 + \hat{z}^2} \right] d\hat{\eta} \right. \\
 &\quad \left. - \int_{\hat{\eta}_m}^{\hat{\eta}_b} \ln \left[(\hat{\xi}_{om} + \hat{\xi}_{im} \hat{\eta}) + \sqrt{(\hat{\xi}_{om} + \hat{\xi}_{im} \hat{\eta})^2 + \hat{\eta}^2 + \hat{z}^2} \right] d\hat{\eta} \right\} \quad E.29
 \end{aligned}$$

Consider the indefinite integral

$$\hat{I}_2 = \int \ln(\hat{\xi} + \hat{\rho}) d\hat{\eta} \quad E.30$$

with $\hat{\xi} = \hat{\xi}_o + \hat{\xi}_1 \hat{\eta}$. Integrating by parts yields
(note that $\partial \hat{\xi} / \partial \hat{\eta} = \hat{\xi}_1$)

$$\begin{aligned}
 \hat{I}_2 &= \hat{\eta} \ln(\hat{\xi} + \hat{\rho}) - \int \hat{\eta} \frac{1}{\hat{\xi} + \hat{\rho}} \left(\hat{\xi}_1 + \frac{\hat{\xi}_1 \hat{\xi} + \hat{\eta}}{\hat{\rho}} \right) d\hat{\eta} \\
 &= \hat{\eta} \ln(\hat{\xi} + \hat{\rho}) - \int \left(\hat{\xi}_1 \hat{\eta} + \frac{\hat{\eta}^2}{\hat{\xi} + \hat{\rho}} \right) \frac{1}{\hat{\rho}} d\hat{\eta} \quad E.31
 \end{aligned}$$

Note that

$$\begin{aligned}
 \frac{\hat{\eta}^2}{\hat{\xi} + \hat{\rho}} \frac{1}{\hat{\rho}} &= \frac{\hat{\eta}^2}{\hat{\xi}^2 - \hat{\rho}^2} \frac{\hat{\xi} - \hat{\rho}}{\hat{\rho}} = -\frac{\hat{\eta}^2}{\hat{\eta}^2 + \hat{z}^2} \left(\frac{\hat{\xi}}{\hat{\rho}} - 1 \right) \\
 &= -\frac{\hat{\eta}^2}{\hat{\eta}^2 + \hat{z}^2} \frac{\hat{\xi}}{\hat{\rho}} + \frac{\hat{\eta}^2}{\hat{\eta}^2 + \hat{z}^2} = -\frac{\hat{\xi}}{\hat{\rho}} + \frac{\hat{\xi}^2}{\hat{\eta}^2 + \hat{z}^2} \frac{\hat{\xi}}{\hat{\rho}} + \frac{\hat{\eta}^2}{\hat{\eta}^2 + \hat{z}^2} \quad E.32
 \end{aligned}$$

Combining Eqs. E.31 and E.32 yields (note that $\hat{\xi}_1 \hat{\eta} - \hat{\xi} = -\hat{\xi}_0$.)

$$\hat{I}_2 = \hat{\eta} \ln(\hat{\xi} + \hat{\rho}) + \hat{\xi}_0 \int \frac{1}{\hat{\rho}} d\hat{\eta} - \hat{\xi}^2 \int \frac{\hat{\xi}}{\hat{\eta}^2 + \hat{\xi}^2} \frac{1}{\hat{\rho}} d\hat{\eta} - \int \frac{\hat{\eta}^2}{\hat{\eta}^2 + \hat{\xi}^2} d\hat{\eta} \quad \text{E.33}$$

Note that

$$\begin{aligned} \int \frac{1}{\hat{\rho}} d\hat{\eta} &= \int [(\hat{\xi}_0 + \hat{\xi}_1 \hat{\eta})^2 + \hat{\eta}^2 + \hat{\xi}^2]^{-1/2} d\hat{\eta} \\ &= \frac{1}{\sqrt{1 + \hat{\xi}_1^2}} \ln \left(\hat{\eta} + \frac{\hat{\xi}_0 \hat{\xi}_1}{1 + \hat{\xi}_1^2} + \frac{1}{\sqrt{1 + \hat{\xi}_1^2}} \hat{\rho} \right) \end{aligned} \quad \text{E.34}$$

Combining Eqs. E.29, E.33 and E.34 yields

$$\begin{aligned} \hat{I}_S &= \frac{-s\bar{\alpha}}{\sqrt{1 + \bar{\alpha}^2 + \bar{\beta}^2}} \left\{ \left[\hat{\eta}_p \ln \left(\frac{\hat{\xi}_{pp} + \hat{\rho}_{pp}}{\hat{\xi}_{mp} + \hat{\rho}_{mp}} \right) - \hat{\eta}_m \ln \left(\frac{\hat{\xi}_{pm} + \hat{\rho}_{pm}}{\hat{\xi}_{nm} + \hat{\rho}_{nm}} \right) \right] \right. \\ &\quad + \frac{\hat{\xi}_{op}}{\sqrt{1 + \hat{\xi}_{ip}^2}} \ln \left(\frac{\hat{\eta}_p + \hat{\xi}_{op} \hat{\xi}_{ip} / (1 + \hat{\xi}_{ip}^2) + \hat{\rho}_{pp} / \sqrt{1 + \hat{\xi}_{ip}^2}}{\hat{\eta}_m + \hat{\xi}_{op} \hat{\xi}_{ip} / (1 + \hat{\xi}_{ip}^2) + \hat{\rho}_{pm} / \sqrt{1 + \hat{\xi}_{ip}^2}} \right) \\ &\quad - \frac{\hat{\xi}_{om}}{\sqrt{1 + \hat{\xi}_{im}^2}} \ln \left(\frac{\hat{\eta}_p + \hat{\xi}_{om} \hat{\xi}_{im} / (1 + \hat{\xi}_{im}^2) + \hat{\rho}_{mp} / \sqrt{1 + \hat{\xi}_{im}^2}}{\hat{\eta}_m + \hat{\xi}_{om} \hat{\xi}_{im} / (1 + \hat{\xi}_{im}^2) + \hat{\rho}_{nm} / \sqrt{1 + \hat{\xi}_{im}^2}} \right) \\ &\quad \left. - |\hat{\xi}| \hat{I} \right\} \end{aligned} \quad \text{E.35}$$

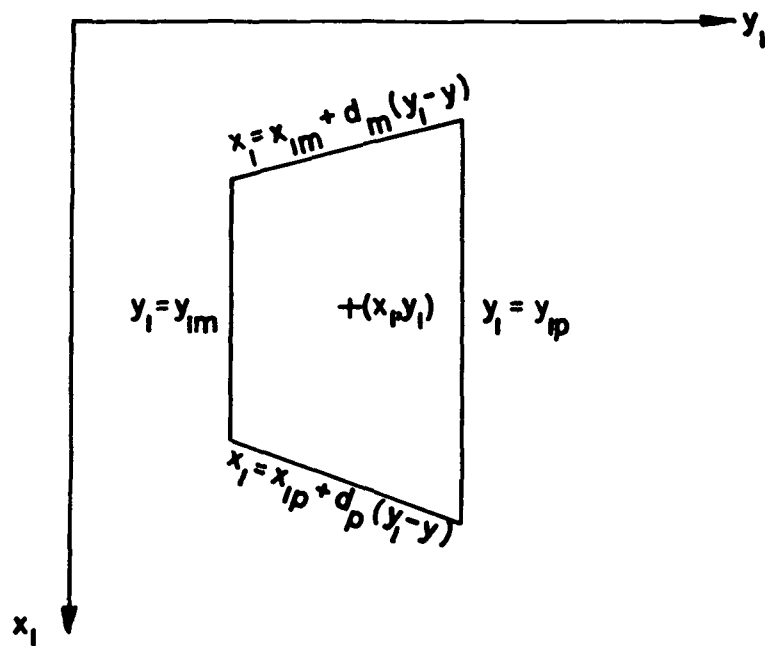


Fig. E.1 The projection of the trapezoidal element in the plane x_1, y_1

APPENDIX F

INITIAL CONDITIONS

In this Appendix, the generalized Huygens' principle is further generalized to cover also the case in which the problem is formulated with initial conditions. In this case, the function E , defined by Eq. 3.1, must be assumed to be zero also for $t \leq 0$. Thus, a branch of the surface Σ is given by the equation*

$$S \equiv t_1 = 0 \quad \text{F.1}$$

For this surface, $\nabla S = 0$ and $\partial S / \partial t_1 = +1$. Furthermore, $S^T = t - T$ and $|\nabla S^T| = |\nabla T|$. Thus, Eq. 3.32 can be generalized by adding to the right-hand side the term

$$\begin{aligned} 4\pi E \varphi_{\text{I.C.}} &= \frac{1}{a_\omega^2} \iint_{\Sigma_{\text{I.C.}}^T} \left(\frac{\partial \varphi}{\partial t_1} \right)^T \frac{1}{r_\beta} \frac{1}{|\nabla T|} d\Sigma^T \\ &\quad - \frac{1}{a_\omega^2} \iint_{\Sigma_{\text{I.C.}}^T} M \frac{\partial}{\partial x_1} \left(\frac{1}{r_\beta} \right) \varphi^T \frac{1}{|\nabla T|} d\Sigma^T \\ &\quad + \frac{1}{a_\omega^2} \frac{\partial}{\partial t} \iint_{\Sigma_{\text{I.C.}}^T} \left(1 + M \frac{\partial T}{\partial x_1} \right) \varphi^T \frac{1}{r_\beta} \frac{1}{|\nabla T|} d\Sigma^T \end{aligned} \quad \text{F.2}$$

*The condition that $\square S$ is directed like the four-dimensional outward normal $\vec{\nu}$ is satisfied (see Fig. 2).

As shown in Appendix B, for $M = 0$, Eq. F.2 reduces to the classical Poisson formula⁹ (Cauchy problem for the wave equation).

Similar results can be obtained for the supersonic flow.

APPENDIX G

SMALL THICKNESS FORMULATION

G.1 Introduction

As mentioned in Section 6, the integral equation for the potential φ has the disadvantage that it becomes singular as the thickness goes to zero. In this Appendix, the characteristics of this equation are analyzed more in detail. In particular, the behaviour at the trailing and the leading edges (where one might consider that the thickness is zero) are examined (Subsection G.2), vortex layer interpretation is given (Subsection G.3) and an alternative approach to solving the problem is suggested (Subsection G.4).

G.2 Leading and Trailing Edges

Consider first the trailing edge. In order to obtain the integral equation at the trailing edge, it is convenient to use the same procedure used in Appendix C, that is, to obtain the integral equation as the limit (when the control point approaches the trailing edge) of Eq. 6.1, or for simplicity, the corresponding one for incompressible flow

$$\varphi = \oint_{\Sigma_B} Q_n \frac{1}{4\pi r} d\Sigma - \oint_{\Sigma_B + \Sigma_w} \varphi \frac{\partial}{\partial n_1} \left(\frac{1}{4\pi r} \right) d\Sigma \quad \text{G.1}$$

For the sake of simplicity, the surface Σ is replaced by the smoothed surface Σ' in an infinitesimal neighborhood of the trailing edge (see Fig. G.1).

Next, the limit value of Eq. G.1 as the control point P goes to P*, is considered. Following the same procedure used in Appendix C, one obtains immediately

$$\varphi_{TE,u} = \left\{ \oint_{\Sigma_B} Q_n \frac{1}{4\pi r} d\Sigma - \oint_{\Sigma_B + \Sigma_w} \varphi \frac{\partial}{\partial n_i} \left(\frac{1}{4\pi r} \right) d\Sigma \right\}_{P=P_*} + \frac{1}{2} (\varphi_{TE,u} - \varphi_{TE,l}) \quad G.2$$

where $\varphi_{TE,u}(\varphi_{TE,l})$ is the upper (lower) value of φ at the trailing edge. Similarly, if P approaches P* from the bottom, one obtains

$$\varphi_{TE,l} = \left\{ \oint_{\Sigma_B} Q_n \frac{1}{4\pi r} d\Sigma - \oint_{\Sigma_B + \Sigma_w} \varphi \frac{\partial}{\partial n_i} \left(\frac{1}{4\pi r} \right) d\Sigma \right\}_{P=P_*} + \frac{1}{2} (\varphi_{TE,l} - \varphi_{TE,u}) \quad G.3$$

However, the two equations are not independent since both are equivalent to

$$\varphi_{TE,u} + \varphi_{TE,l} = \left\{ \oint_{\Sigma_B} Q_n \frac{1}{2\pi r} d\Sigma - \oint_{\Sigma_B + \Sigma_w} \varphi \frac{\partial}{\partial n_i} \left(\frac{1}{2\pi r} \right) d\Sigma \right\}_{P=P_*} \quad G.4$$

Note that in general for lifting bodies $\varphi_{TE,u} \neq \varphi_{TE,l}$. Thus, one has only one equation (Eq. G.4) for two unknowns $\varphi_{TE,u}$ and $\varphi_{TE,l}$. Hence, an additional condition, the Kutta condition, must be given in order to make the problem complete:

$$\Delta c_{p,TE} = (c_{p,u} - c_{p,l})_{TE} = \left(\frac{d\varphi_u}{dt} - \frac{d\varphi_l}{dt} \right)_{TE} = 0 \quad G.5$$

The implication of this on the numerical formulation described in Section 6 are obvious. If the control points of the upper

and lower surface are very close to the trailing edge, the two equations are both very close to Eq. G.4 and thus, the determinant is very close to zero. Hence, use of small boxes in the neighborhood of the trailing edge yields elimination of significant figures even for thick wings. An alternative formulation is then required (Subsection G.3).

It may be noted that the above problem does not exist at the leading edge since there, the upper and lower values of the potential are equal. Incidentally, however, it may be worth noting that, as is well known, at the leading edge the hypothesis of small perturbation fails. For, at the leading edge, the boundary conditions are given by

$$\frac{\partial \phi}{\partial n} = - \frac{\partial S / \partial x}{|\nabla S|} = - \eta_x \approx -1 \quad \text{G.6}$$

(since the normal \vec{n} is almost parallel to the x-axis), which is in contradiction to Eqs. 4.5 and 4.6. It may be noted however, that the boundary condition is still used in its exact form and that the terms neglected in Section 4 are still of the same order of the nonlinear term of the differential equation. Moreover, this yields only a local effect which eventually can be analyzed with the method of matched asymptotic expansions (see for instance, Ref. 24). In any case, the error involved is smaller than the one obtained in the lifting surface theory where the value of $\partial \phi / \partial x$ is infinitely large.

G.3 Vortex Layer

As is well known, a discontinuity in the potential corresponds to a vortex layer. The direction of the vortices in the layer is given by the direction of the line $\Delta\varphi = \text{constant}$ and the intensity of the vortex is given by variation of $\frac{\partial \Delta\varphi}{\partial s}$ where s is the direction (in the layer) normal to the "constant $\Delta\varphi$ lines", that is, the direction of the perturbation velocity component in the plane of the vortex layer. Physically speaking, the doublet integral can be interpreted as a (zero-thickness) boundary layer (note that, with this interpretation, $E = 0$ inside Σ should be replaced by $\varphi = 0$ inside Σ , which implies that the perturbation velocity is identically equal to zero inside Σ). Finally, it may be noted that this implies that this formulation does not yield any phenomena of the type encountered in lifting-surface formulations (with elements inclined to the flow), for which "wakes emanating from points near the body leading edge will thread through the body surface near its trailing edge" (Ref. 25 p. 446). It should be noted that the tangent plane approximation (Section 7) yields a similar phenomenon. However, the tangent plane approximation should be considered only as a numerical approximate procedure (with controlled error) to solve a physically well posed formulation.

G.4 Alternative Formulations

Finally, it is worth noting that alternative numerical formulations can be used in connection with the theoretical

formulation presented here. Again, for the sake of simplicity, the discussion is carried out for the steady incompressible case. Consider first the normal derivative of the basic equation

$$\frac{\partial \varphi}{\partial n} = \oint_{\Sigma} \frac{\partial \varphi}{\partial n_1} \frac{\partial}{\partial n} \left(\frac{1}{4\pi R} \right) d\Sigma - \oint_{\Sigma} \varphi \frac{\partial^2}{\partial n \partial n_1} \left(\frac{1}{4\pi R} \right) d\Sigma \quad G.7$$

By taking the limit as the control point approaches Σ , one obtains an integral equation (different from Eq. 6.2), which has the advantage that if the thickness is equal to zero, the operator is not singular: the limit equation is the one used by Haviland.²⁶

Two other alternative formulations are obtained by introducing a convenient flow field inside the surface Σ (see Lamb²⁷). If the value of the potential is continuous across the surface, one obtains

$$\varphi = \oint_{\Sigma} S \frac{1}{4\pi R} d\Sigma \quad G.8$$

where S is the intensity of the source distribution (equal to the discontinuity in normal velocity). On the other hand, if the normal velocity is continuous across the surface, then one obtains

$$\varphi = \oint_{\Sigma} D \frac{\partial}{\partial n_1} \left(\frac{1}{4\pi R} \right) d\Sigma \quad G.9$$

where D is the intensity of the doublet distribution (equal to the discontinuity of φ). By taking the normal derivative

of Eqs. G.8 and G.9 and imposing the boundary conditions, one obtains two integral equations for the unknowns S and D, respectively. These methods are used, for instance, by Hess and Smith²⁸ and Djojodihardjo and Widnall,⁶ respectively.

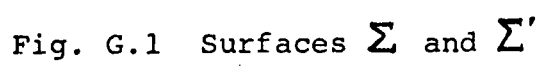
It may be noted that more complex formulations can be obtained by combining two or more of these four basic methods, Eqs. 6.2, G.7, G.8 and G.9. The advantages and disadvantages of the four basic methods are briefly discussed here. Note first that the "source method", Eq. G.8, is limited to nonlifting bodies: extensions to lifting configurations must include doublet distributions as well.²⁹ On the other hand, the other two methods, Eqs. G.7 and G.9, if applied to a closed surface, involve a singular operator (which yields a determinant equal to zero). For, according to Eq. 6.6, one obtains, outside Σ ,

$$\oint_{\Sigma} \frac{\partial}{\partial n_1} \left(\frac{1}{4\pi R} \right) d\Sigma = -\frac{1}{4\pi} \oint_{4\pi} d\Omega = 0 \quad (G.10)$$

and thus its normal derivative is zero: hence, Eqs. G.7 and G.9 have a nontrivial (constant) solution for the homogeneous problem.* Thus, the method presented here is the only one of the four basic methods, which can be applied to "closed-surface"

* It should be noted however, that these two methods can be used for open surfaces (lifting surfaces²⁶), or for the analysis of the transient response.⁶

description of lifting configurations. On the other hand, as mentioned above, combinations of two or more of the four basic methods can be usefully employed. Various combinations are now being explored.



APPENDIX H

SUPERSONIC DOUBLET

H.1 Introduction

It should be noted that, as mentioned in Subsection 3.5, the supersonic Green function (Eq. 3.44) has an infinitely large discontinuity at the Mach cone. Hence, the normal derivative $\partial G / \partial n_1$ (supersonic doublet) has meaning only in the theory of distributions.⁷

The scope of this Appendix is to obtain the correct definition of the supersonic doublet within the theory of functions (as distinct from distributions). In order to obtain this, the Lighthill definition of distribution, or generalized functions (as limit of regular functions) will be employed. For simplicity, the steady case is considered. The potential steady supersonic flow around a body of arbitrary shape is described by the equation

$$\varphi = \oint_{\Sigma} \frac{\partial \varphi}{\partial n_1} G d\Sigma - \oint_{\Sigma} \varphi \frac{\partial G}{\partial n_1} d\Sigma \quad \text{H.1}$$

where φ is the perturbation potential, Σ is a surface surrounding the body and the wake and (see Eq. 3.44)

$$G = \frac{-1}{2\pi r_B} = -\frac{1}{2\pi} \left[(x-x_1)^2 - (y-y_1)^2 - (z-z_1)^2 \right]^{-\frac{1}{2}} \quad \begin{matrix} x-x_1 > [(y-y_1)^2 + (z-z_1)^2]^{\frac{1}{2}} \\ x-x_1 < [(y-y_1)^2 + (z-z_1)^2]^{\frac{1}{2}} \end{matrix} \quad \text{H.2}$$

$$= 0$$

is the steady supersonic source or Green's function. In Eq.

B.2, it is assumed for simplicity that $B = \sqrt{M^2 - 1} \equiv 1$, since by using the supersonic Prandtl-Glauert transformation, expressions formally equal to Eqs. H.1 and H.2 can be obtained.

For the sake of simplicity, an element of planar surface Σ_0 , parallel to the x-axis is considered. By suitable change of coordinates, this element can be reduced to be lying in the plane $z_1 = 0$. In this case

$$\frac{\partial}{\partial n_1} = \frac{\partial}{\partial z_1} = - \frac{\partial}{\partial z} \quad \text{H.3}$$

Furthermore, the origin will be assumed to be moved to the point $(x, y, 0)$, so that Eq. H.2 reduces to

$$\begin{aligned} G &= - \frac{1}{2\pi} (x_1^2 - y_1^2 - z^2)^{-\frac{1}{2}} & x_1 < -[y_1^2 + z^2]^{\frac{1}{2}} \\ &= 0 & x_1 > -[y_1^2 + z^2]^{\frac{1}{2}} \end{aligned} \quad \text{H.4}$$

In conclusion, the supersonic doublet integral reduces to

$$I_D \equiv - \iint_{\Sigma_0} \frac{\partial G}{\partial n_1} d\Sigma = \iint_{\Sigma_0} \frac{\partial G}{\partial z} dx_1 dy_1 \quad \text{H.5}$$

with G given by Eq. H.4. This integral is analyzed in the following.

H.2 Modified Supersonic Doublet Integral

As mentioned before, following the Lighthill approach, the Eq. H.4 will be considered as the limit of a more manageable function. A suitable choice is (see Fig. H.1)

$$\begin{aligned} \hat{G} &= - \frac{1}{2\pi} \frac{1}{r_B} & r_B &\geq \varepsilon \\ &= - \frac{1}{2\pi} \frac{r_B}{\varepsilon^2} & r_B &\leq \varepsilon \end{aligned} \quad \text{H.6}$$

Furthermore,

$$\hat{G} = 0 \quad x_1 > -[y_1^2 + z^2]^{\frac{1}{2}} \quad \text{H.7}$$

Hence, the function has no discontinuity for all the values of x_1 and y_1 . In conclusion, the modified supersonic source G is given by

$$\begin{aligned} \hat{G} &= -\frac{1}{2\pi} (x_1^2 - y_1^2 - z^2)^{-\frac{1}{2}} & -\infty \leq x_1 \leq -(y_1^2 + z^2 + \varepsilon^2)^{\frac{1}{2}} \\ &= -\frac{1}{2\pi\varepsilon^2} (x_1^2 - y_1^2 - z^2)^{-\frac{1}{2}} & -(y_1^2 + z^2 + \varepsilon^2)^{\frac{1}{2}} \leq x_1 \leq -(y_1^2 + z^2)^{\frac{1}{2}} \\ &= 0 & -(y_1^2 + z^2)^{\frac{1}{2}} \leq x_1 \leq \infty \end{aligned} \quad \text{H.8}$$

Consider the modified supersonic doublet integral

$$\hat{I}_D = \iint_{\Sigma_0 = \Sigma_1 + \Sigma_2 + \Sigma_3} \frac{\partial \hat{G}}{\partial z} dx_1 dy_1 \quad \text{H.9}$$

where Σ_1 , Σ_2 and Σ_3 are shown in Fig. H.2. For the sake of simplicity, two edges of Σ_0 have been assumed to be parallel to the x -axis. Hence,

$$\hat{I}_D = -\frac{1}{2\pi} (\hat{I}_1 + \hat{I}_2) \quad \text{H.10}$$

where

$$\begin{aligned} \hat{I}_1 &= \iint_{\Sigma_1} \frac{\partial}{\partial z} \left(\frac{1}{r_B} \right) dx_1 dy_1 \\ &= 2z \int_0^Y dy_1 \int_{-X(y_1)}^{-\sqrt{y_1^2 + z^2 + \varepsilon^2}} \frac{1}{r_B^3} dx_1 \end{aligned} \quad \text{H.11}$$

and

$$\begin{aligned} \hat{I}_2 &= \frac{1}{\varepsilon^2} \iint_{\Sigma_2} \frac{\partial r_B}{\partial z} dx_1 dy_1 \\ &= -\frac{2z}{\varepsilon^2} \int_0^Y dy_1 \int_{-\sqrt{y_1^2 + z^2 + \varepsilon^2}}^{-\sqrt{y_1^2 + z^2}} \frac{1}{r_B} dx_1 \end{aligned} \quad \text{H.12}$$

Using the transformation

$$x_1 = -\sqrt{r_1^2 + y_1^2 + z^2} \quad \text{H.13}$$

one obtains

$$dx_1 = -\frac{r_1}{x_1} dr_1 \quad \text{H.14}$$

and

$$\begin{aligned} \hat{I}_1 &= 2z \int_0^Y dy_1 \int_0^{R=\sqrt{X^2-y_1^2-z^2}} \frac{1}{r_1} \frac{1}{\sqrt{r_1^2+y_1^2+z^2}} dr_1 \\ &= -2z \int_0^Y dy_1 \frac{1}{y_1^2+z^2} \left[\frac{\sqrt{r_1^2+y_1^2+z^2}}{r_1} \right]_E^R \\ &= I + \frac{2z}{\varepsilon} \int_0^Y \frac{\sqrt{\varepsilon^2+y_1^2+z^2}}{y_1^2+z^2} dy_1 \\ &= I + \frac{2z}{\varepsilon} \left[\ln(y_1 + \sqrt{\varepsilon^2+y_1^2+z^2}) + \frac{\varepsilon}{|z|} \tan^{-1} \frac{\varepsilon y_1}{|z|\sqrt{\varepsilon^2+y_1^2+z^2}} \right]_{y_1=0}^{y_1=Y} \\ &= I + \frac{2z}{\varepsilon} \ln \left(\frac{Y + \sqrt{\varepsilon^2+Y^2+z^2}}{\varepsilon^2+z^2} \right) + 2 \frac{z}{|z|} \tan^{-1} \left(\frac{\varepsilon Y}{|z|\sqrt{\varepsilon^2+Y^2+z^2}} \right) \quad \text{H.15} \end{aligned}$$

where

$$I = -2z \int_0^Y \frac{\sqrt{R^2+y_1^2+z^2}}{y_1^2+z^2} \frac{dy_1}{R} = -2z \int_0^Y \frac{X}{y_1^2+z^2} \frac{dy_1}{\sqrt{X^2-y_1^2-z^2}} \quad \text{H.16}$$

is the contribution from the edge $x = X(y)$.

On the other hand, combining Eqs. H.12 to H.14 yields

$$\begin{aligned}
\hat{I}_2 &= \frac{-2z}{\varepsilon^2} \int_0^Y dy_1 \int_{-\sqrt{y_1^2 + z^2}}^{-\sqrt{y_1^2 + \varepsilon^2}} \frac{1}{r_B} dx_1 = -\frac{2z}{\varepsilon^2} \int_0^Y dy_1 \int_0^\varepsilon \frac{dr_1}{\sqrt{r_1^2 + y_1^2 + z^2}} \\
&= -\frac{2z}{\varepsilon^2} \int_0^Y \left[\ln(\varepsilon + \sqrt{\varepsilon^2 + y_1^2 + z^2}) - \ln(\sqrt{y_1^2 + z^2}) \right] dy_1 \\
&= -\frac{2z}{\varepsilon^2} \left\{ \left[y_1 \ln(\varepsilon + \sqrt{\varepsilon^2 + y_1^2 + z^2}) - y_1 \ln(\sqrt{y_1^2 + z^2}) \right]_0^Y \right. \\
&\quad \left. - \int_0^Y y_1 \left[\frac{1}{\varepsilon + \sqrt{\varepsilon^2 + y_1^2 + z^2}} \frac{y_1}{\sqrt{\varepsilon^2 + y_1^2 + z^2}} - \frac{1}{\sqrt{y_1^2 + z^2}} \frac{y_1}{\sqrt{y_1^2 + z^2}} \right] dy_1 \right\} \\
&= -\frac{2z}{\varepsilon^2} \left\{ Y \ln \left(\frac{\varepsilon + \sqrt{\varepsilon^2 + Y^2 + z^2}}{\sqrt{Y^2 + z^2}} \right) - \int_0^Y y_1^2 \left[\frac{-\varepsilon + \sqrt{\varepsilon^2 + y_1^2 + z^2}}{(y_1^2 + z^2)\sqrt{\varepsilon^2 + y_1^2 + z^2}} - \frac{1}{y_1^2 + z^2} \right] dy_1 \right\} \\
&= -\frac{2z}{\varepsilon^2} \left\{ Y \ln \left(\frac{\varepsilon + \sqrt{\varepsilon^2 + Y^2 + z^2}}{\sqrt{Y^2 + z^2}} \right) + \varepsilon \int_0^Y \frac{1}{\sqrt{\varepsilon^2 + y_1^2 + z^2}} dy_1 - \varepsilon z^2 \int_0^Y \frac{1}{y_1^2 + z^2} \frac{dy_1}{\sqrt{\varepsilon^2 + y_1^2 + z^2}} \right\} \\
&= -\frac{2z}{\varepsilon^2} \left\{ Y \ln \left(\frac{\varepsilon + \sqrt{\varepsilon^2 + Y^2 + z^2}}{\sqrt{Y^2 + z^2}} \right) + \varepsilon \ln \left(\frac{Y + \sqrt{\varepsilon^2 + Y^2 + z^2}}{\sqrt{\varepsilon^2 + z^2}} \right) \right. \\
&\quad \left. - |z| \tan^{-1} \left(\frac{\varepsilon Y}{|z| \sqrt{\varepsilon^2 + Y^2 + z^2}} \right) \right\} \tag{H.17}
\end{aligned}$$

Finally, combining Eq. H.15 and H.17, one obtains

$$\begin{aligned}
\hat{I}_1 + \hat{I}_2 &= I + 2z \left[\frac{1}{\varepsilon} \ln \frac{Y + \sqrt{\varepsilon^2 + Y^2 + z^2}}{\sqrt{\varepsilon^2 + z^2}} + \frac{1}{|z|} \tan^{-1} \left(\frac{\varepsilon Y}{|z| \sqrt{\varepsilon^2 + Y^2 + z^2}} \right) \right. \\
&\quad \left. - \frac{Y}{\varepsilon^2} \ln \left(\frac{\varepsilon + \sqrt{\varepsilon^2 + Y^2 + z^2}}{\sqrt{Y^2 + z^2}} \right) - \frac{1}{\varepsilon} \ln \left(\frac{Y + \sqrt{\varepsilon^2 + Y^2 + z^2}}{\sqrt{\varepsilon^2 + z^2}} \right) + \frac{|z|}{\varepsilon^2} \tan^{-1} \left(\frac{\varepsilon Y}{|z| \sqrt{\varepsilon^2 + Y^2 + z^2}} \right) \right] \tag{H.18} \\
&= I + 2z \left[-\frac{Y}{\varepsilon^2} \ln \left(\frac{\varepsilon}{\sqrt{Y^2 + z^2}} + \sqrt{\frac{\varepsilon^2}{Y^2 + z^2} + 1} \right) + \left(1 + \frac{z^2}{\varepsilon^2} \right) \frac{1}{|z|} \tan^{-1} \left(\frac{\varepsilon Y}{|z| \sqrt{\varepsilon^2 + Y^2 + z^2}} \right) \right]
\end{aligned}$$

By expanding in power of ϵ one obtains

$$\begin{aligned}
 \hat{I}_1 + \hat{I}_2 &= I + 2z \left\{ -\frac{\Psi}{\epsilon^2} \ln \left[\frac{\epsilon}{\sqrt{\Psi^2 + z^2}} + \left(1 + \frac{1}{2} \frac{\epsilon^2}{\Psi^2 + z^2} + \dots \right) \right] \right. \\
 &\quad \left. + \left(1 + \frac{z^2}{\epsilon^2} \right) \frac{1}{|z|} \tan^{-1} \left[\frac{\epsilon \Psi}{|z| \sqrt{\Psi^2 + z^2}} \left(1 - \frac{1}{2} \frac{\epsilon^2}{\Psi^2 + z^2} + \dots \right) \right] \right\} \\
 &= I + 2z \left\{ \frac{\Psi}{\epsilon^2} \left[\left(\frac{\epsilon}{\sqrt{\Psi^2 + z^2}} + \frac{1}{2} \frac{\epsilon^2}{\Psi^2 + z^2} + O(\epsilon^3) \right) - \frac{1}{2} \left(\frac{\epsilon}{\sqrt{\Psi^2 + z^2}} + O(\epsilon^3) \right)^2 + O(\epsilon^3) \right] \right. \\
 &\quad \left. + \left(1 + \frac{z^2}{\epsilon^2} \right) \frac{1}{|z|} \left(\frac{\epsilon \Psi}{|z| \sqrt{\Psi^2 + z^2}} + O(\epsilon^3) \right) \right\} \\
 &= I + 2z \left\{ \left[-\frac{1}{\epsilon} \frac{\Psi}{\sqrt{\Psi^2 + z^2}} + O(\epsilon) \right] + \left[\frac{z^2}{\epsilon^2} \frac{\epsilon}{|z|^2} \frac{\Psi}{\sqrt{\Psi^2 + z^2}} + O(\epsilon) \right] \right\} \\
 &= I + O(\epsilon)
 \end{aligned}$$

H.19

Finally, combining Eq. H.10 and H.19, one obtains

$$\hat{I}_D = -\frac{1}{2\pi} I + O(\epsilon)$$

H.20

H.3 The Supersonic Doublet Integral

By letting ϵ go to zero, one obtains

$$I_D = \lim_{\epsilon \rightarrow 0} \hat{I}_D = -\frac{1}{2\pi} I$$

H.21

where I , given by Eq. H.15, is the contribution of the boundary $x = x(y_1)$. Hence, the rule is that the contribution of the boundary $r_B = 0$ (which is infinity if the theory of function

is applied carelessly) is zero.

Note in particular that if $X = \text{const.}$

$$I_D = -\frac{1}{2\pi} I = \text{sign}(z) \frac{1}{\pi} \tan^{-1} \frac{X Y}{|z| \sqrt{X^2 - Y^2 - z^2}} \quad \text{H.22}$$

Finally, note that

$$I_D(z=0) = I_D(X=Y=\infty) = \frac{1}{2} \text{sign}(z) \quad \text{H.23}$$

which is the same result used in subsonic flow to prove that

$E = 1/2$ on the surface Σ .

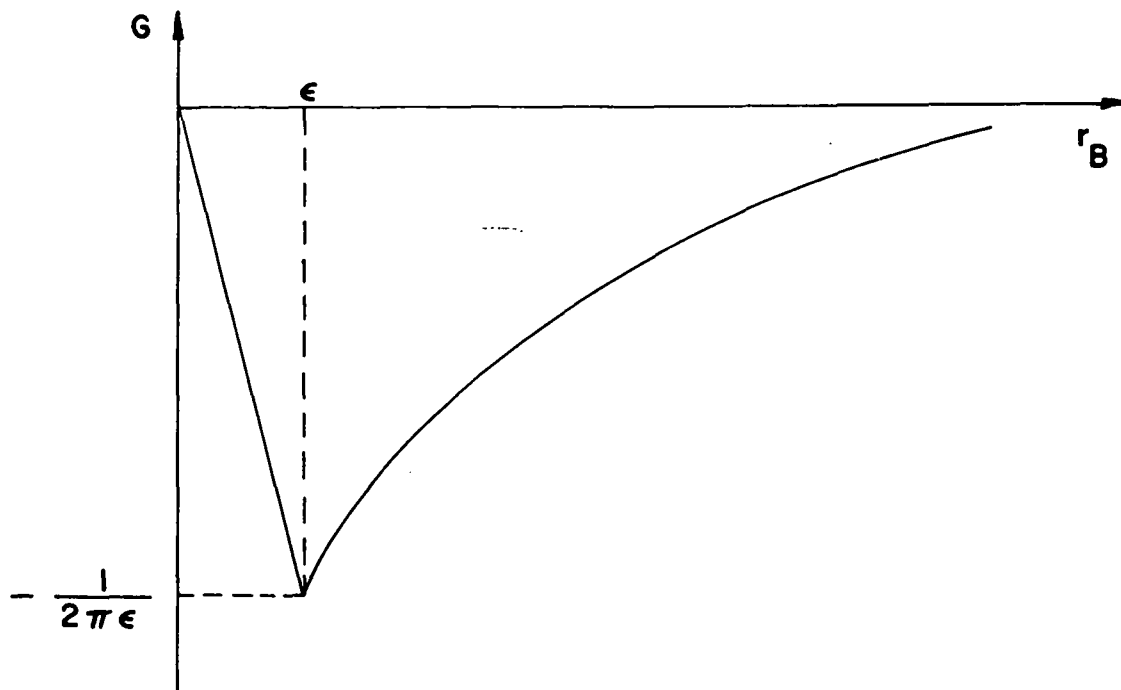


Fig. H.1 Modified Supersonic Source

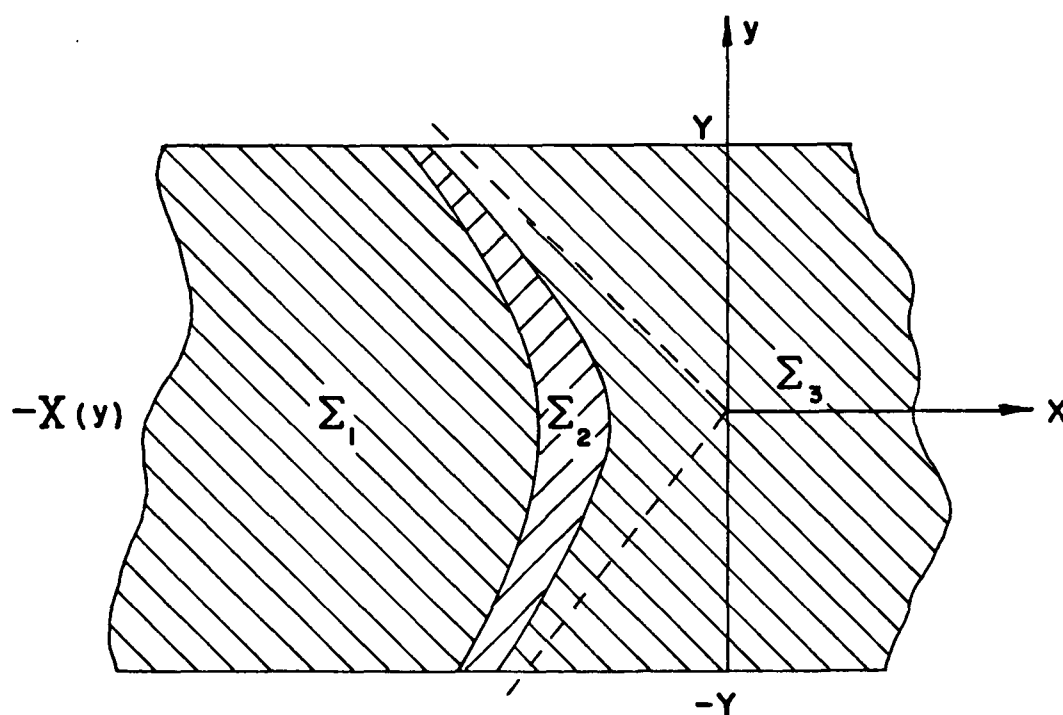


Fig. H.2 Surface $\Sigma_0 = \Sigma_1 + \Sigma_2 + \Sigma_3$